NASA TECHNICAL NOTE

NASA TN D-5941

C. 1

NASA TN D-5941

PARAMETRIC DESIGN OF INTERPLANETARY AND ORBITAL TRAJECTORIES WITH EXAMPLES FOR MARS 1973, 1975, AND 1977 OPPORTUNITIES

by John F. Newcomb and William F. Hampshire II

Langley Research Center
Hampton, Va. 23365

NATIONAL AERONAUTICS AND SPACE ADMINISTRATION • WASHINGTON, D. C. • AUGUST 1970

1. Report No. NASA TN D-5941	2. Government Accession No.	3. Recipient's Catalog No.
4. Title and Subtitle PARAMETRIC DESIGN OF INTERPLANETARY AND ORBITAL TRAJECTORIES WITH EXAMPLES FOR MARS 1973, 1975, AND 1977 OPPORTUNITIES		5. Report Date August 1970
		6. Performing Organization Code
7. Author(s) John F. Newcomb and William F. Hampshire II		8. Performing Organization Report No. L-6564
		10. Work Unit No. 815-00-00-00
9. Performing Organization Name and Address NASA Langley Research Center Hampton, Va. 23365		11. Contract or Grant No.
		13. Type of Report and Period Covered Technical Note
12. Sponsoring Agency Name and Address National Aeronautics and Space Administration Washington, D.C. 20546		14. Sponsoring Agency Code

15. Supplementary Notes

16. Abstract

A method for parametrically studying the general interplanetary trajectory design problem is discussed; the method couples the design of interplanetary trajectories with the resulting planetary orbits obtainable from various launch and arrival opportunities. The procedure is applied to the trajectories which could be launched to Mars in the years 1973, 1975, and 1977, and for those opportunities, a set of parametric charts for use in designing Mars missions is included. The important mission parameters are presented and discussed, and launch windows are established which maximize payload in planetary orbit for a coplanar periapsis deboost.

17. Key Words (Suggested by Author(s)) Interplanetary missions Trajectory design	18. Distribution Statement Unclassified – Unlimited

19. Security Classif. (of this report) Unclassified	20. Security Classif. (of this page) Unclassified	21. No. of Pages 78	22. Price* $3.00

*For sale by the Clearinghouse for Federal Scientific and Technical Information
Springfield, Virginia 22151

PARAMETRIC DESIGN OF INTERPLANETARY AND ORBITAL TRAJECTORIES WITH EXAMPLES FOR MARS 1973, 1975, AND 1977 OPPORTUNITIES

By John F. Newcomb and William F. Hampshire II
Langley Research Center

SUMMARY

A procedure is described for parametrically studying the general interplanetary mission design problem. This procedure is applied to the analysis of the Mars 1973, 1975, and 1977 type I (heliocentric travel angle less than 180°) and type II (heliocentric travel angle greater than 180°) opportunities. First, the general heliocentric orbital parameters and accompanying planetary approach conditions for launch and arrival opportunities were determined. The actual launch and arrival energies were examined, and a launch window was established which maximized the payload in the planetary orbit. For the opportunities examined, all the resulting planetary approach asymptotes lay in a small region of planetary right ascension and declination. This fact, coupled with a philosophy of a coplanar periapsis deboost at the planet, yields families of orbits for particular launch opportunities. Representative subsets of these families were examined, and the occultations of the Sun, Earth, and Canopus by the planet are displayed as well as the illumination under orbital traces. Thus, a set of parametric charts for use in designing Mars missions and in selecting experiments for the aforementioned opportunities is presented.

INTRODUCTION

One important factor in designing interplanetary missions is the coordination of the heliocentric trajectory geometry with the planetary orbit geometry. This coordination is necessary to establish the capability of performing particular integrated missions within the boundaries of constraints generated by experimentation and by spacecraft design. In other studies such as references 1 and 2, for example, only the heliocentric trajectory parameters and planetary approach conditions are considered. The intent of this paper is to extend previous analyses by presenting the available planetary orbit designs and other parameters which result from the approach conditions and which are influenced by the heliocentric geometry.

The difficulty in studying any general planetary mission of this nature lies in the fact that the problem is highly multidimensional. Therefore, if a meaningful parametric study is to be undertaken, an attempt must be made to determine those parameters which have a profound effect on mission design; thereby, those parameters which remain relatively invariant from mission to mission and have less effect on particular mission design options are eliminated. In the study presented herein, an attempt has been made to minimize the number of parameters to be examined by making use of similarities in the planetary approach trajectories and also by assuming a simple planetary orbit injection technique. The most important similarity in the approach conditions resulting from a particular launch opportunity is the small variation in the direction of $\vec{S}$ (a unit vector at the target planet, parallel to the asymptote of the incoming hyperbola but translated to the center of the planet). For the orbit injection maneuver, an impulsive velocity is applied at periapsis of the incoming hyperbolic orbit, thus a coplanar elliptic orbit with the same periapsis is produced. The result of the relative constancy in position of the approach asymptote and the adoption of the simple orbit injection maneuver is to produce families of feasible orbits about the planet which show little variation as a function of launch and arrival dates.

The many diverse experiments that may be performed with a planetary orbiting vehicle result in additional constraints on the mission design problem. However, two fundamental types of constraints appear to be involved in most of the experiments under consideration. First, some type of imagery of the planetary surface may be desirable, or it may be desirable to place a probe on the surface at some particular lighting condition. Therefore, the orbital placement with respect to the Sun illumination on the planet is of interest. Second, another set of constraints is created by more general experiment and spacecraft-generated requirements. These constraints are the occurrence and time duration of occultation of the Sun, Earth, or some other celestial reference, such as the star Canopus. Therefore, as a first approach to designing an interplanetary mission, only these two types of constraints need be examined for each launch opportunity in order to determine which integrated sets of experiments can be readily performed.

For the duration of the planetary arrival window corresponding to the launch opportunity, the celestial geometry of the Sun, Mars, Earth, and Canopus is relatively constant. It has already been noted that the approach asymptote location is relatively invariant. Therefore, only a few representative arrival conditions need be examined to almost completely describe the family of feasible orbits and the associated occultations and lighting conditions available in a given launch opportunity. Thus, the feasibility of mission objectives and associated experimentation for a given launch opportunity can be readily assessed.

SYMBOLS

C_3 vis viva integral or twice the launch energy per unit mass, $(km/sec)^2$

G angle between planet-Sun vector and local vertical on surface of planet, deg

$\vec{S}$ unit vector at center of planet in direction of asymptote of traveled leg of hyperbola

V_∞ hyperbolic excess velocity, km/sec

Z angle between planet-Sun vector and planetary hyperbolic approach asymptote, deg

β pseudoinclination, deg

δ declination of $\vec{S}$, deg

λ right ascension of $\vec{S}$, deg

Subscripts:

$\oplus$ quantity measured at Earth (If quantity is an angle, then Earth right-ascension—declination system is used as basic coordinate system.)

♂ quantity measured at Mars (If quantity is an angle, then Mars right-ascension—declination system is used as basic coordinate system.)

ABBREVIATIONS

DEC declination

RA right ascension

ANALYSIS

In the following analysis a procedure for the trajectory design of general planetary missions is developed. Herein, the word "general" implies that no particular set of experiments and no particular spacecraft have been selected; thus there are no mission-dependent constraints to shape the interplanetary and planetary orbit design.

Consequently, the problem must be studied parametrically so that when a definitive mission is proposed, the resulting constraints can be considered in the light of the parametric analysis. Such a study is feasible in the interplanetary part of the trajectory design. However, since design of the planetary orbit is a multidimensional problem, a completely parametric analysis is prohibitive. Therefore, in the planetary part of the trajectory design, representative values for some of the parameters were chosen, and those particular cases were investigated.

As a first step, the heliocentric trajectory and its associated earth departure and planetary arrival conditions were generated by a simple computer program which fit a heliocentric orbit between two vectors for a given transfer time. For details of the computer algorism, see reference 3, page 213. The computer algorism utilized was similar to that described in reference 4. Most of the earth departure and arrival parameters which evolved are available from several sources in slightly different form. (For example, see ref. 2.) Plots of the data are most useful when arrival date is held constant. For example, in sketch (a) parameters such as C_3 at earth (twice the launch energy per unit mass) and V_∞ (hyperbolic excess velocity) at the planet are plotted against launch date for several constant arrival dates.

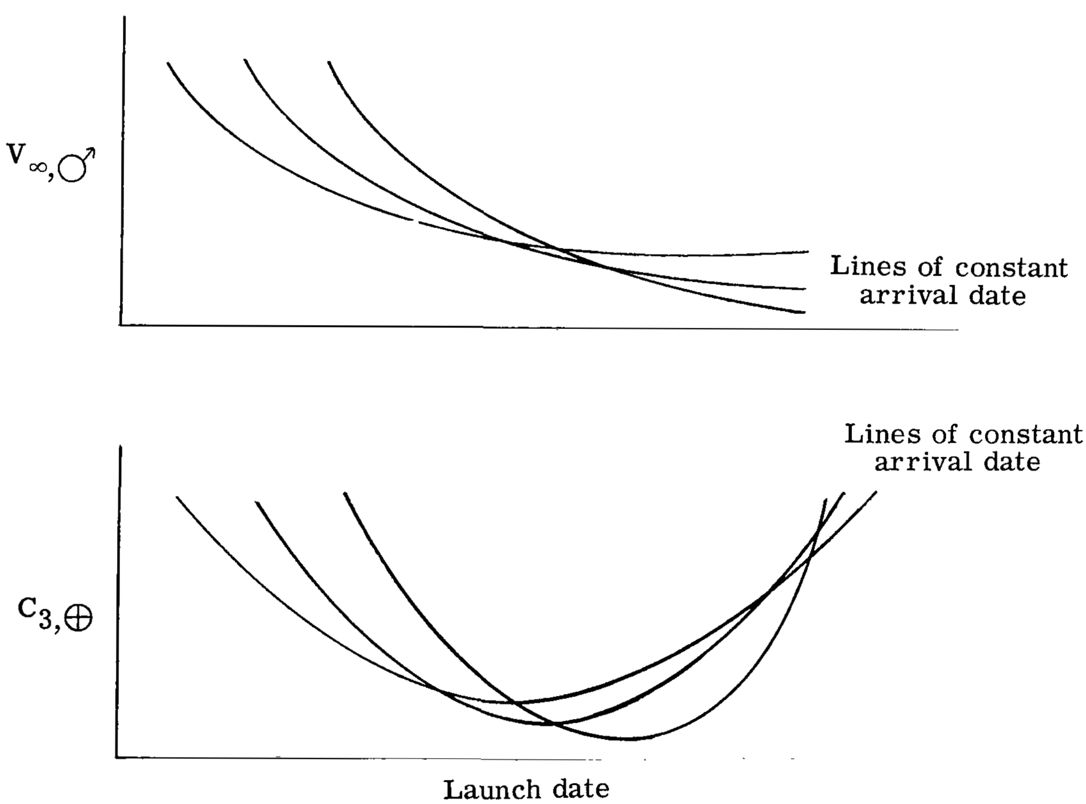

Sketch (a)

Once the desired launch window duration is known, the actual launch and arrival windows can be found by maximizing the payload in planetary orbit. That is, for each interplanetary trajectory, a launch energy and a planetary arrival velocity can be calculated. Here it is assumed that the launch vehicle delivers the maximum payload onto the interplanetary trajectory on each launch day. At the planet it is assumed that the ideal velocity equation is a good approximation for determining the mass fraction in planetary orbit. Thus the payload delivered to the planet multiplied by the mass fraction determines the in-orbit payload. This method implies that on each launch day the spacecraft carries only enough fuel to inject it into planetary orbit. Also in this analysis, no fuel is allotted for error corrections. (The purpose of this study is to obtain and to present general launch and arrival windows and trends, not to generate a detailed payload study.) The resulting payload weight can be plotted against launch date for various constant arrival dates, as shown in sketch (b).

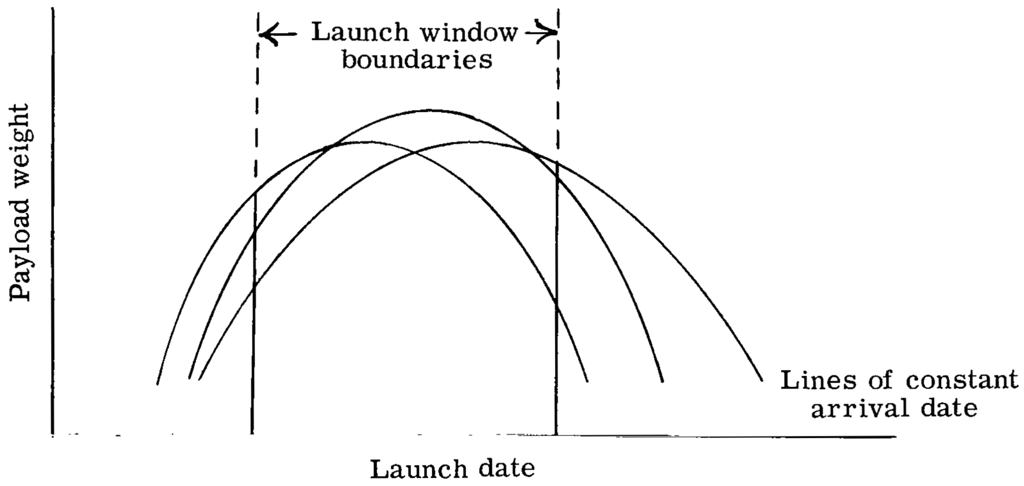

Sketch (b)

With these data and a chosen launch window duration, the maximum payloads and the accompanying launch and arrival date boundaries can be found. If these boundaries were transferred to other graphs, for example the approach asymptote location plot, the actual bounds on the asymptote could be established.

In this study the spacecraft orbit injection maneuver at the planet is assumed to be an impulsive coplanar transfer from the periapsis of the incoming hyperbolic trajectory to the periapsis of the elliptic orbit. For the actual mission, departure from this ideal orbit injection maneuver may be necessary in order to satisfy mission particular constraints. However, with departure from this approach, the deboost velocity requirements mount rapidly. Because of these rapidly mounting velocity requirements, the resulting orbital orientations cannot vary significantly from these "nominals" without consumption of much larger amounts of fuel. Therefore, this approach not only results in nominal orbital placements from which only small excursions will be taken, but has the additional advantage of imposing the same constraint on all missions; thereby one degree of freedom is effectively eliminated from the problem.

Next, various orbital inclinations are assumed to be obtained at the planet by rotation of the hyperbolic trajectory about $\vec{S}$, where the rotation is performed either at the Earth injection maneuver or during the midcourse maneuver. Therefore, a family of possible orbital inclinations can be obtained. The following spacecraft-oriented parameters can then be investigated: duration of Sun occultation, Earth occultation, and Canopus occultation by the planet, as well as the orbital positionings with respect to the sunlighting bands. These data were generated by utilizing a computer program described in reference 5. With the investigation performed for several sizes of orbits, the parametric mission design problem is solved in that a launch opportunity is chosen and the resulting orbital geometry is investigated. This analysis therefore serves as a first step toward investigating a general interplanetary mission design.

The approach described above was derived through a need to study possible missions to Mars during the 1973, 1975, and 1977 launch opportunities. The results of that study are presented in "Results and Discussion"; however, prior to that presentation, the areocentric coordinate and the parameter β must be introduced. In the areocentric system, shown in figure 1, the Mars equator forms the reference plane. The point at which the Sun appears to cross the planet equator in a south-to-north direction forms the reference axis. Two angular coordinates are necessary to define an object in the coordinate system: right ascension measured from the reference axis counterclockwise (+) as seen from above, and declination measured from the planet equator in a northerly (+) or southerly (-) direction. The pseudoinclination β is used in place of the normally defined inclination and may be best described by referring to figure 1. In the figure, β is always measured counterclockwise from the orbital node which is nearest the approach asymptote. This node can be the ascending or descending node. If β is between 0° and 90°, then this is an ascending node and the orbit is posigrade. If β is between 90° and 180°, then this is an ascending node and the orbit is retrograde.

RESULTS AND DISCUSSION

The approach presented in the analysis toward formulation of trajectories for interplanetary missions was applied to the proposed 1973, 1975, and 1977 Mars missions. This section contains primarily a discussion of the methods and results of that study. It was stated that launch and arrival windows could be determined on the basis of the requirement to maximize payload in planetary orbit; for the purpose of this example, a 30-day launch window duration was arbitrarily chosen. This selection implies the use of some launch vehicle and a representative performance of that vehicle. In order to generalize the analyses as much as possible, three different launch vehicles were assumed. These vehicles were chosen to span the reasonable range of possible booster systems which may be used in the 1973 to 1977 opportunities. The three vehicles chosen were the Titan IIIC, the Titan IIIF-Centaur, and the Saturn V. Typical performance curves for these vehicles are shown in figure 2; gross payload weight is defined as total weight injected on to the interplanetary trajectory.

The interplanetary trajectory was determined by finding the unique heliocentric ellipse passing through the launch planet at the launch date and the target planet at the target date via Lambert's theorem. A mean-element ephemeris was used to generate the planetary positions and velocities. The vector velocity of the launch planet at the launch date is subtracted vectorially from the vector velocity of the heliocentric ellipse to determine the sphere-of-influence velocity. This velocity is then assumed to be the hyperbolic excess velocity at departure. Likewise, the arrival hyperbolic excess velocity and direction of the approach asymptote are calculated at the target planet arrival. Shown in figure 3 are the trajectory characteristics for the single conic transfers between Earth and Mars for the 1973 type I opportunity. The following trajectory geometry classification, described in reference 2, will be used: A type I trajectory indicates that the heliocentric travel angle of the spacecraft is less than 180°, and a type II trajectory indicates a travel angle greater than 180°. Shown in the figure are various parameters plotted against the launch date for several lines of constant arrival date at 20-day intervals. The date of arrival is indicated by the symbol at the extremity of each line. In figure 3(a) twice the required launch energy per unit mass $C_{3,\oplus}$ and the hyperbolic excess velocity at Mars arrival $V_{\infty,♂}$ are shown as functions of launch date for various arrival dates, as first introduced in sketch (a). Here and in the rest of the analysis, generation of trajectories was limited to those having $C_{3,\oplus}$ requirements of less than 36 $(km/sec)^2$ (which represents a reasonable limit on the basis of present launch vehicle capabilities). Figure 3(b) presents data on the angle between the hyperbolic approach asymptote at Mars and the vector pointing from Mars to the Sun. This angle Z is commonly called the ZAP angle and is important because it relates the possible orbital orientation with respect to the sunlighting. Also shown in figure 3(b) is the geocentric declination of the launch asymptote $\delta_{\oplus}$. Figure 3(c) presents the areocentric right ascension and declination of the approach asymptote as a function of launch date for various arrival dates. The relative invariance in position of the vector should be noted for further reference.

Shown in figure 4 is the payload in Mars orbit as a function of launch and arrival dates for the three launch vehicles considered, the Titan IIIC, the Titan IIIF-Centaur, and the Saturn V. A specific impulse of 290 seconds was assumed for the orbit injection engine, and the ideal velocity equation was used to determine the actual weight in Mars orbit. It was also assumed that the injection maneuver placed the spacecraft in an orbit with a 1000-km periapsis altitude and with a period equal to 1 Martian day (24 h 37 min). Whereas these stipulations are pertinent to a total description of the analysis, the prime use of figure 4 is to produce a launch window. It can be seen from a comparison of the dotted vertical lines in each segment of the figure that the choice of a 30-day launch window, which maximizes the payload in Mars orbit, is almost independent of the particular launch vehicle used. However, to keep the analysis as general as possible, a launch opportunity was established which encompasses the three individual 30-day windows. This overall launch opportunity, or launch window boundary, is shown by the solid vertical lines in the figure. In an actual mission the payload weight is defined by the value at the boundaries of the window, and once the spacecraft is sized for these boundaries, the middle part of the window simply allows additional capability at launch and arrival. With this boundary established, it was possible to select typical trajectories which, with their encounter geometries, are representative of the total window. Thus, data need not be generated for all of the points in the launch window. From figure 4 three heliocentric trajectories representative of launches during the 1973 type I opportunity were chosen, and the pertinent parameters are shown in table I. (Also shown are values for type II trajectory parameters which will be discussed subsequently.) These trajectories represent launches at the beginning, middle, and end of the overall window.

Figure 5 represents the lighting conditions under the areocentric orbits resulting from the encounter conditions of the three selected trajectories. In figure 5(a) is shown the sunlighting conditions which would exist under the family of possible areocentric orbits resulting from a launch at the beginning of the launch period. The coordinate system used is again the Mars right-ascension—declination system. In the figure the dashed lines represent lines of constant Sun illumination G of 30°, 60°, and 90°. The subsolar point is shown as $\odot$. The location of the approach asymptote is shown as a square symbol $\boxdot$. Also shown in the figure is a cluster of orbit traces which can be generated by rotation of the incoming hyperbola about the approach asymptote. The locus of periapsis for a 1000-km hyperbolic periapsis altitude is also shown. The parameter β, as described in the "Analysis" section, has been used to describe orbital inclination. Each orbit trace shown in the figure represents two values of β, one for a posigrade orbit and one for a retrograde orbit. This also accounts for the fact that the locus-of-periapsis circle crosses each orbit trace twice, since the posigrade and retrograde orbits have different periapsis locations. In every case the spacecraft will travel through the periapsis position before it travels through the approach asymptote position. With this description in mind, the figure can be viewed and conclusions drawn as to the orbit orientation best suited to a photographic mission, given whatever constraints that may be imposed. For example, suppose the area of the planet near a declination of -40° is the prime target for pictures. An orbital inclination might be chosen such that part of orbital trace is nearly parallel to the -40° declination line. This mission would require an orbit where $\beta = 40^{\circ}$, $\beta = 140^{\circ}$, $\beta = 220^{\circ}$, or $\beta = 320^{\circ}$ as can be seen in figure 5(a). However, it also can be seen that the $\beta = 140^{\circ}$ and $\beta = 320^{\circ}$ orbits are essentially parallel to the -40° declination line in the region where there is no sunlighting on the planet for the day of arrival (in between terminators). On the other hand, the $\beta = 40^{\circ}$ and $\beta = 220^{\circ}$ orbits are parallel to the desired declination in a lighting band of $G = 30^{\circ}$ to $G = 90^{\circ}$. Of the latter two, the $\beta = 40^{\circ}$ might be chosen because it is near periapsis during the region of interest and hence closer to the photographic target. Like figure 5(a), figures 5(b) and 5(c) present the conditions which exist for launches in the middle and end of the launch opportunity. Therefore, the part of the launch opportunity that can best be utilized to satisfy a given set of mission constraints can be determined with the use of figure 5.

Now that the lighting conditions have been displayed for the three conditions chosen, the accompanying occultation characteristics remain to be displayed, and these are shown in figure 6. In figure 6(a), for example, the occultation times of the Sun, Earth, and Canopus are shown as functions of the pseudoinclination β for the conditions resulting from the earliest launch, as shown in table I. The hatched areas in the figure represent areas of unattainable orbit inclination due to the coplanar orbit injection maneuver. The boundaries of the areas are numerically equal to the declination of the approach asymptote at Mars. In figure 6(a) and in similar figures, several orbit sizes have been assumed. This assumption was essential because occultations are not only a function of orbit orientation but of orbit size itself. Therefore in the lower part of figure 6(a), two different orbits were investigated. Both orbits have periapsis altitudes of 1000 km, but one has a period equal to 1 Martian day and the other has a period equal to 1/2 Martian day. In the upper part of the figure, the same two orbital periods are again investigated, but the periapsis altitudes of both are 3000 km. From figure 6(a) the effect of orbit orientations and sizes and their desirability can be determined from the point of view of occultation characteristics. From figures 6(a), 6(b), and 6(c), the changes in these occultation conditions as the launch opportunity progresses can be determined, and this knowledge, with the lighting geometry displayed in figure 5, can be used to make a first-order judgment of the feasibility of a particular integrated mission during the 1973 type I launch opportunity.

An investigation into the Mars 1973 type II opportunity yielded the data presented in figures 7 to 10. They are presented in the same form and the same order as figures 3 to 6, respectively, and therefore need not be described in detail. A comparison of the two types of trajectories available in 1973 shows that the type I trajectories have slightly more payload capability. (See figs. 4 and 8.) The type I trajectories in general also have the advantage of requiring significantly shorter trip times. However, one advantage found with type II trajectories in 1973 is that the launch window can be widened without a significant sacrifice in payload weight capacity; this is not true of the 1973 type I trajectories, where the payload weight capability falls off rapidly in any attempt to widen the launch window.

The 1975 type I and type II opportunities have also been investigated, and the results are presented in figures 11 to 18. In contrast to the 1973 trajectories, more payload capability is available from 1975 type II trajectories than from type I. (See figs. 12 and 16.) In general, the 1975 type II payload capacity is also greater than that associated with either type of 1973 trajectory; whereas the 1975 type I payload capacity is, in general, less than that available with either type of 1973 trajectory. Another disadvantage that might rule out 1975 type I missions is shown in the upper half of figure 11(b). The declination of the launch asymptote for those trajectories is almost always higher than the normal $+34^{\circ}$ limit imposed on launches from the Eastern Test Range. Therefore, unless the vehicle is launched from another location, either the constraint must be relaxed or some dog-leg maneuver would be required. (A dog-leg maneuver of the magnitude required here would be very costly from a fuel standpoint, and thus would significantly reduce the payload capability shown in fig. 12.) For each 1975 launch window, three trajectories were chosen as representative for both type I and type II, and the important parameters relating to those trajectories are shown in table II.

The 1977 launch opportunity has also been investigated, and the results are shown in figures 19 to 22 for the type I trajectories and figures 23 to 26 for the type II trajectories. Like the 1975 trajectories, the 1977 type II trajectories afford larger payload weight capability than the type I trajectories. (See figs. 20 and 24.) Moreover, the 1977 trajectories allow slightly larger payload capability than their respective 1975 types. The problem that existed with the 1975 type I trajectories also is exhibited in the 1977 type I trajectory analysis; the declination of the launch asymptote for almost all of the trajectories in this group is above the $+34^{\circ}$ limit imposed on launches from the Eastern Test Range (fig. 19(b)), thus the payload weights capability shown in figure 20 is reduced. Table III exhibits the parameters representative of launches during the beginning, middle, and end of each 1977 launch window.

The variation of $\vec{S}$ may be of particular importance for mission planning, since the declination of the hyperbolic approach asymptote at Mars determines the minimum inclination of the areocentric orbit for a coplanar deboost maneuver. It is therefore interesting to note the declination of the asymptotes for the various launch opportunities. Figure 27 displays, on the right-ascension—declination grid, the loci of the approach asymptotes for the three launch opportunities and launch window boundaries investigated. In the figure the solid lines indicate the boundaries of the asymptote locations for type I trajectories, and dashed lines indicate the boundaries for the type II trajectories. In

1973 reasonably low inclination orbits (0° to 20°) can be easily achieved with the type I trajectories, whereas higher inclination (20° to 50° minimum inclination) orbits would normally be deduced from the use of type II trajectories. In 1975 the minimum inclination orbits achievable from both type I and type II trajectories would be approximately the same; whereas 1977 type II trajectories would, in general, yield lower inclination orbits than the type I trajectories. The variation in planet lighting and occultation is a major factor in determining the desirable orbit sizes and orientations. These data may also be used to determine the preferable arrival dates. However, particular conclusions cannot be made without a familiarity with the detailed mission objectives. Thus, the reader may use these data for additional analysis in the light of any proposed mission objectives which he may wish to consider.

CONCLUDING REMARKS

A method has been presented for visualizing the overall trajectory design problem for missions to the planets; this method has been applied to the 1973, 1975, and 1977 Mars launch opportunities. A launch window boundary has been selected for each year and type of heliocentric trajectory. Three typical trajectories and their associated Mars encounter conditions were then chosen for each launch window boundary for both the type I (heliocentric travel angle less than 180°) and the type II (heliocentric travel angle greater than 180°) trajectories. For each of these typical trajectories the family of possible areocentric orbits, which could be formed by a rotation of the hyperbola about the approach asymptote, was then investigated. Two prime conditions indicative of orbit accommodation were investigated: the orbit-sunlight geometry and the occultations of the Sun, Earth, and Canopus.

The 1977 type II opportunity was shown to be the most favorable for putting the maximum payload in orbit. The 1975 type II trajectories exhibit nearly equal capability. However, because of lower payload weights and range safety constraints, the type I trajectories available for launching in 1975 and 1977 are probably not feasible. Either type of trajectory launched in 1973 can yield reasonable payload weights in orbit but has less capability than the 1975 and 1977 type II trajectories. For each of these opportunities, definition of mission objectives is required to ascertain acceptable lighting conditions and occultations. However, the required orbital design data have been presented so that these variables can be considered as soon as mission objectives are defined.

Langley Research Center,
National Aeronautics and Space Administration,
Hampton, Va., June 11, 1970.

REFERENCES

1. Clarke, V. C., Jr.; Roth, R. Y.; et al.: Earth-Mars Trajectories, 1964-77. Tech. Mem. No. 33-100, Vols. I to VII, Jet Propulsion Lab., California Inst. Technol., 1964.
2. Clarke, V. C., Jr.; Bollman, W. E.; Roth, R. Y.; and Scholey, W. J.: Design Parameters for Ballistic Interplanetary Trajectories – Pt. I. One-Way Transfers to Mars and Venus. Tech. Rep. No. 32-77 (Contract NAS 7-100), Jet Propulsion Lab., California Inst. Technol., Jan. 16, 1963.
3. Escobal, Pedro Ramon: Methods of Orbit Determination. John Wiley & Sons, Inc., 1965.
4. Zoryan, M. D.: Space Research Conic Program, Phase III. 900-130; Rev. A, Jet Propulsion Lab., California Inst. Technol., May 1, 1969.
5. Green, Richard N.: Investigation of Occultation and Imagery Problems for Orbital Missions to Venus and Mars. NASA TN D-5104, 1969.

TABLE I.- TRAJECTORY AND MARS ENCOUNTER PARAMETERS FOR THE 1973 LAUNCH OPPORTUNITY

	1973 type I trajectories			1973 type II trajectories		
Launch date	July 17, 1973	Aug. 4, 1973	Aug. 24, 1973	July 11, 1973	Aug. 4, 1973	Aug. 28, 1973
Arrival date	Feb. 8, 1974	Feb. 28, 1974	Mar. 20, 1974	May 19, 1974	July 18, 1974	Oct. 6, 1974
Trip time, days	206	208	208	312	348	404
Communication distance at arrival, km	180×10^6	210×10^6	239×10^6	317×10^6	371×10^6	392×10^6
$C_{3,\oplus}$, $(km/sec)^2$	16.050	15.118	21.740	22.513	18.098	16.060
$\delta_{\oplus}$, deg	36.39	31.73	22.30	-10.35	-7.97	8.80
$\delta_{♂}$, deg	-8.90	-8.11	-2.45	50.23	45.94	29.94
$\lambda_{♂}$, deg	124.35	123.95	118.91	108.25	124.04	147.00
$V_{\infty,♂}$, km/sec	3.040	2.650	2.421	2.750	3.067	3.639
DEC of Sun at Mars, deg	0.06	3.99	7.73	17.15	22.85	22.69
RA of Sun at Mars, deg	0.14	9.03	17.75	43.89	71.24	109.98

TABLE II. - TRAJECTORY AND MARS ENCOUNTER PARAMETERS FOR THE 1975 LAUNCH OPPORTUNITY

	1975 type I trajectories			1975 type II trajectories		
Launch date	Sept. 5, 1975	Sept. 23, 1975	Oct. 13, 1975	Aug. 20, 1975	Sept. 7, 1975	Sept. 25, 1975
Arrival date	Apr. 2, 1976	May 12, 1976	June 21, 1976	July 11, 1976	Aug. 20, 1976	Sept. 29, 1976
Trip time, days	210	232	252	326	348	370
Communication distance at arrival, km	213×10^6	268×10^6	315×10^6	334×10^6	362×10^6	376×10^6
$C_{3,\oplus}$, $(km/sec)^2$	20.301	20.785	31.738	18.212	14.145	13.888
$\delta_{\oplus}$, deg	53.19	48.76	37.25	1.22	5.77	15.09
$\delta_{♂}$, deg	-24.09	-25.60	-13.03	32.61	28.90	19.91
$\lambda_{♂}$, deg	188.23	183.76	170.14	183.32	180.14	180.04
$V_{\infty,♂}$, km/sec	4.026	2.833	2.335	2.430	2.588	2.982
DEC of Sun at Mars, deg	16.74	21.17	23.60	23.97	22.88	19.27
RA of Sun at Mars, deg	42.58	60.57	79.31	88.94	108.52	128.24

TABLE III. - TRAJECTORY AND MARS ENCOUNTER PARAMETERS FOR THE 1977 LAUNCH OPPORTUNITY

	1977 type I trajectories			1977 type II trajectories		
Launch date	Oct. 12, 1977	Oct. 30, 1977	Nov. 17, 1977	Sept. 20, 1977	Oct. 6, 1977	Oct. 22, 1977
Arrival date	June 6, 1978	July 16, 1978	Sept. 14, 1978	Aug. 25, 1978	Aug. 25, 1978	Sept. 14, 1978
Trip time, days	237	259	301	339	323	327
Communication distance at arrival, km	251×10^6	295×10^6	339×10^6	327×10^6	327×10^6	339×10^6
$C_{3,\oplus}$, $(km/sec)^2$	19.165	20.119	26.486	13.405	10.973	12.288
$\delta_{\oplus}$, deg	60.33	47.24	25.92	16.28	14.29	22.06
$\delta_{♂}$, deg	-36.75	-28.60	-0.53	5.56	7.13	3.30
$\lambda_{♂}$, deg	232.80	224.79	209.14	216.89	221.72	215.18
$V_{\infty,♂}$, km/sec	3.876	2.667	2.828	2.450	2.457	2.553
DEC of Sun at Mars, deg	23.96	22.35	15.31	18.24	18.25	15.31
RA of Sun at Mars, deg	92.84	112.47	142.04	132.19	132.19	142.04

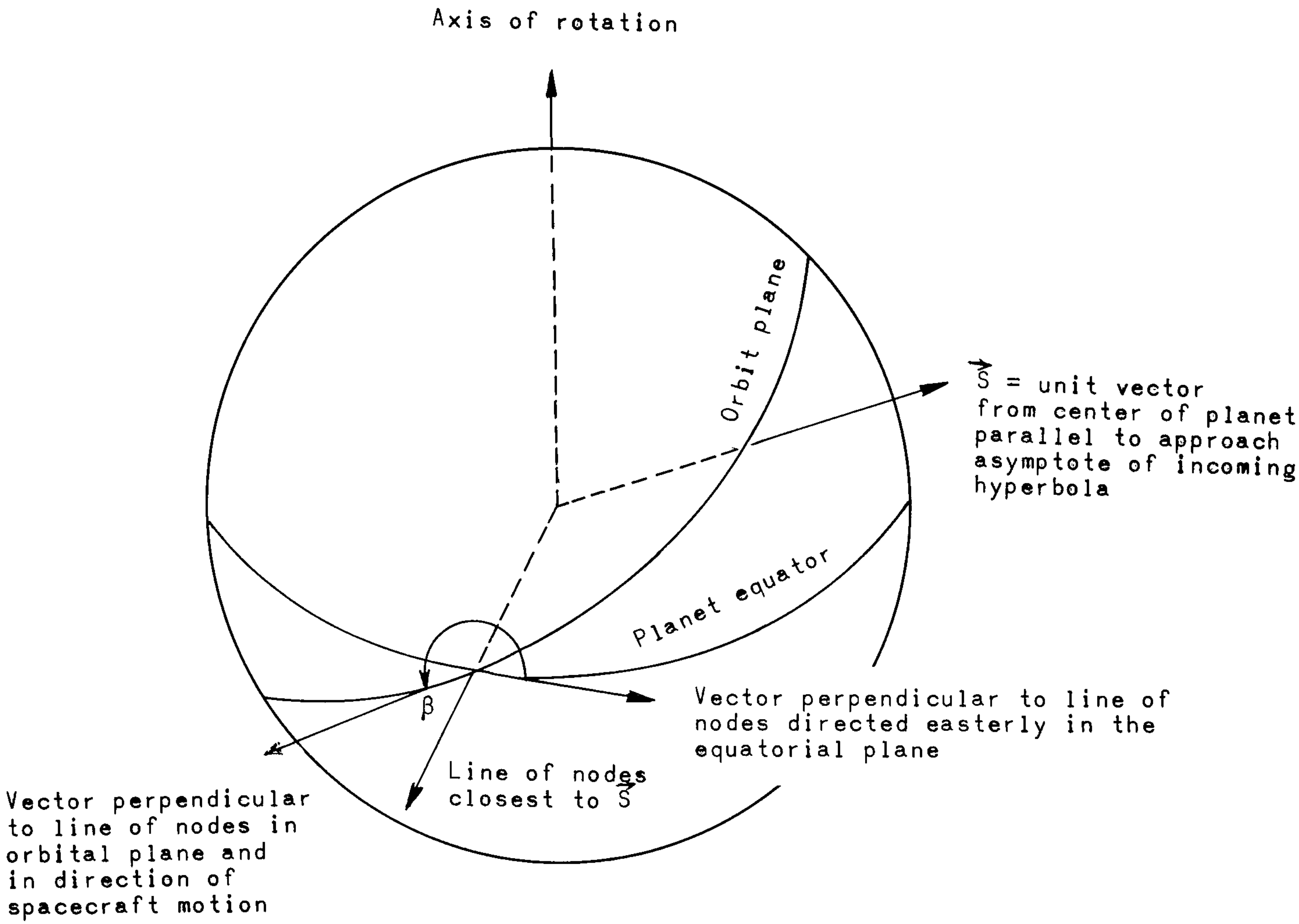

NOTE: β is measured counter-clockwise in plane perpendicular to line of nodes

Figure 1.- Orbital-plane geometry.

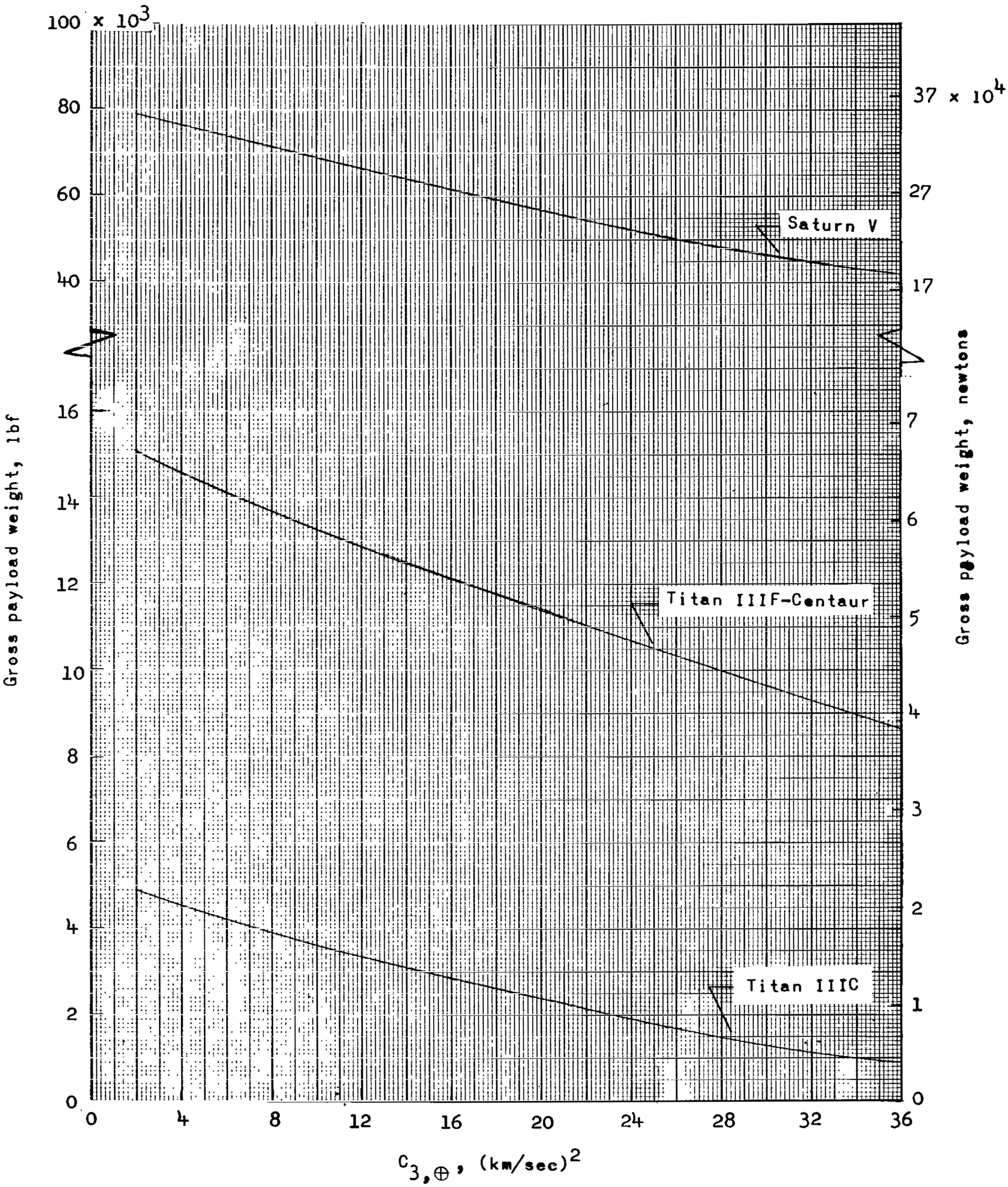

Figure 2.- Typical performance curves for three launch vehicles.

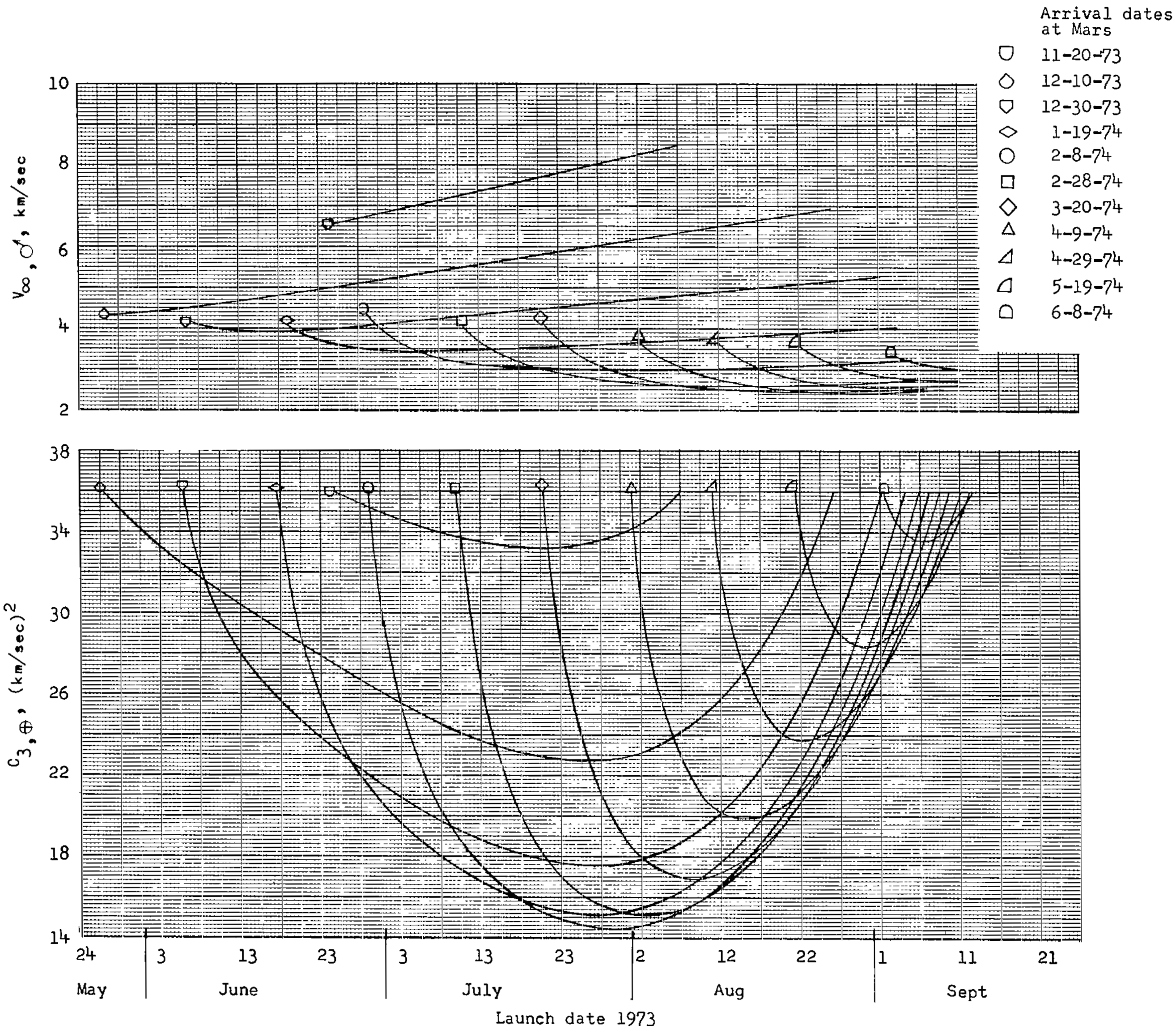

(a) Excess energy at Earth and hyperbolic excess velocity at Mars as functions of launch date for several arrival dates.

Figure 3.- Trajectory characteristics from Earth to Mars for the 1973 type I opportunity.

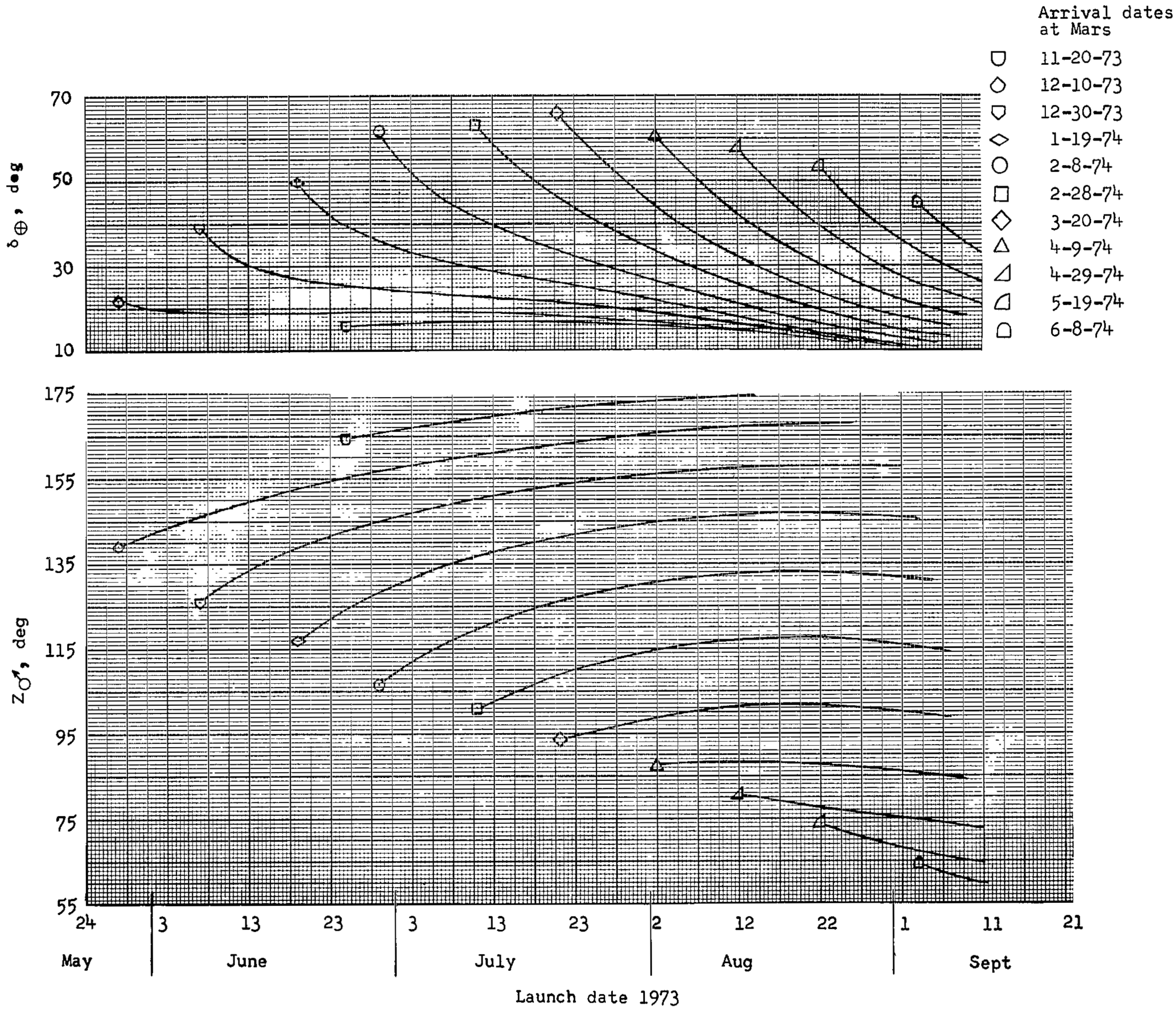

(b) Sun-$\vec{S}$ angle and declination of launch asymptote as functions of launch date for several arrival dates.

Figure 3.- Continued.

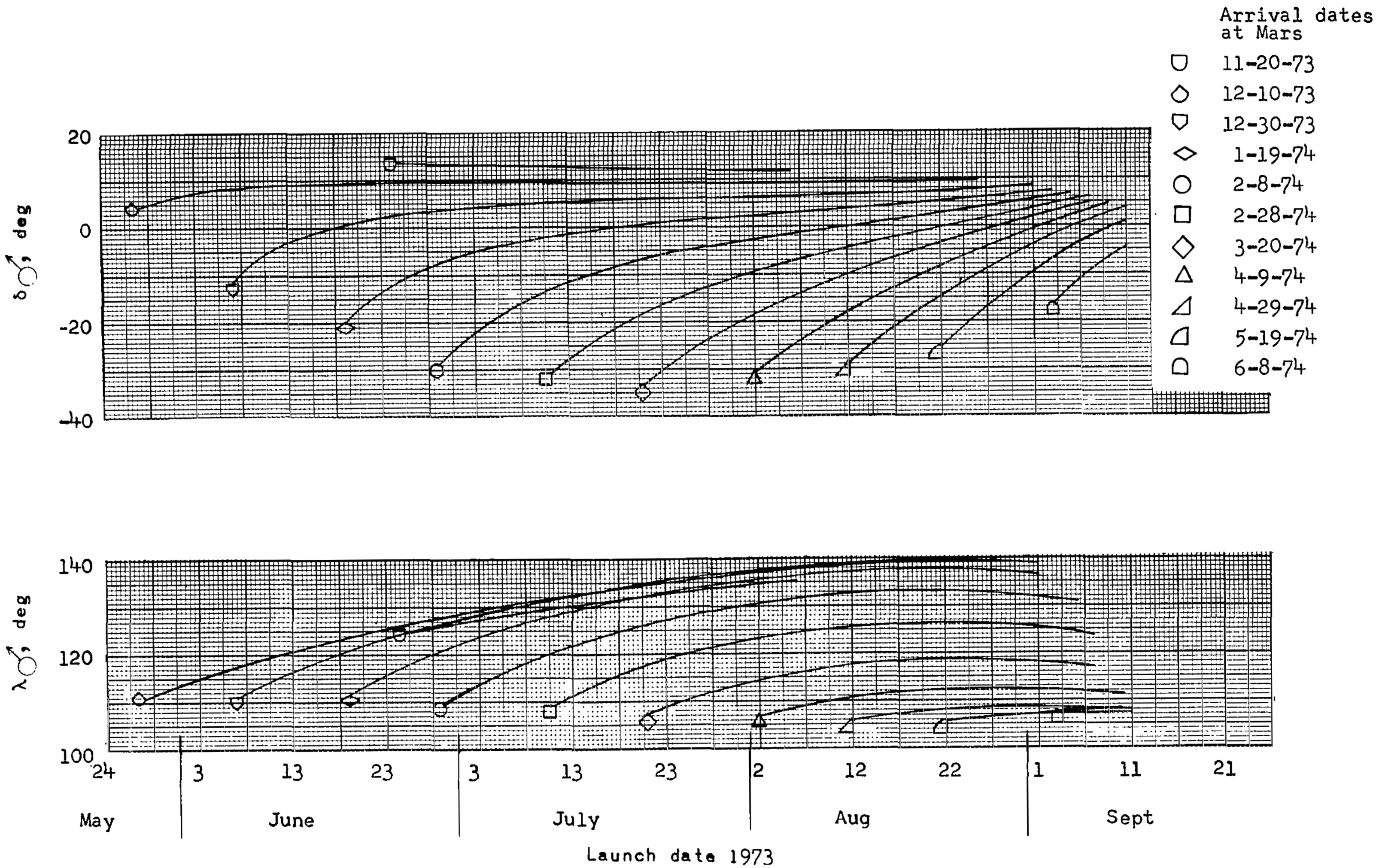

(c) Mars right ascension and declination of $\vec{S}$ as functions of launch date for several arrival dates.

Figure 3.- Concluded.

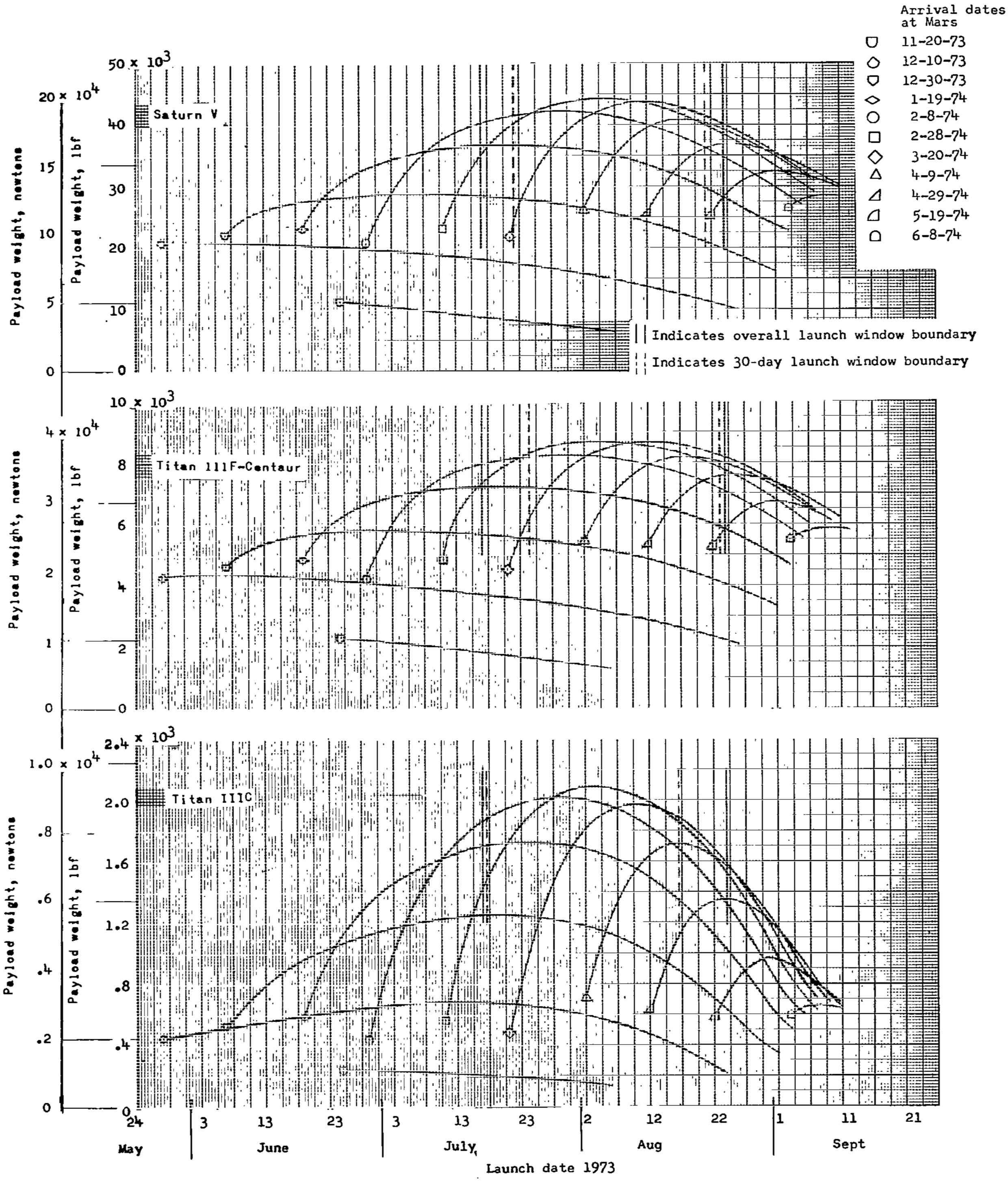

Figure 4.- Payload in Mars orbit as a function of launch date for three launch vehicles for 1973 type I opportunity.

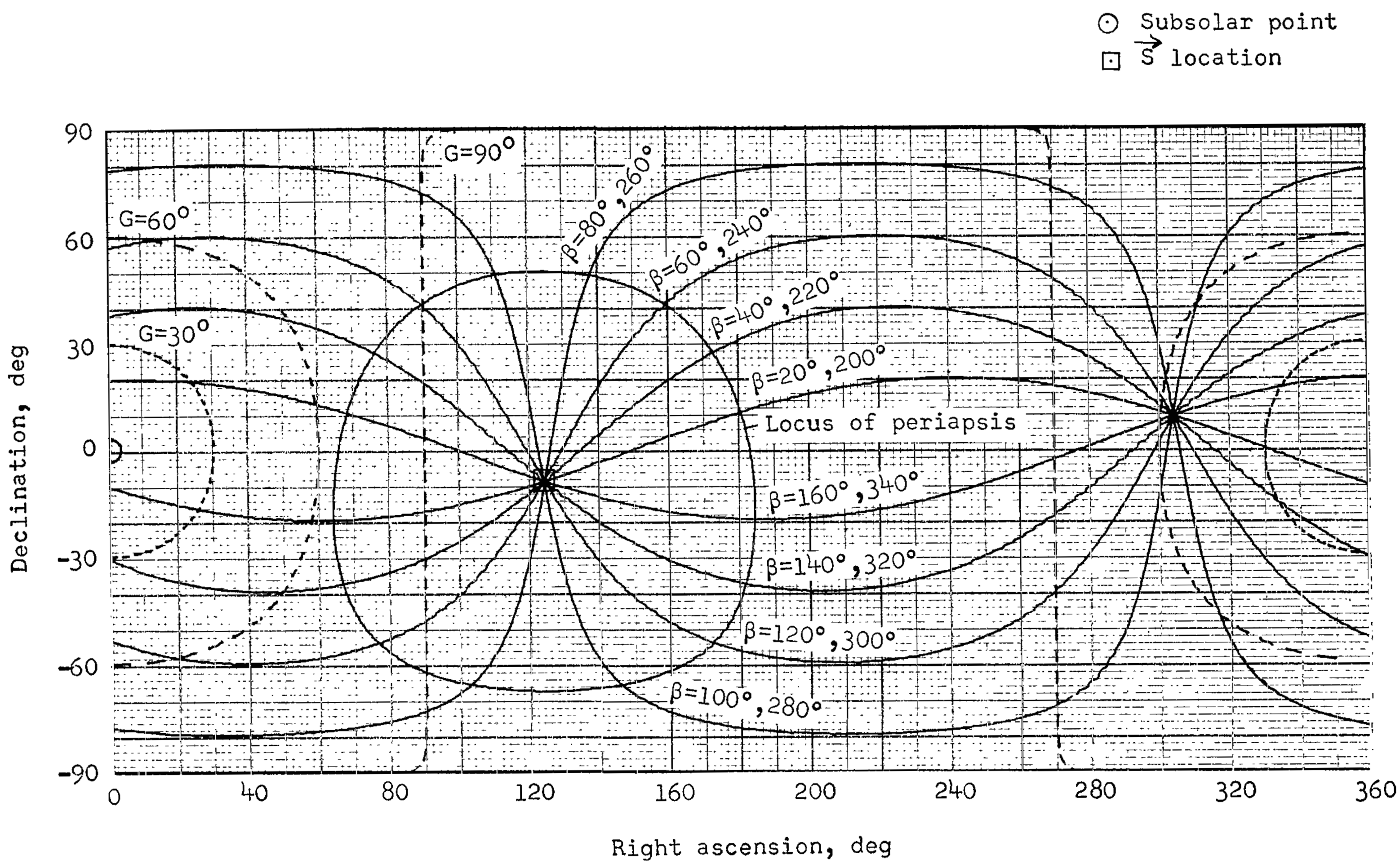

(a) July 17, 1973, launch and February 8, 1974, arrival.

Figure 5.- Relative orbit and sunlighting geometry for typical 1973 type I trajectories.

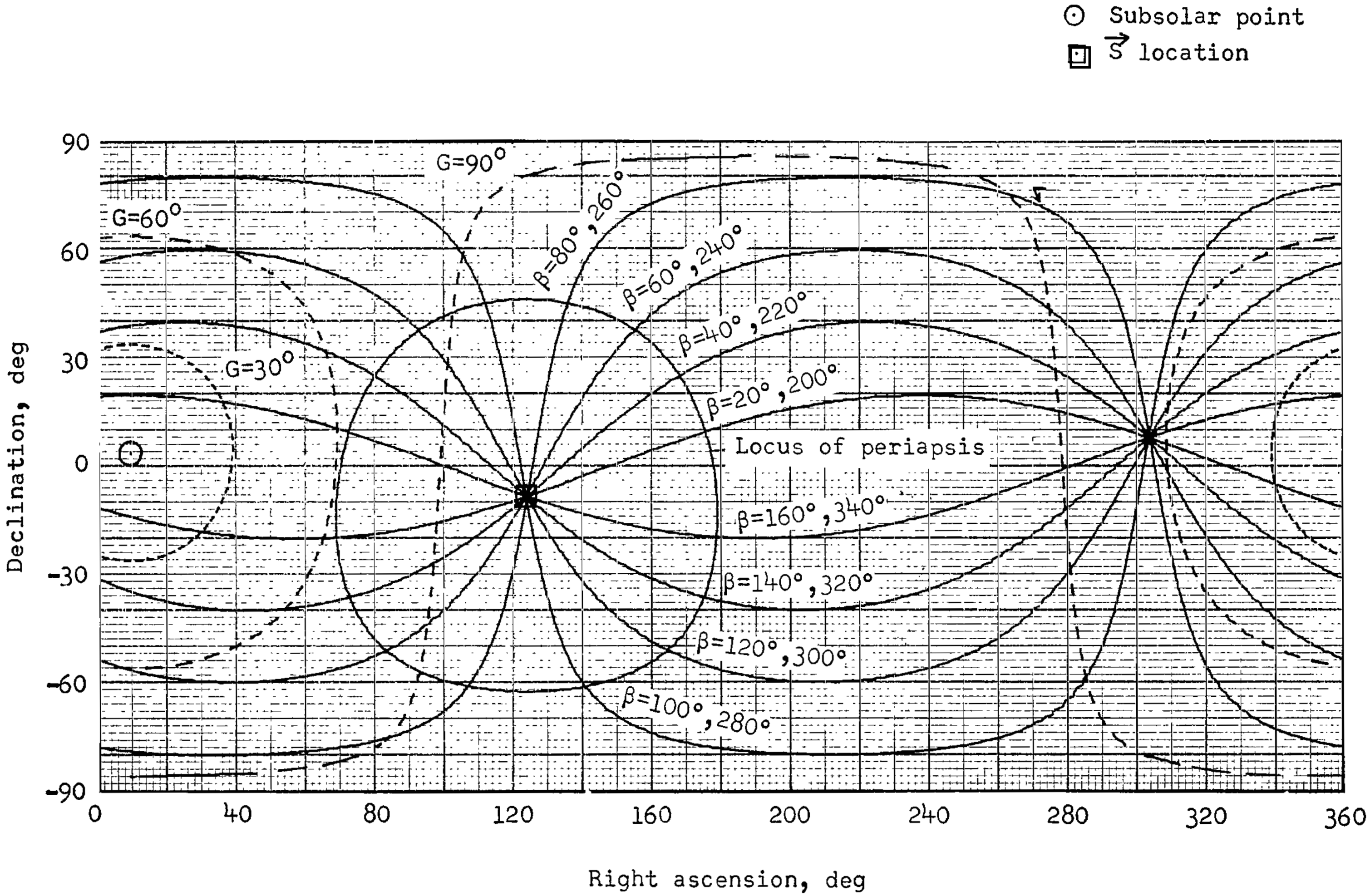

(b) August 4, 1973, launch and February 28, 1974, arrival.

Figure 5.- Continued.

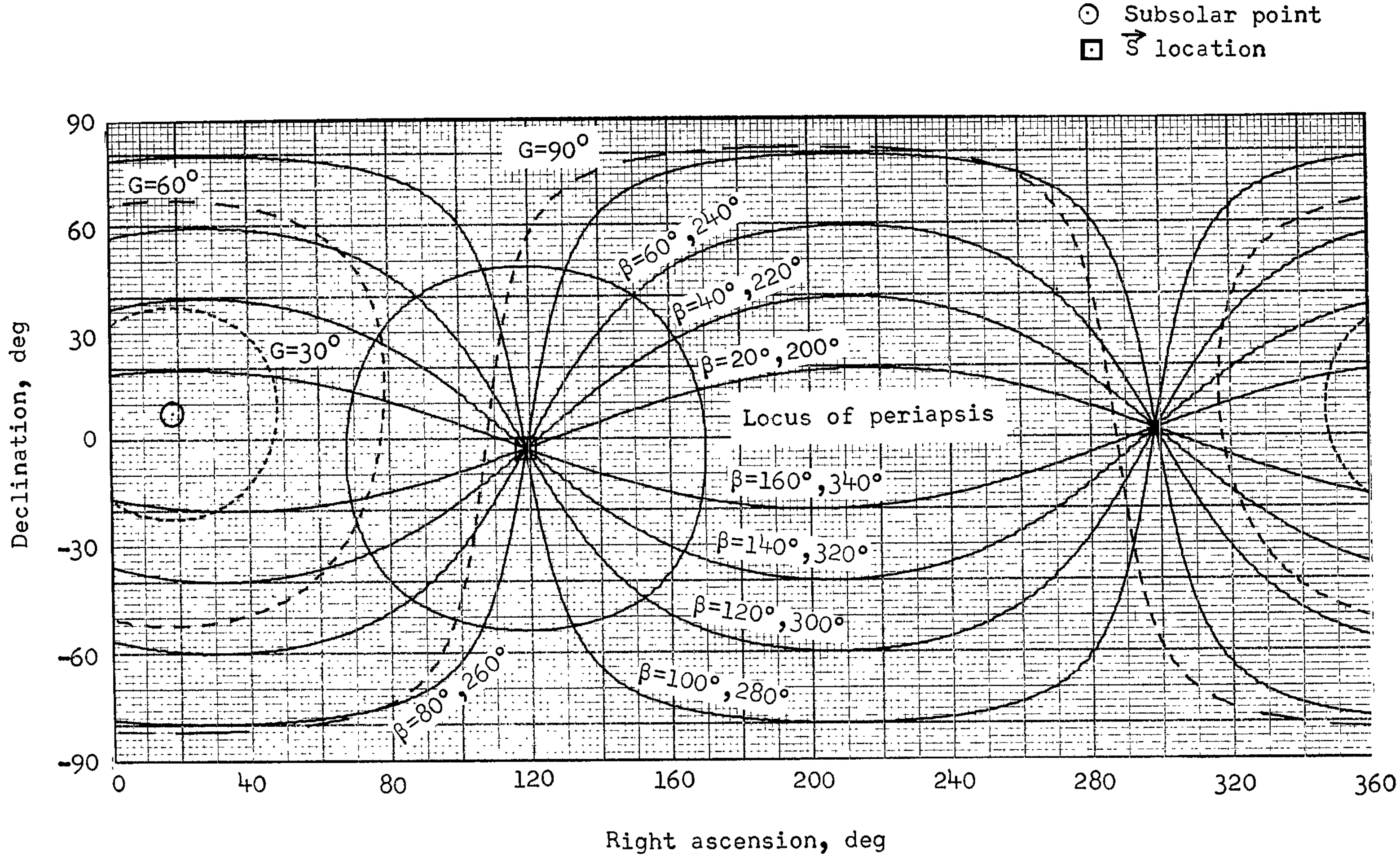

(c) August 24, 1973, launch and March 20, 1974, arrival.

Figure 5.- Concluded.

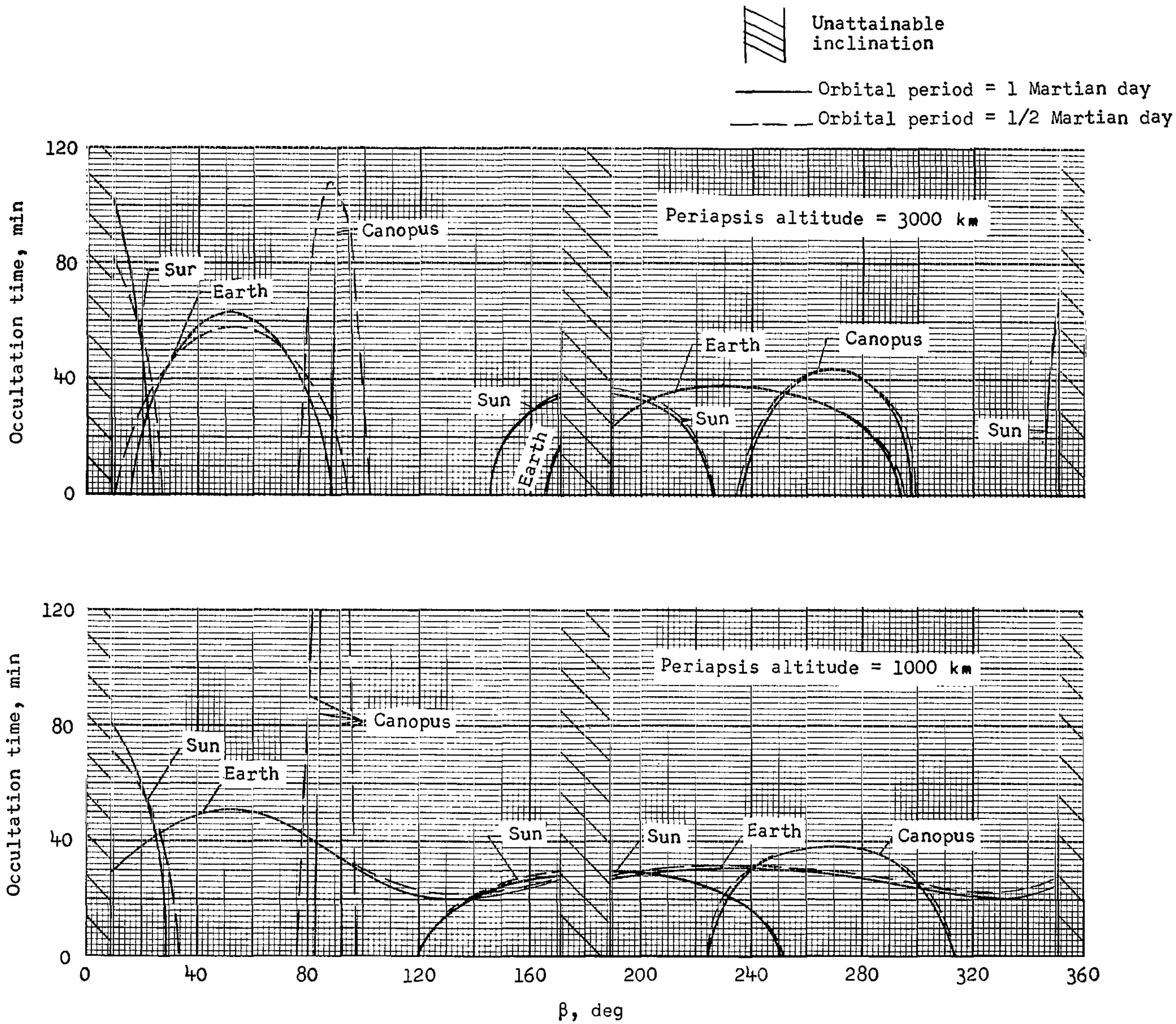

(a) July 17, 1973, launch and February 8, 1974, arrival.

Figure 6.- Occultation characteristics for Mars orbits resulting from typical 1973 type I trajectories.

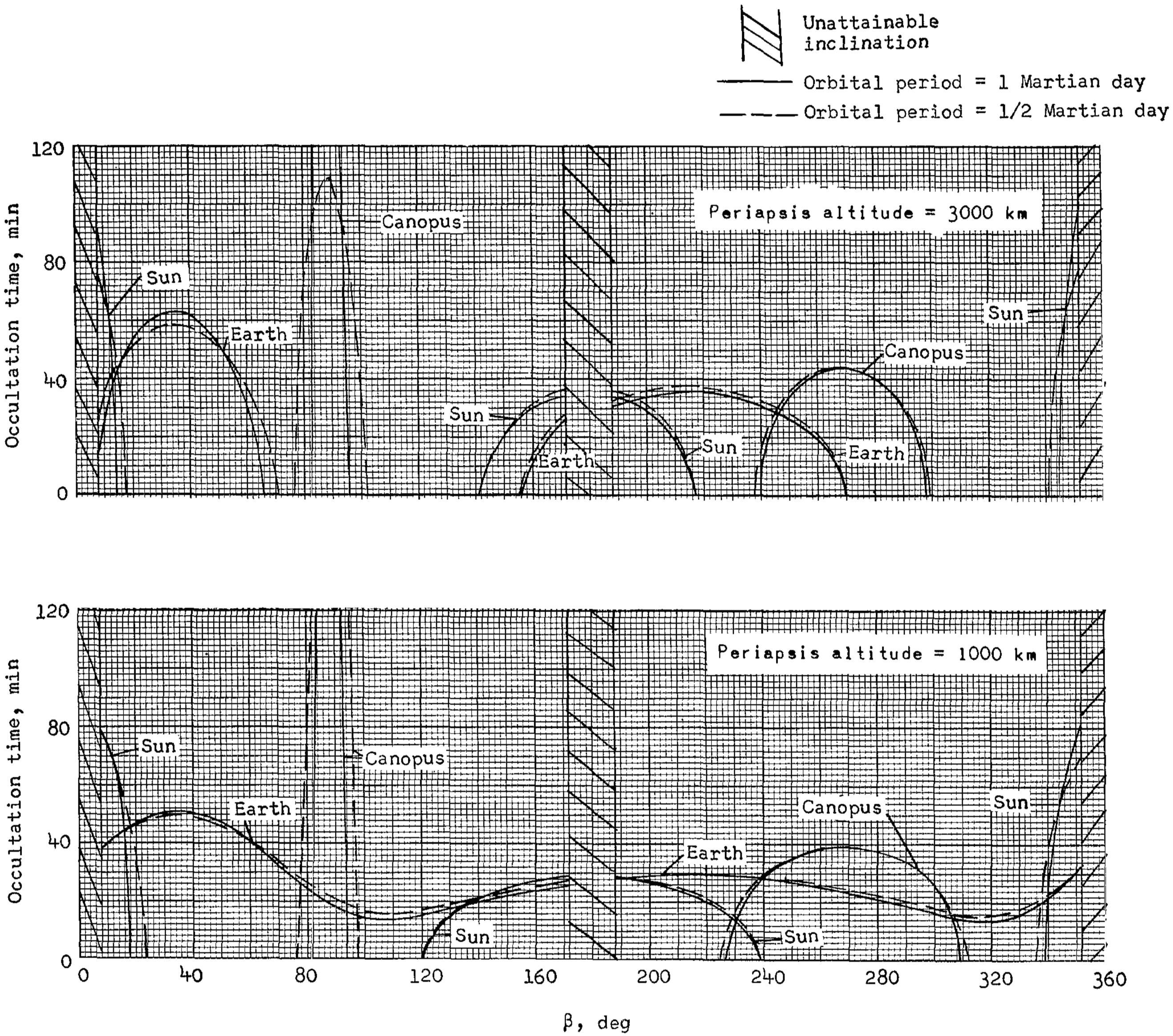

(b) August 4, 1973, launch and February 28, 1974, arrival.

Figure 6.- Continued.

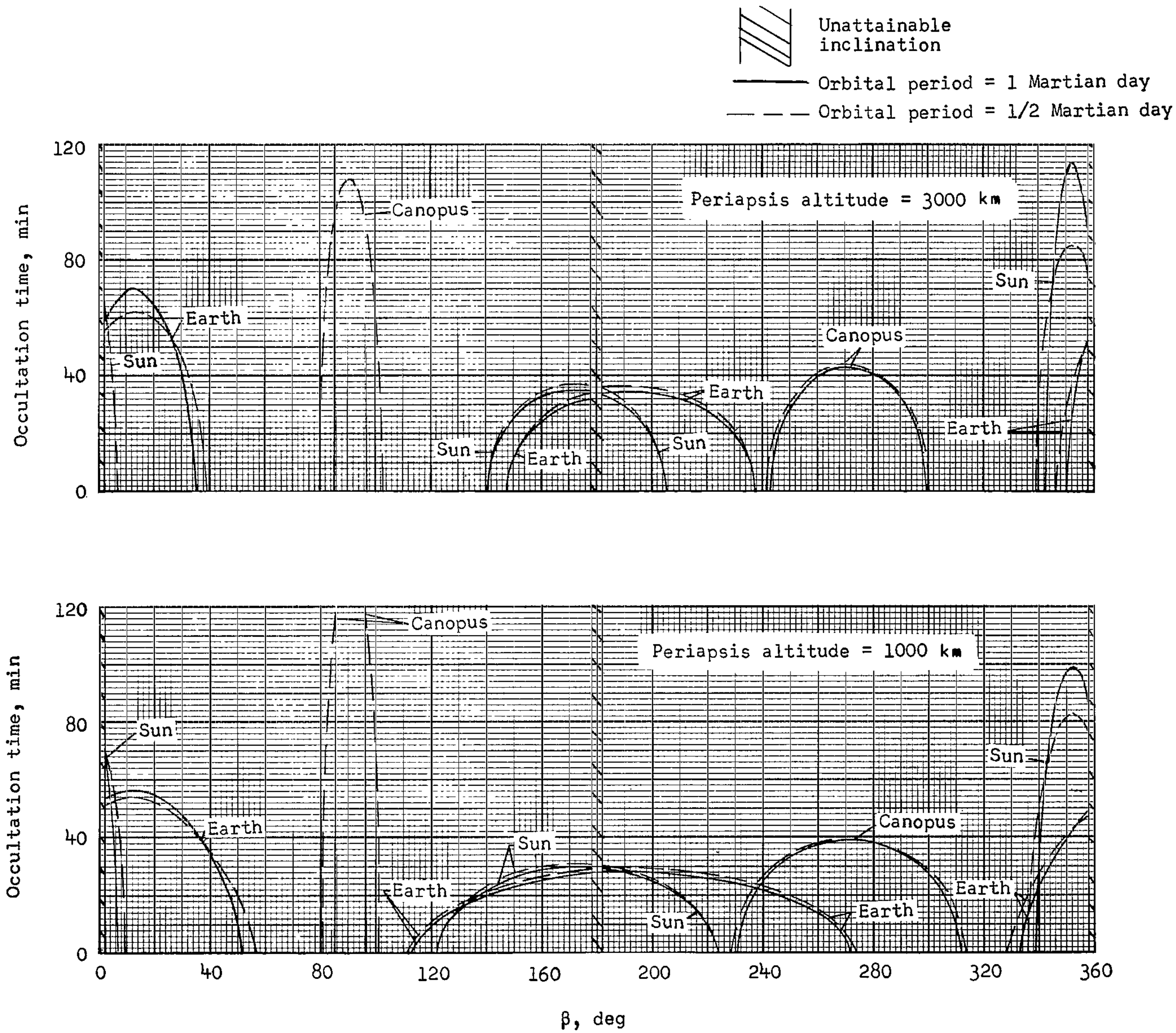

(c) August 24, 1973, launch and March 20, 1974, arrival.

Figure 6.- Concluded.

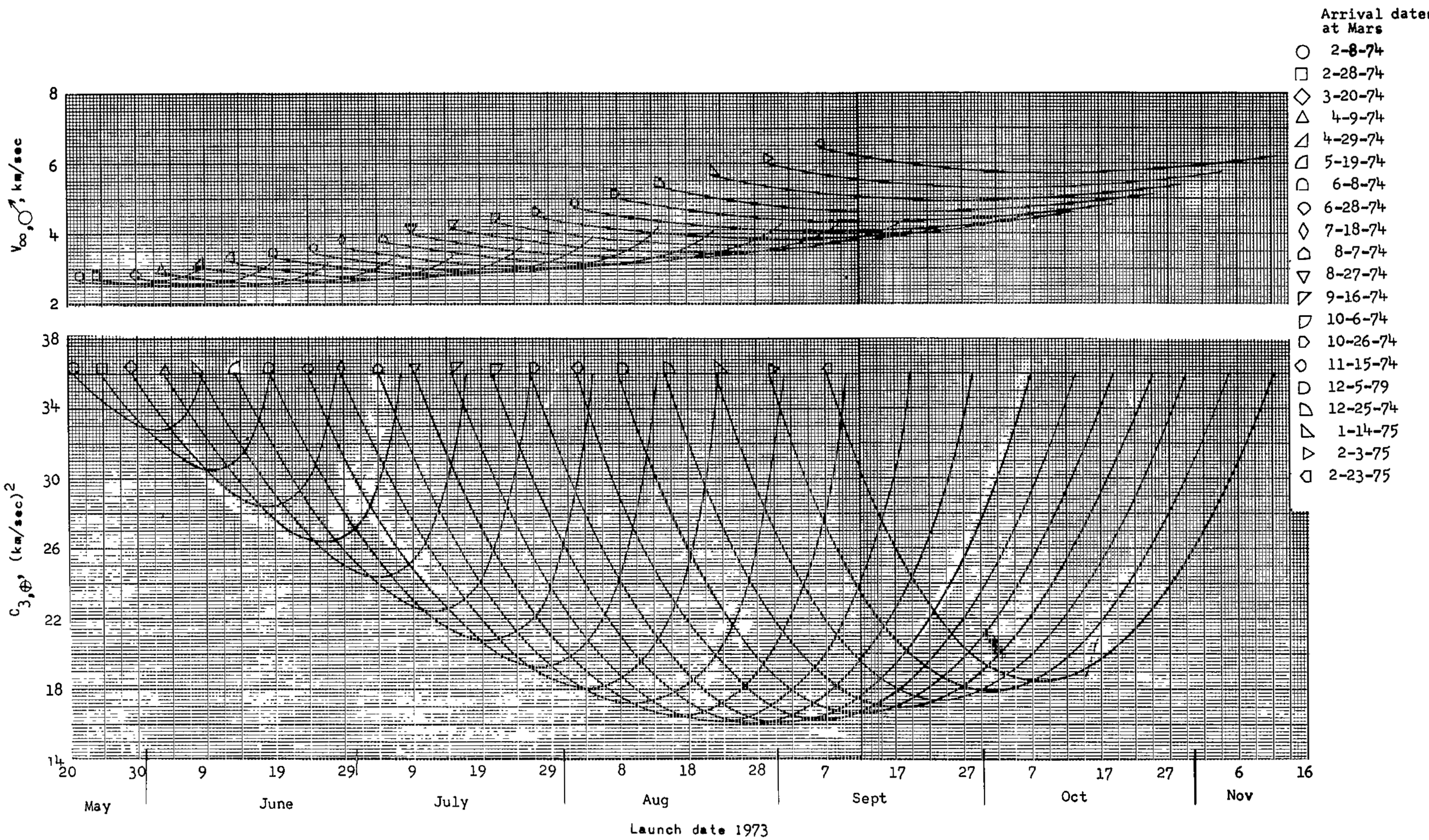

(a) Excess energy at Earth and hyperbolic excess velocity at Mars as functions of launch date for several arrival dates.

Figure 7.- Trajectory characteristics from Earth to Mars for 1973 type II opportunity.

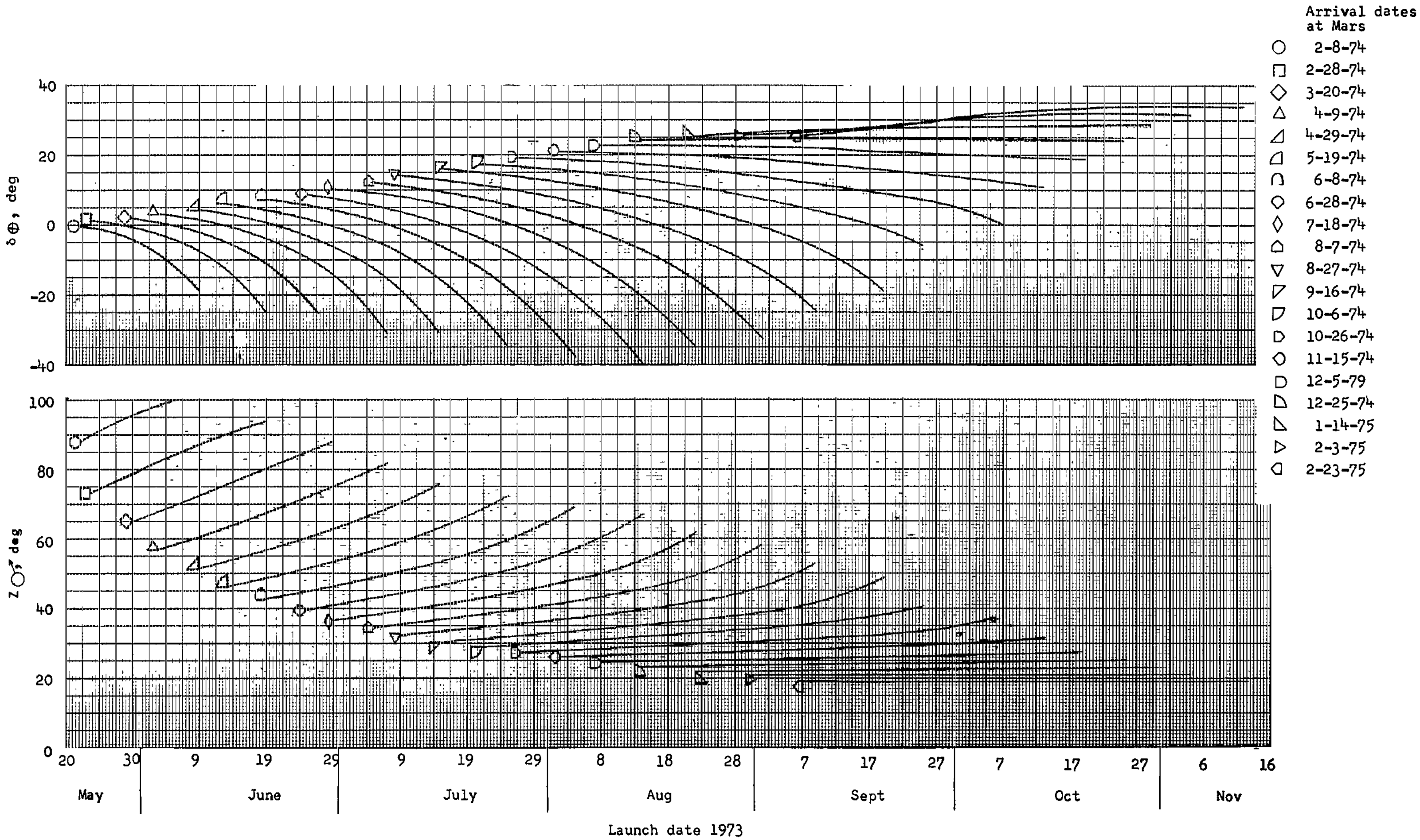

(b) Sun-$\vec{S}$ angle and declination of launch asymptote as functions of launch date for several arrival dates.

Figure 7.- Continued.

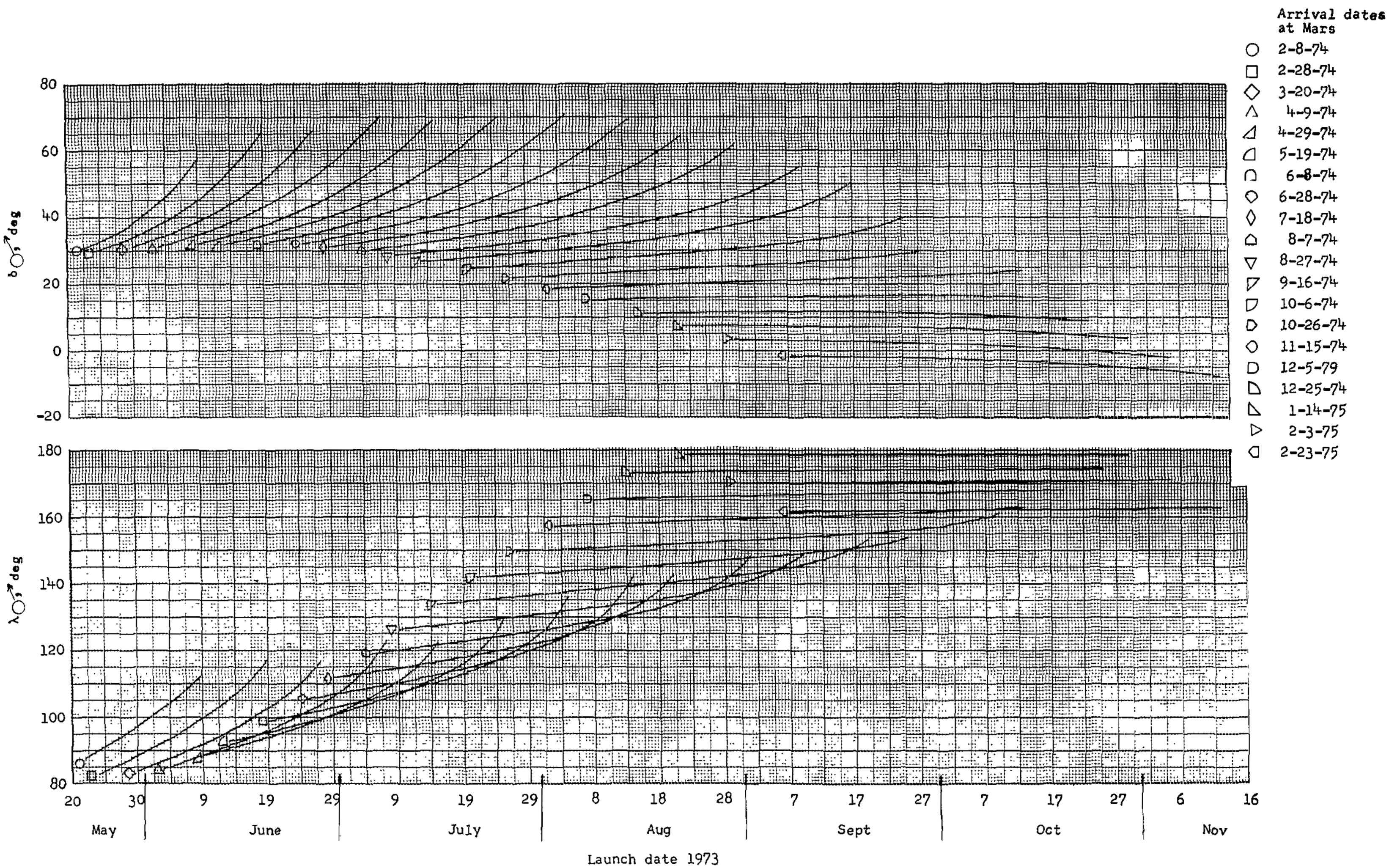

(c) Mars right ascension and declination of $\vec{S}$ as functions of launch date for several arrival dates.

Figure 7.- Concluded.

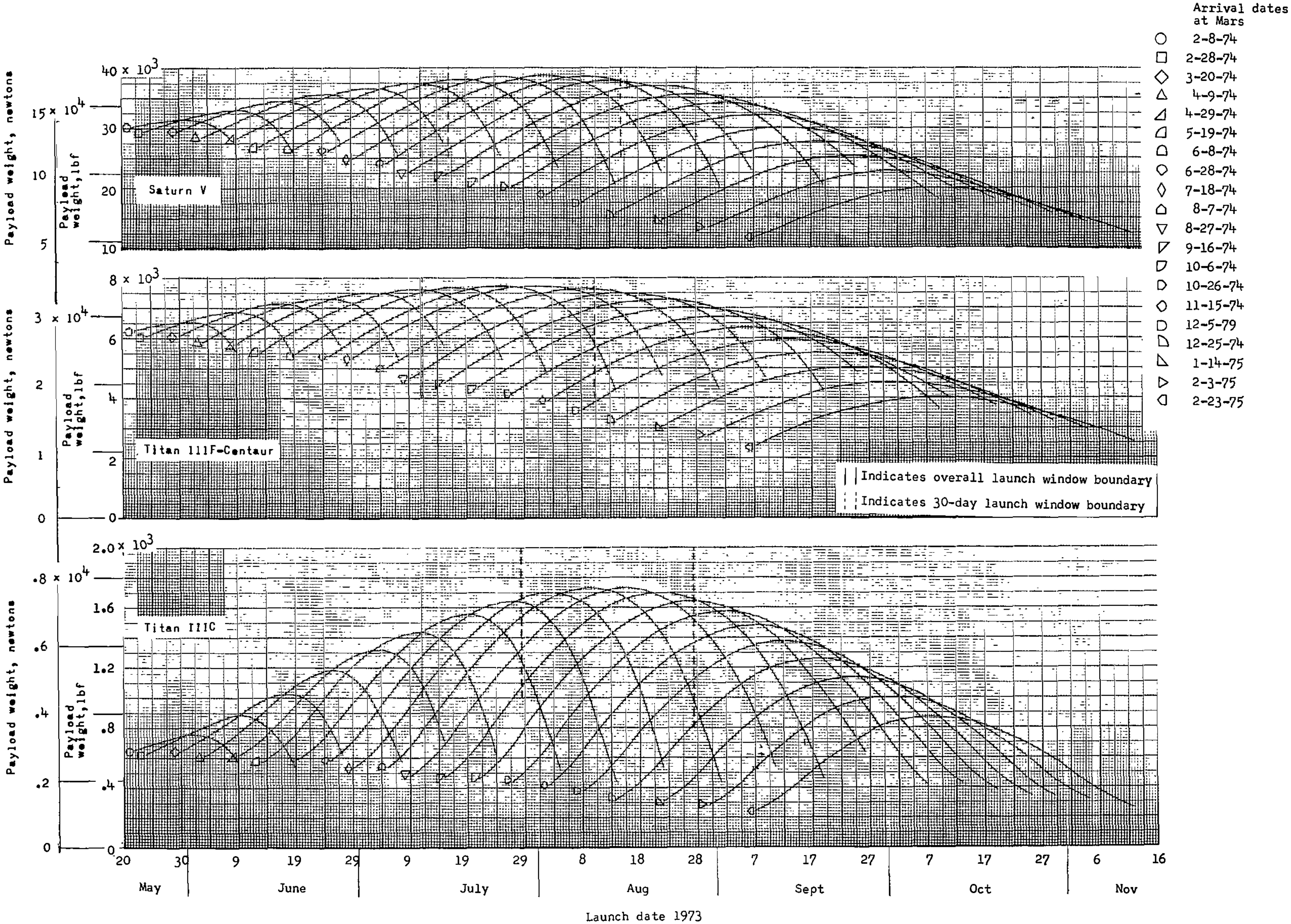

Figure 8.- Payload in Mars orbit as a function of launch date for three launch vehicles for 1973 type II opportunity.

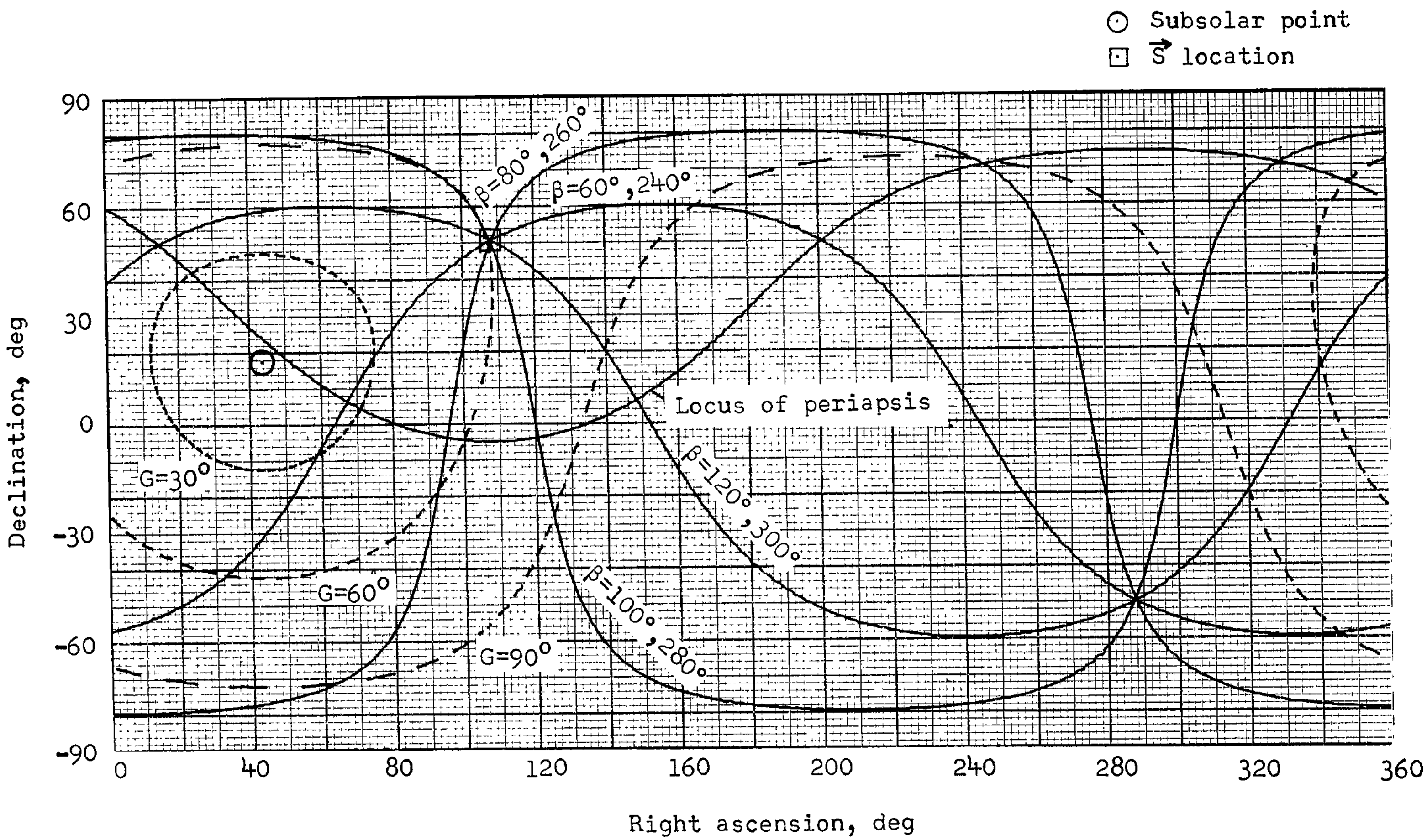

(a) July 11, 1973, launch and May 19, 1974, arrival.

Figure 9.- Relative orbit and sunlighting geometry for typical 1973 type II trajectories.

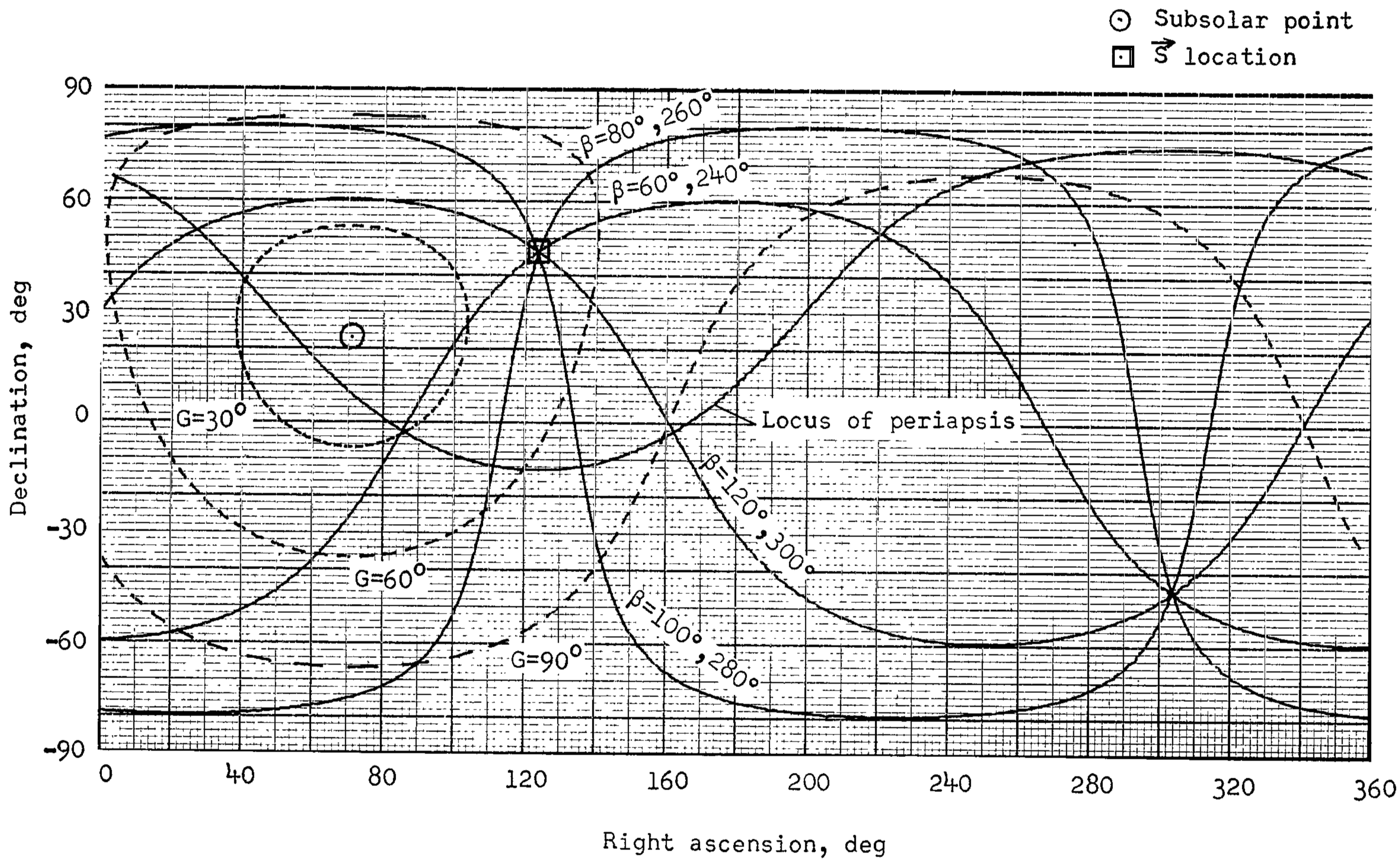

(b) August 4, 1973, launch and July 18, 1974, arrival.

Figure 9.- Continued.

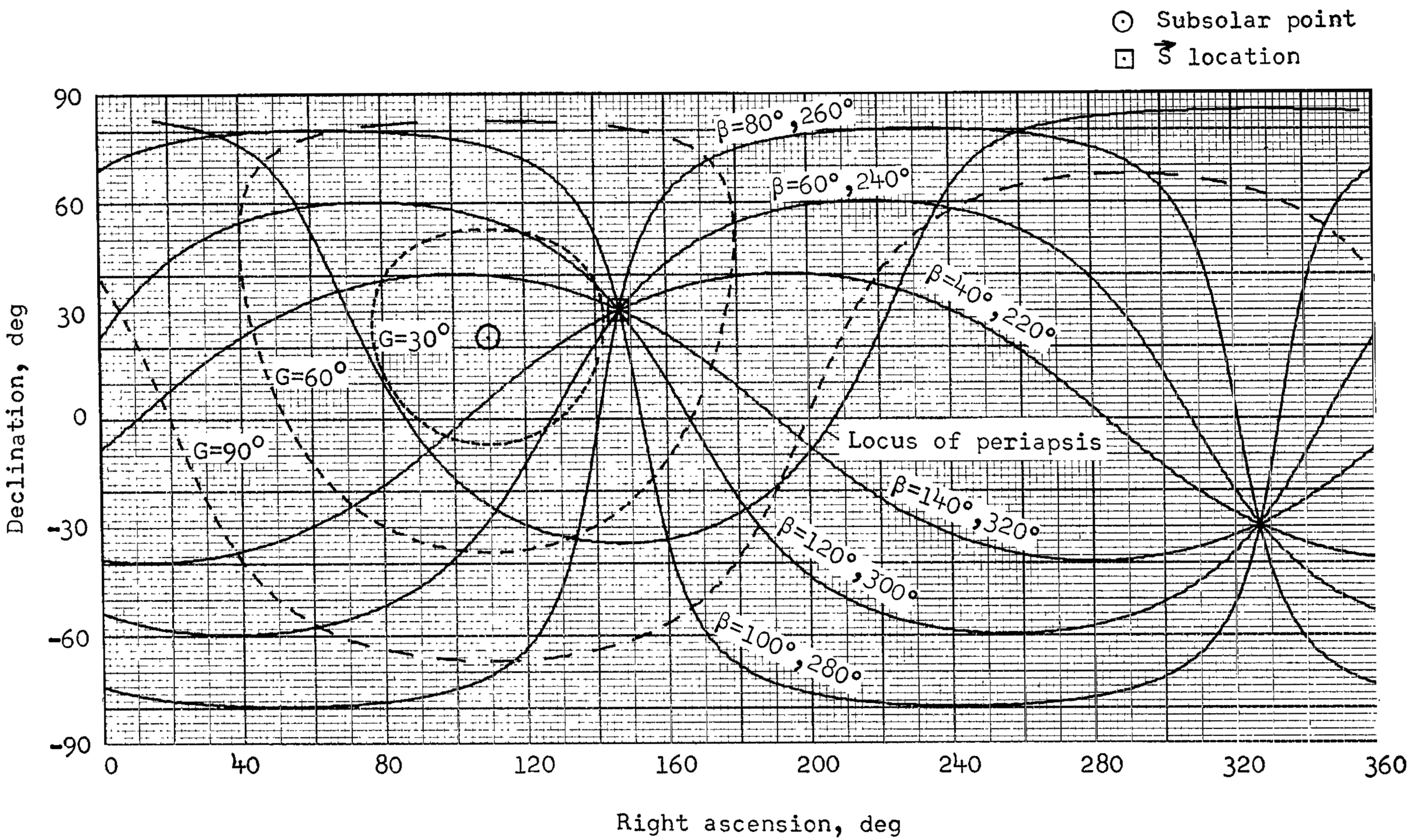

(c) August 28, 1973, launch and October 6, 1974, arrival.

Figure 9.- Concluded.

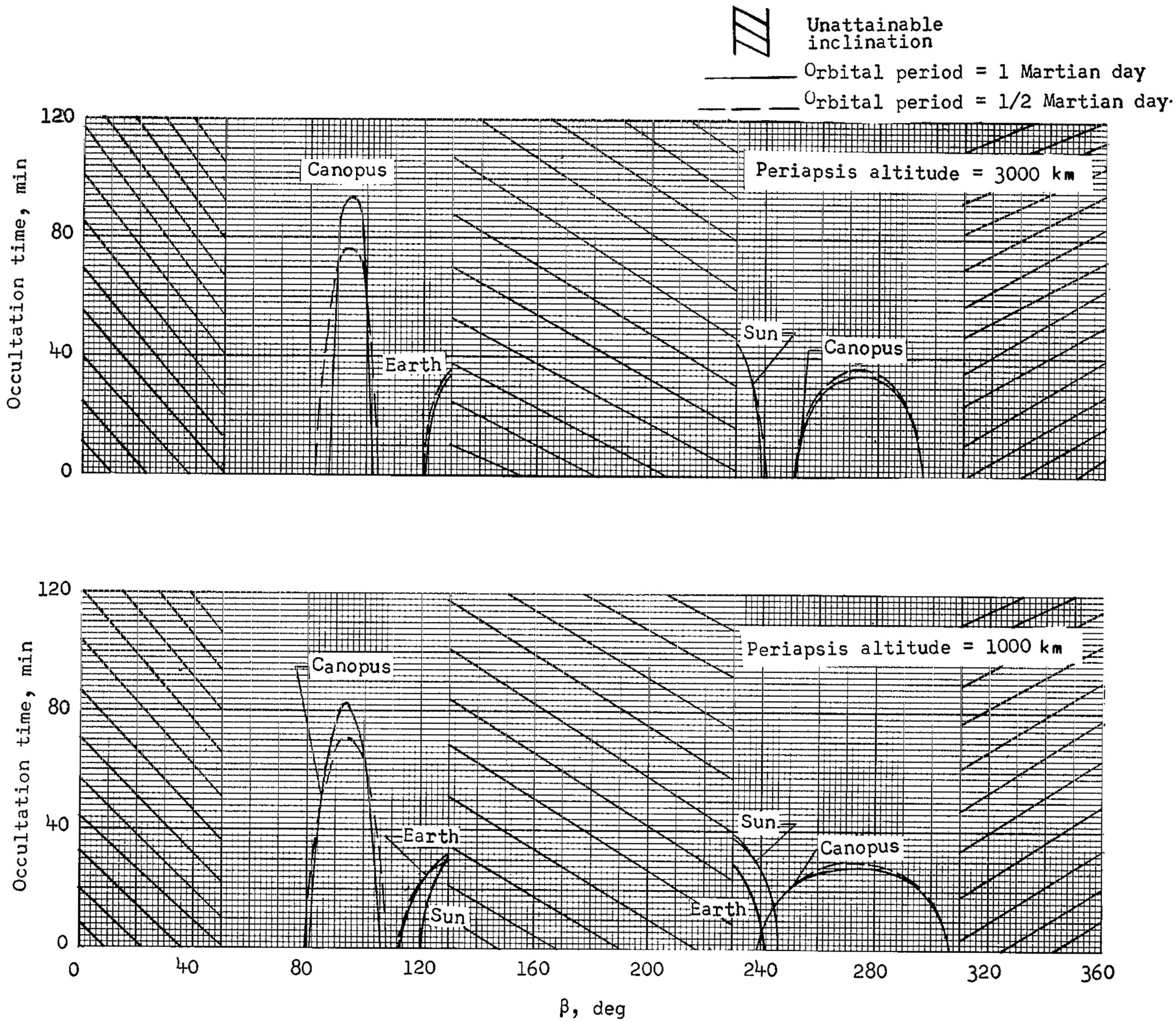

(a) July 11, 1973, launch and May 19, 1974, arrival.

Figure 10.- Occultation characteristics for Mars orbits resulting from typical 1973 type II trajectories.

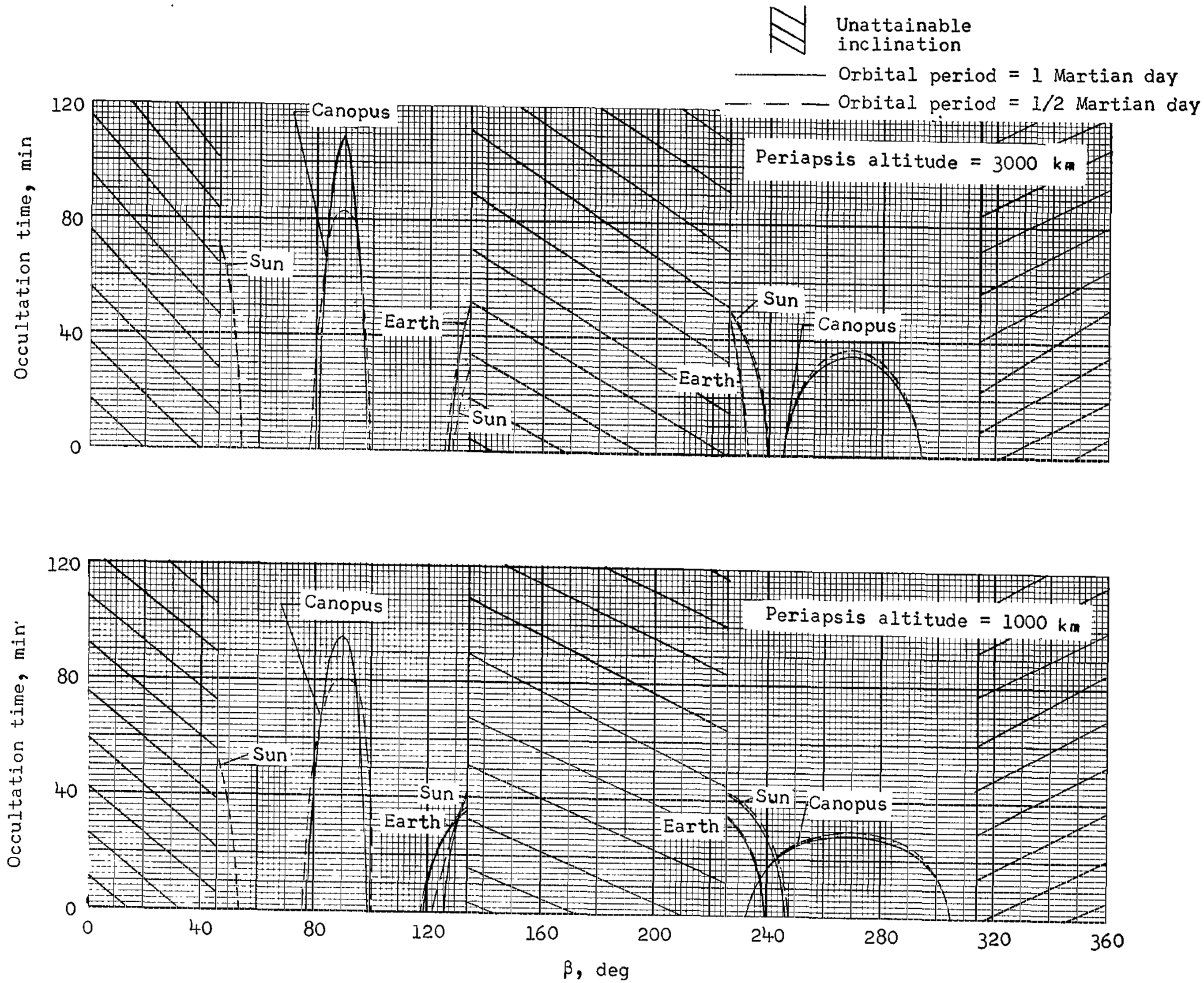

(b) August 4, 1973, launch and July 18, 1974, arrival.

Figure 10.- Continued.

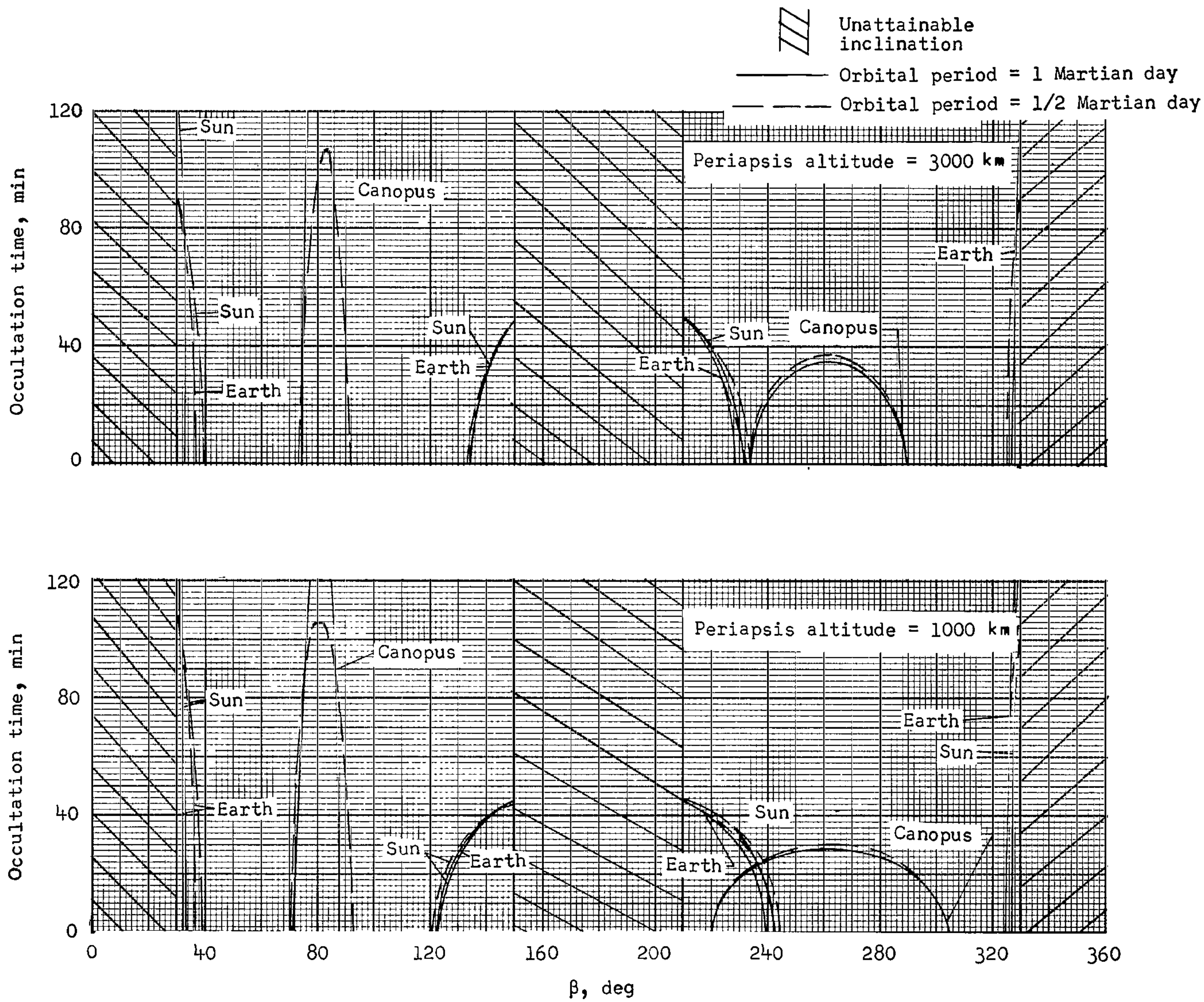

(c) August 28, 1973, launch and October 6, 1974, arrival.

Figure 10.- Concluded.

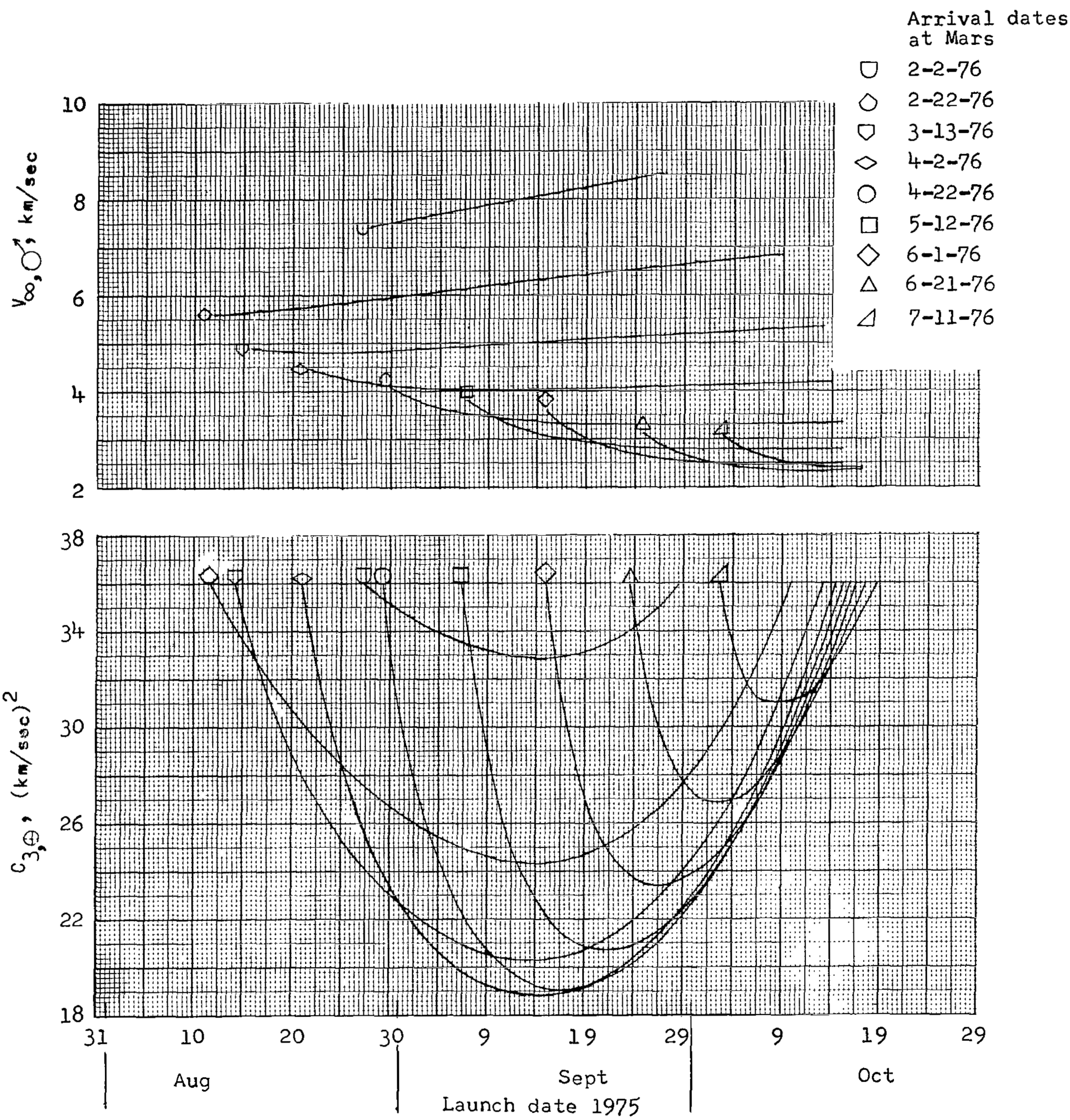

(a) Excess energy at Earth and hyperbolic excess velocity at Mars as functions of launch date for several arrival dates.

Figure 11.- Trajectory characteristics from Earth to Mars for 1975 type I opportunity.

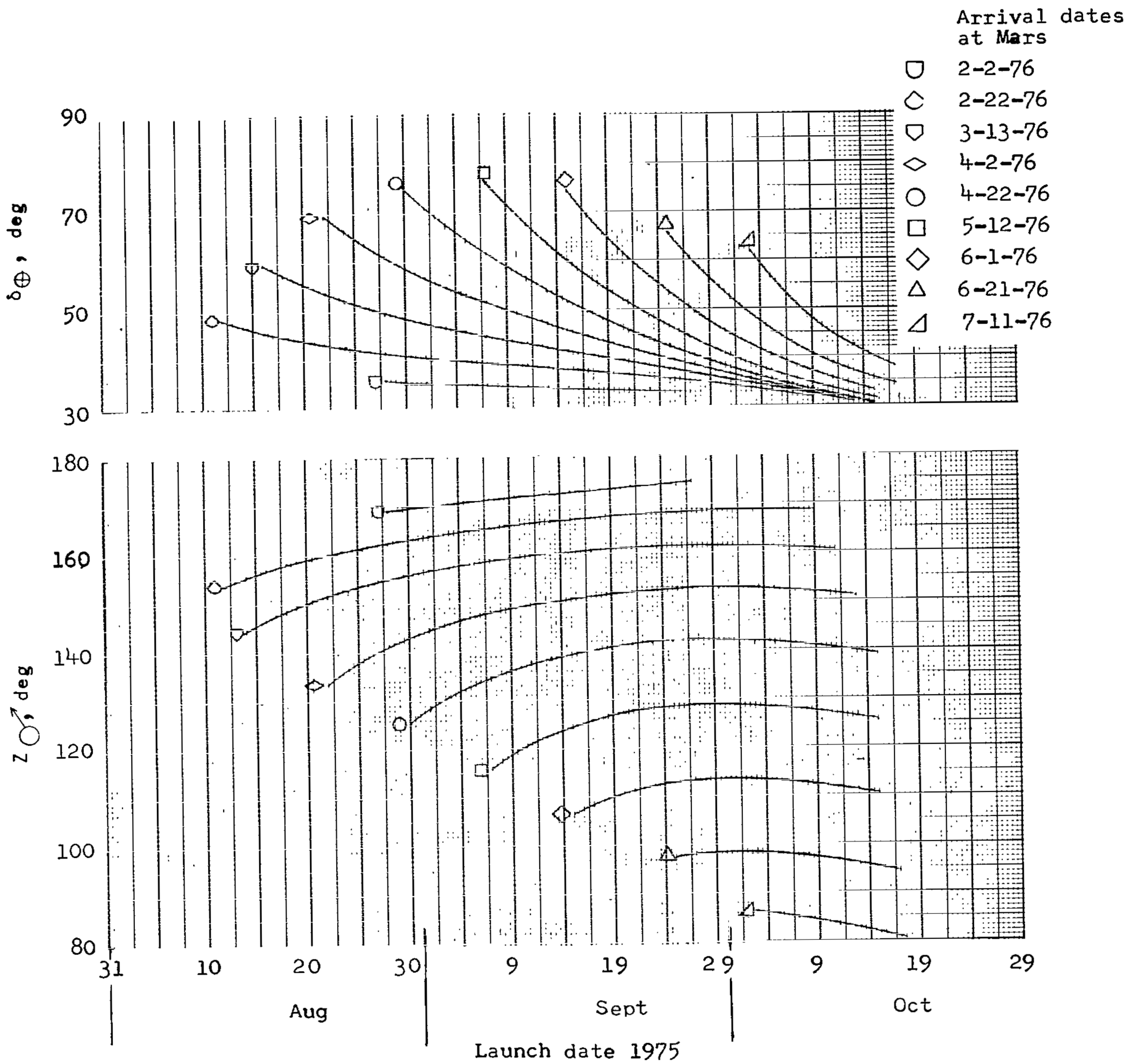

(b) Sun-$\vec{S}$ angle and declination of launch asymptote as functions of launch date for several arrival dates.

Figure 11.- Continued.

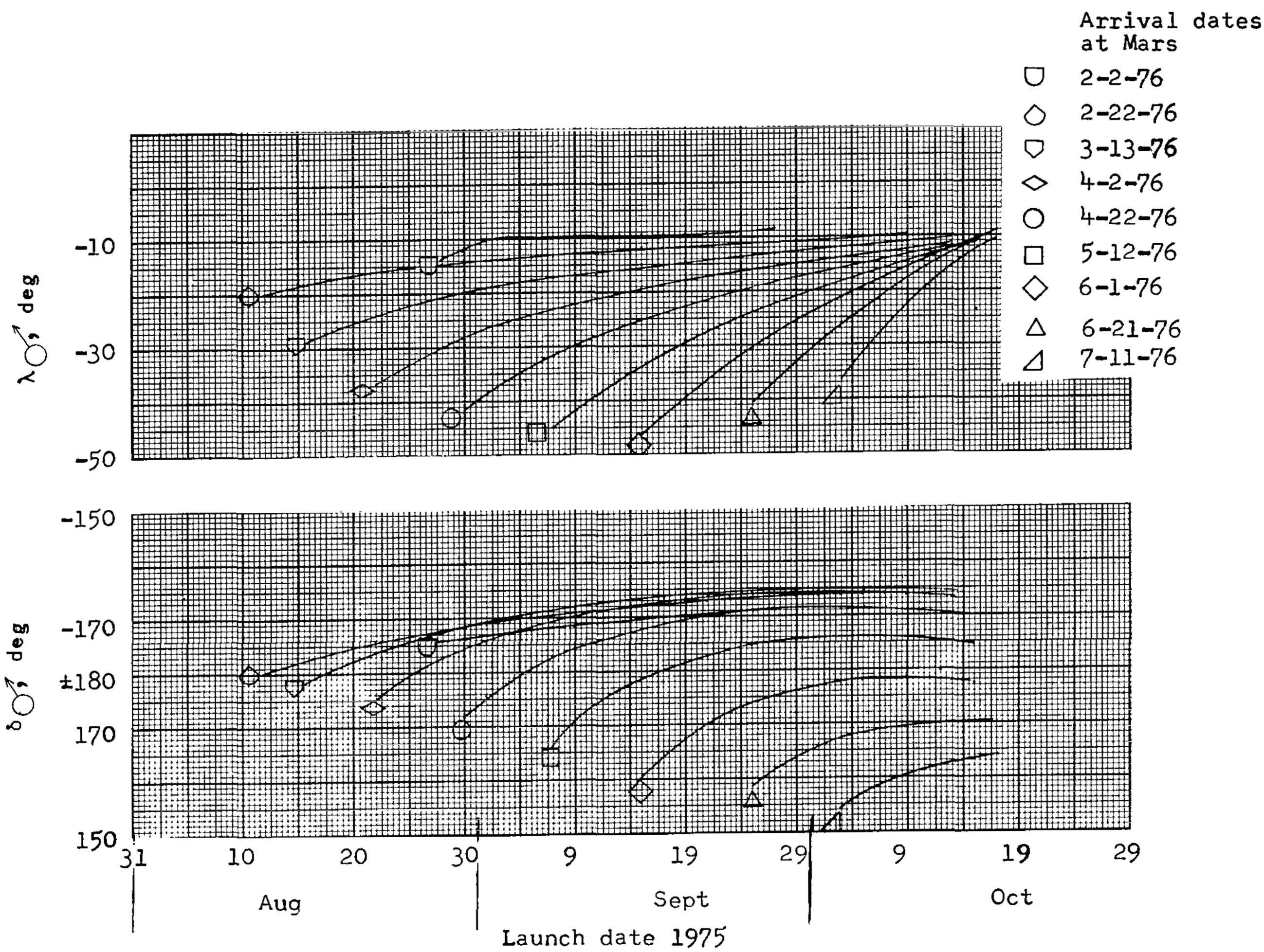

(c) Mars right ascension and declination of $\vec{S}$ as functions of launch date for several arrival dates.

Figure 11.- Concluded.

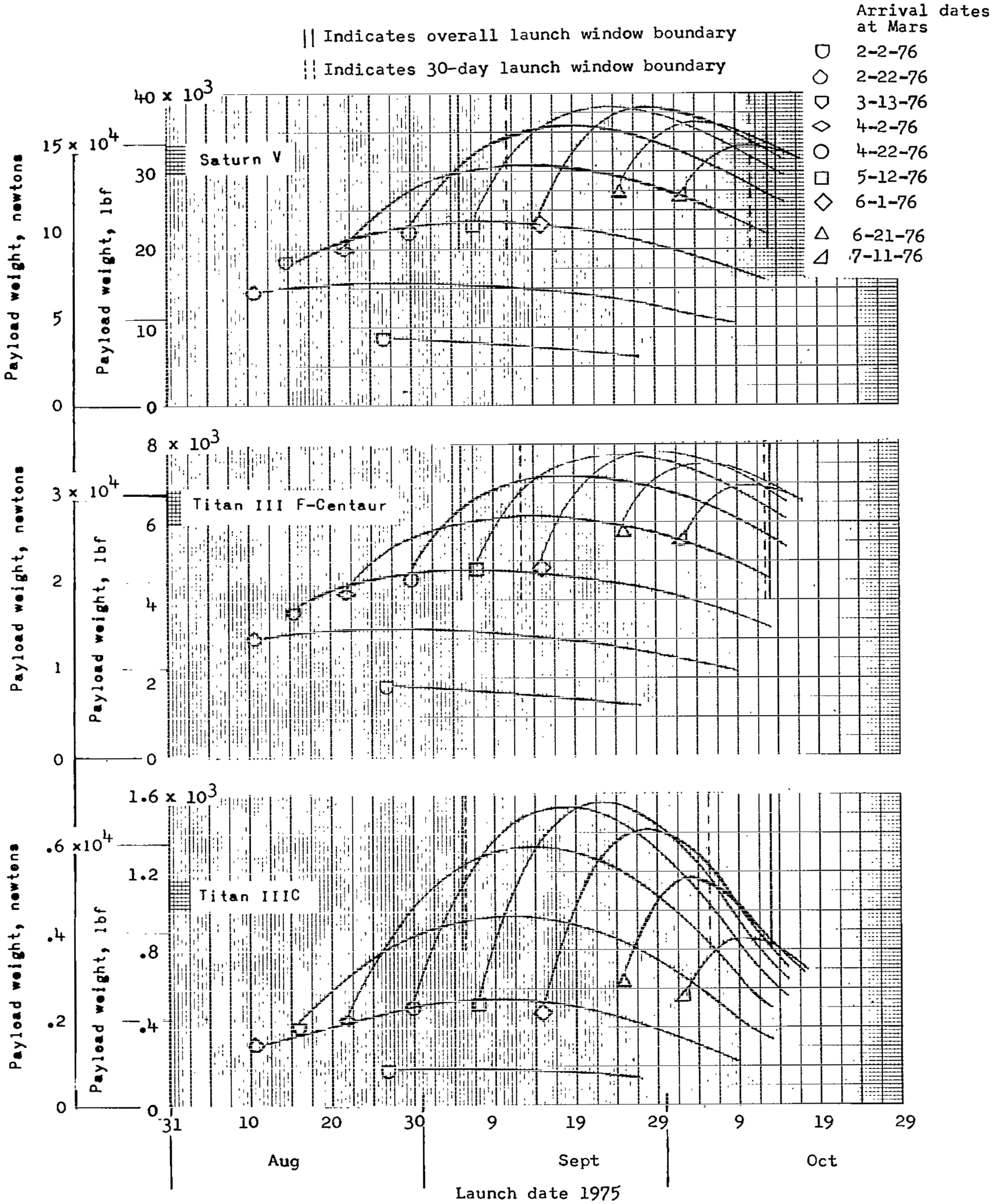

Figure 12.- Payload in Mars orbit as functions of launch date for three launch vehicles for 1975 type I opportunity.

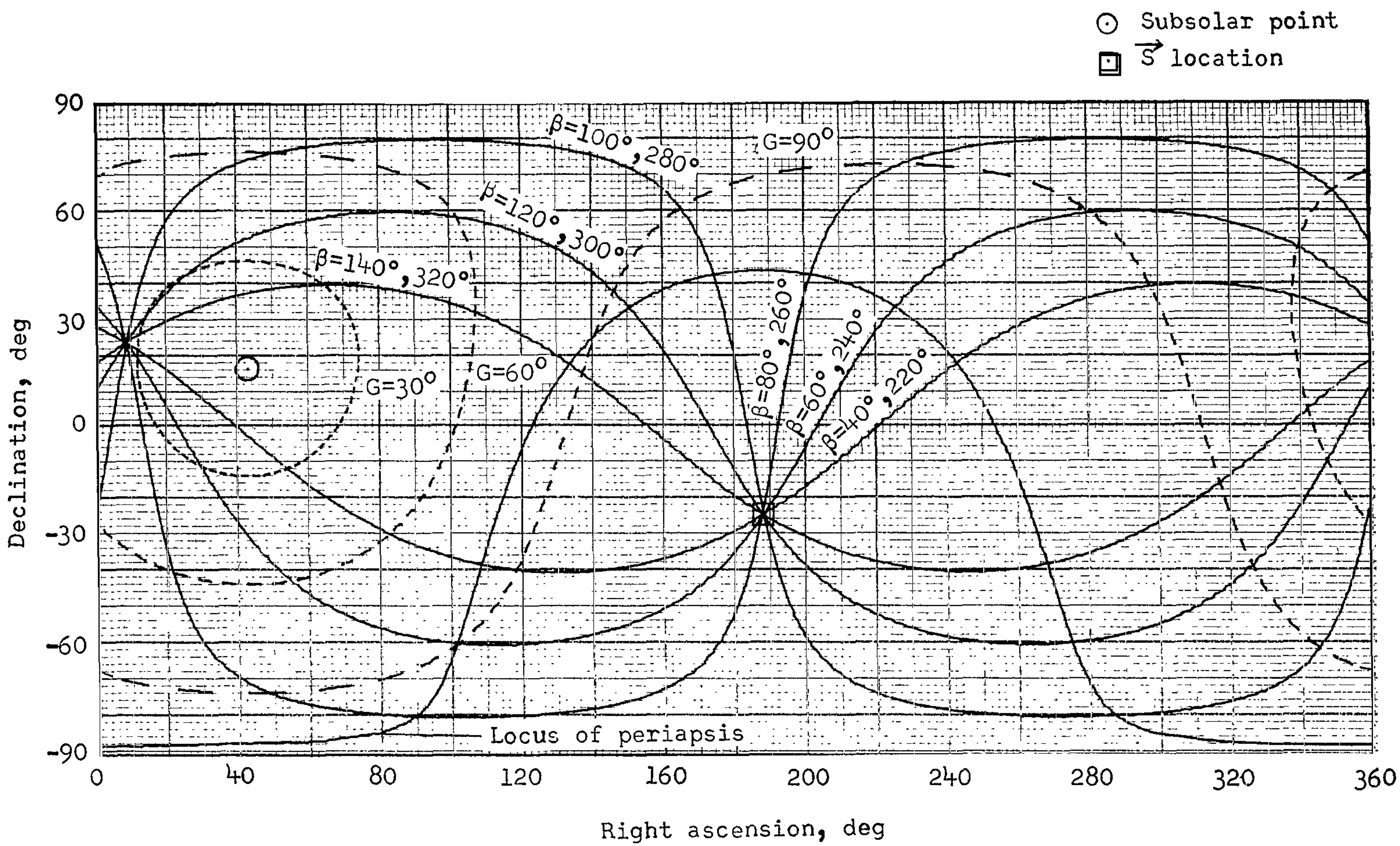

(a) September 5, 1975, launch and April 2, 1976, arrival.

Figure 13.- Relative orbit and sunlighting geometry for typical 1975 type I trajectories.

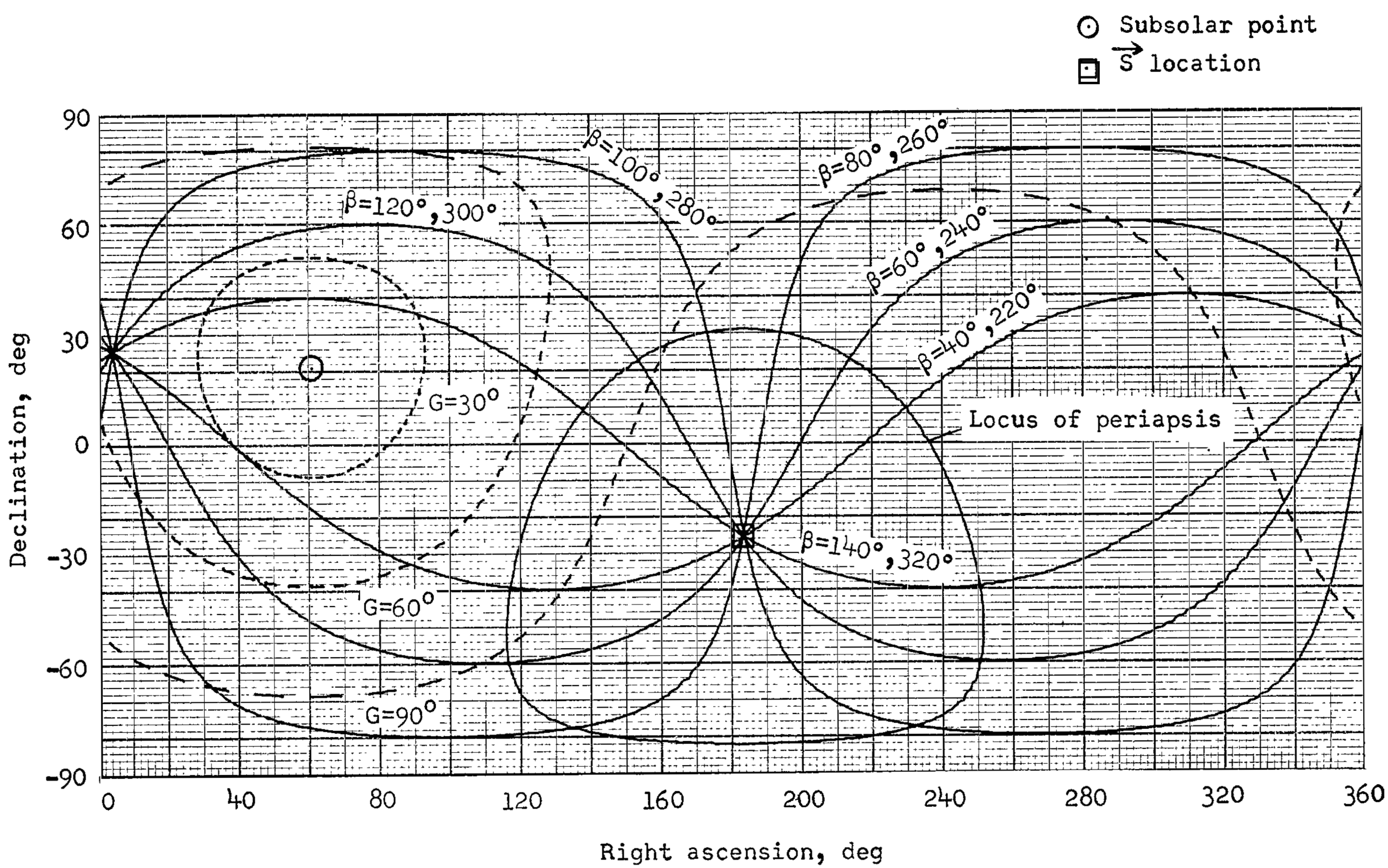

(b) September 23, 1975, launch and May 12, 1976, arrival.

Figure 13.- Continued.

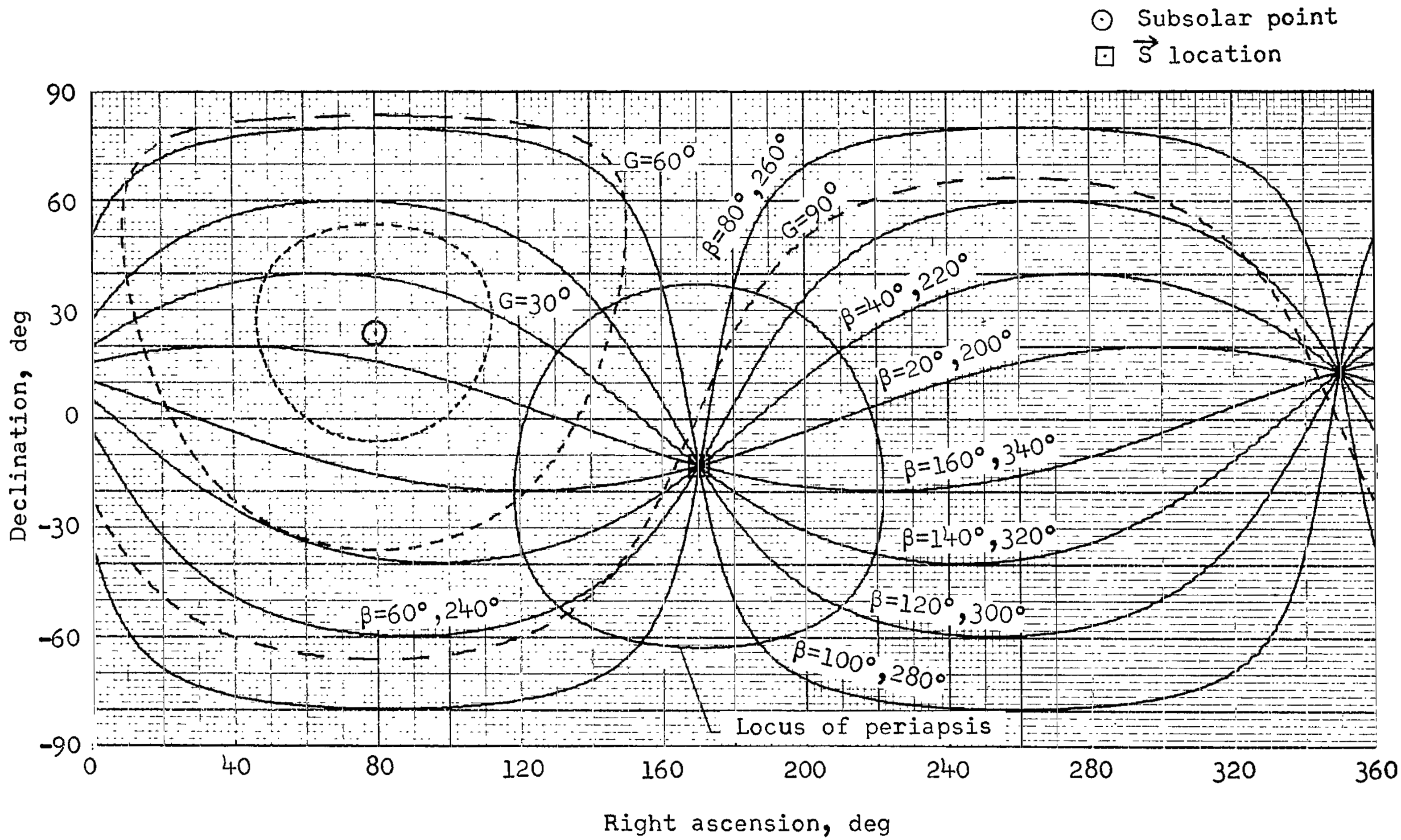

(c) October 13, 1975, launch and June 21, 1976, arrival.

Figure 13.- Concluded.

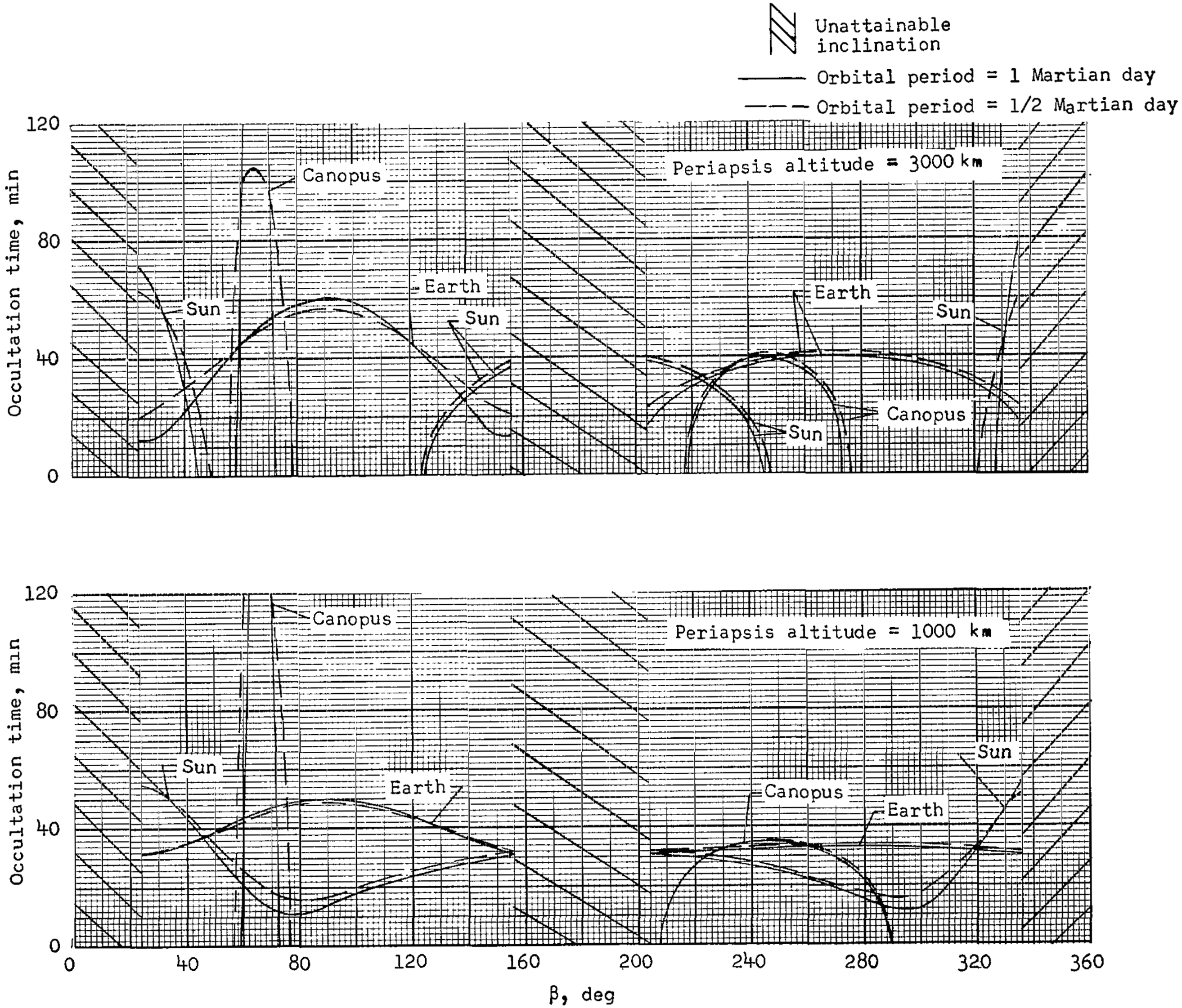

(a) September 5, 1975, launch and April 2, 1976, arrival.

Figure 14.- Occultation characteristics for Mars orbits resulting from typical 1975 type I trajectories.

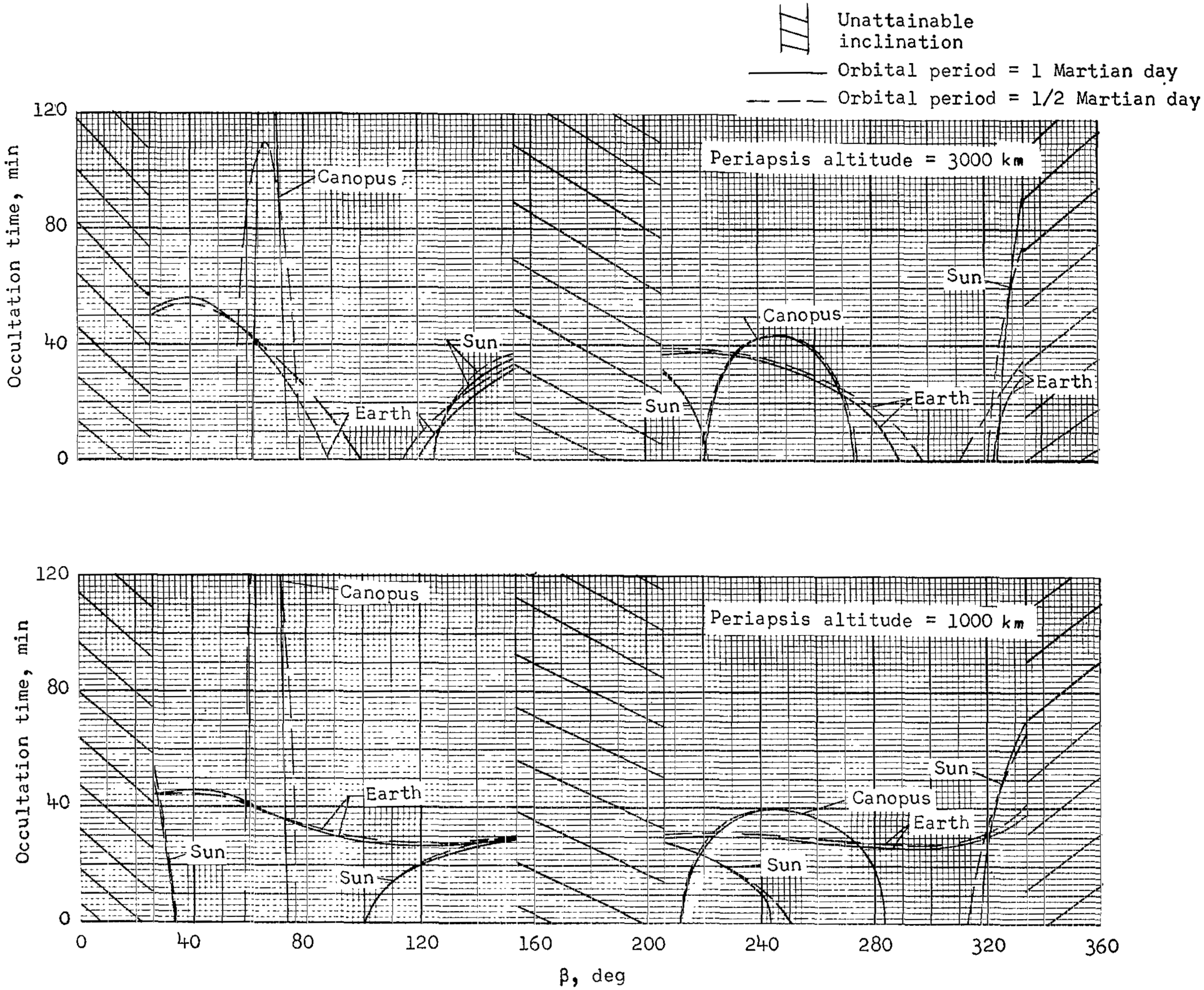

(b) September 23, 1975, launch and May 12, 1976, arrival.

Figure 14.- Continued.

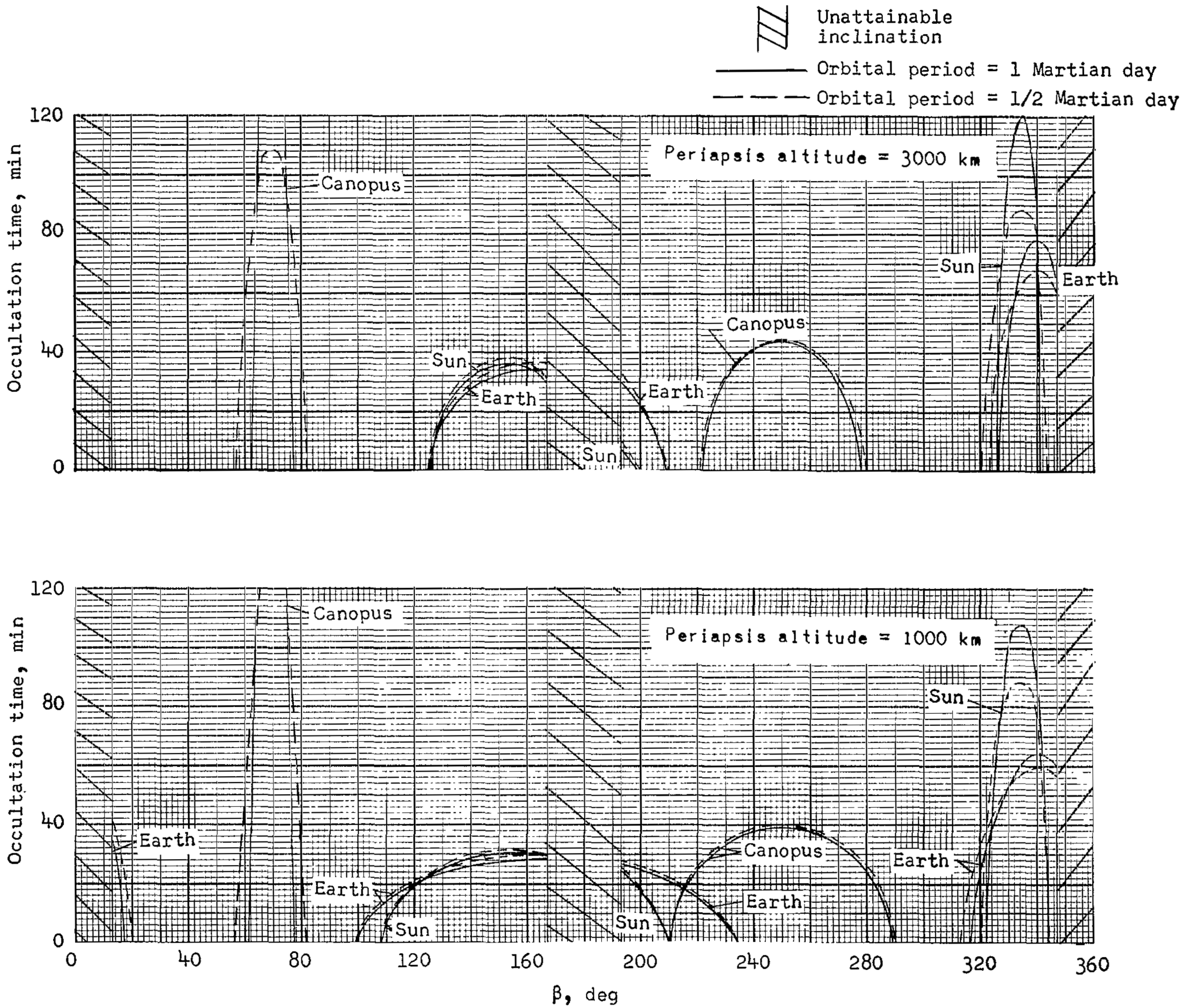

(c) October 13, 1975, launch and June 21, 1976, arrival.

Figure 14.- Concluded.

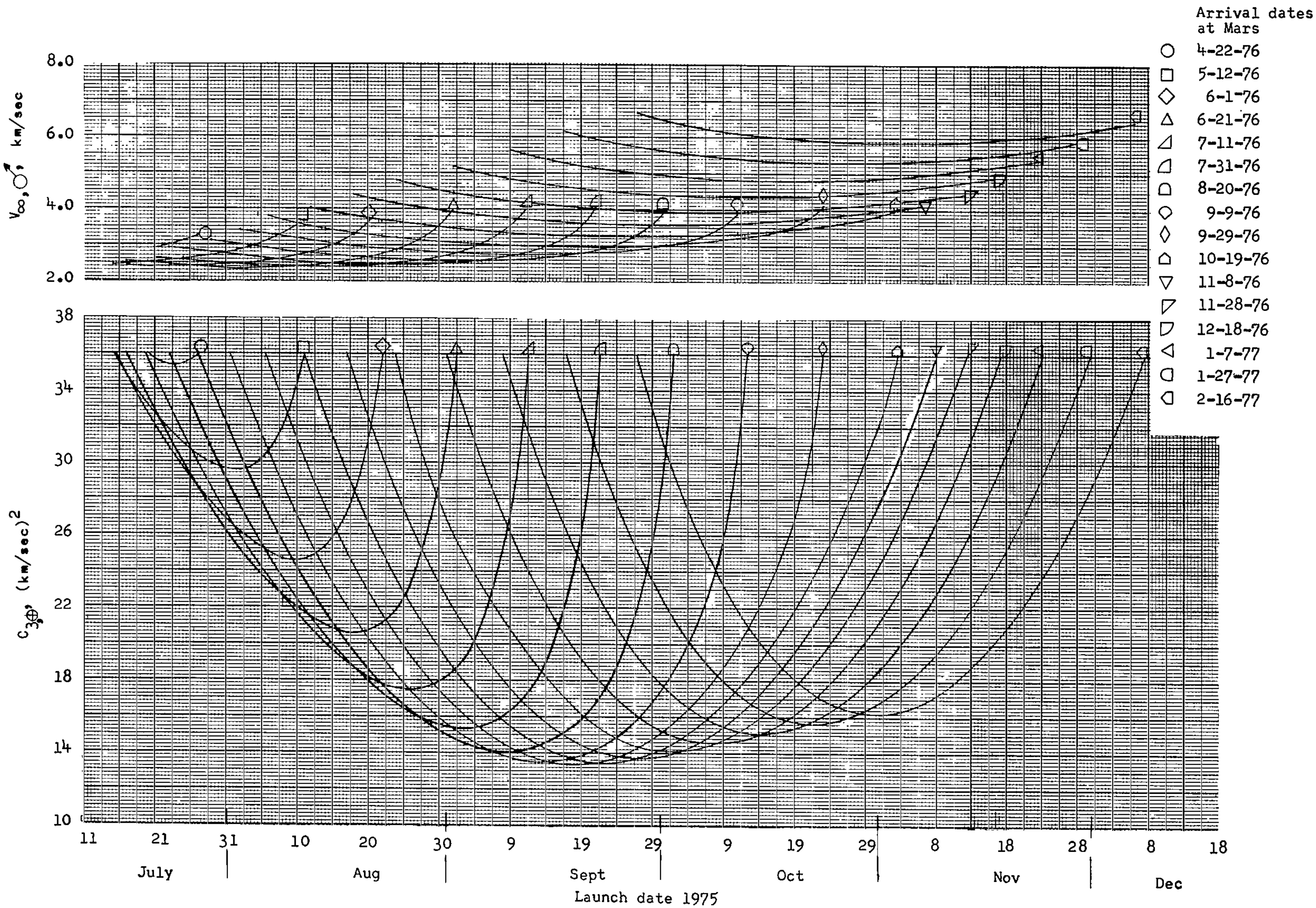

(a) Excess energy at Earth and hyperbolic excess velocity at Mars as functions of launch date for several arrival dates.

Figure 15.- Trajectory characteristics from Earth to Mars for the 1975 type II opportunity.

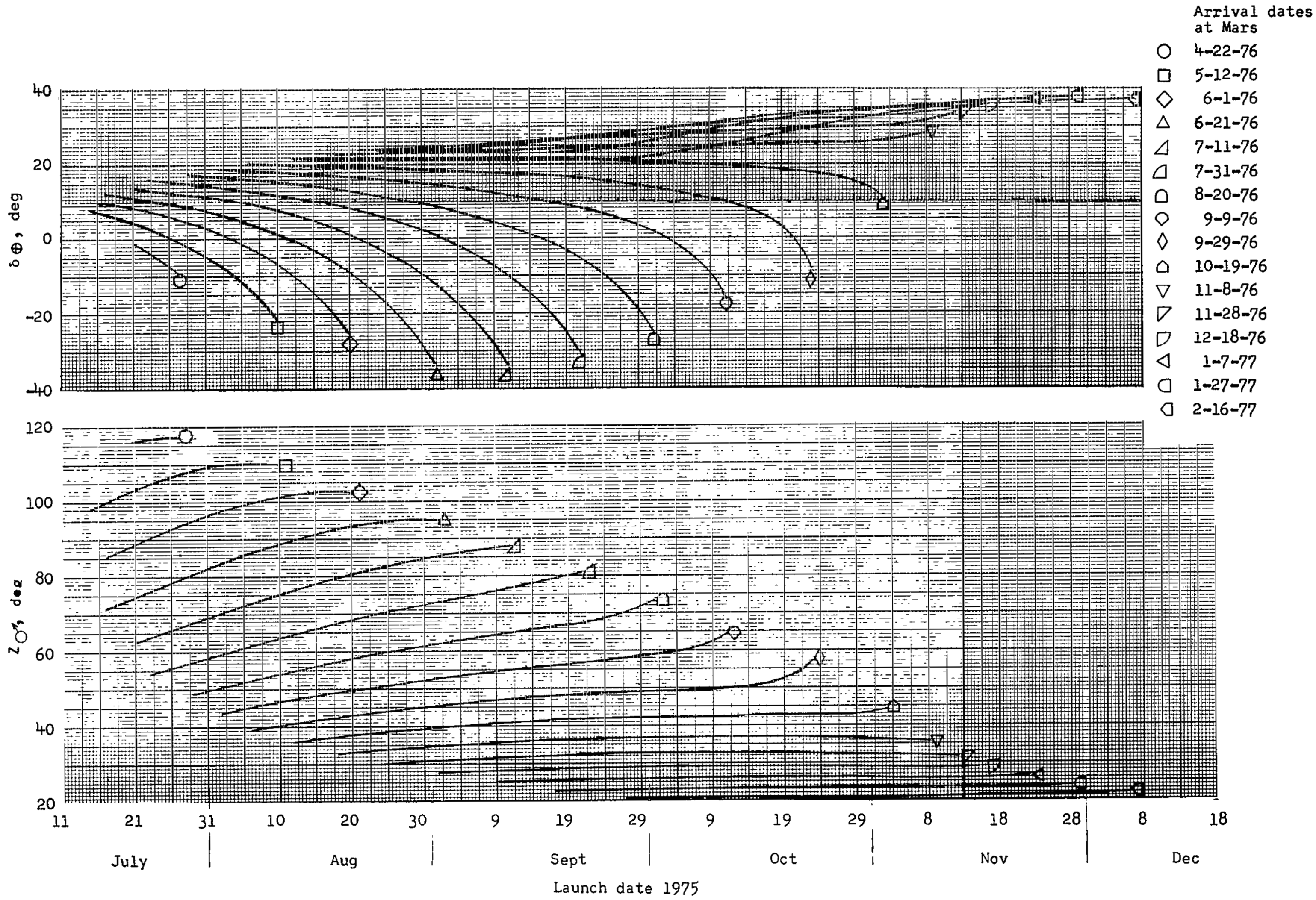

(b) Sun-$\vec{S}$ angle and declination of launch asymptote as functions of launch date for several arrival dates.

Figure 15.- Continued.

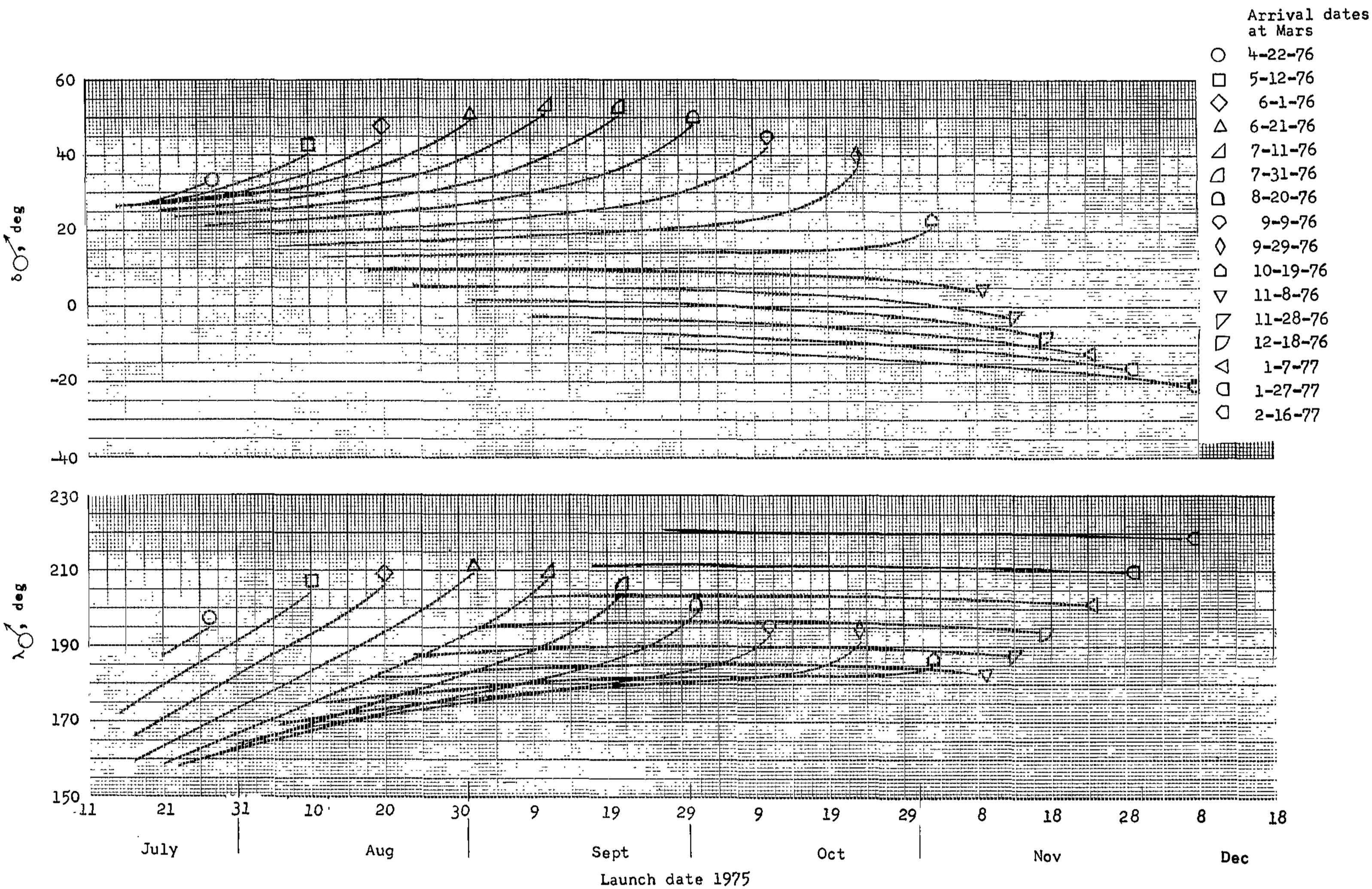

(c) Mars right ascension and declination of $\vec{S}$ as functions of launch date for several arrival dates.

Figure 15.- Concluded.

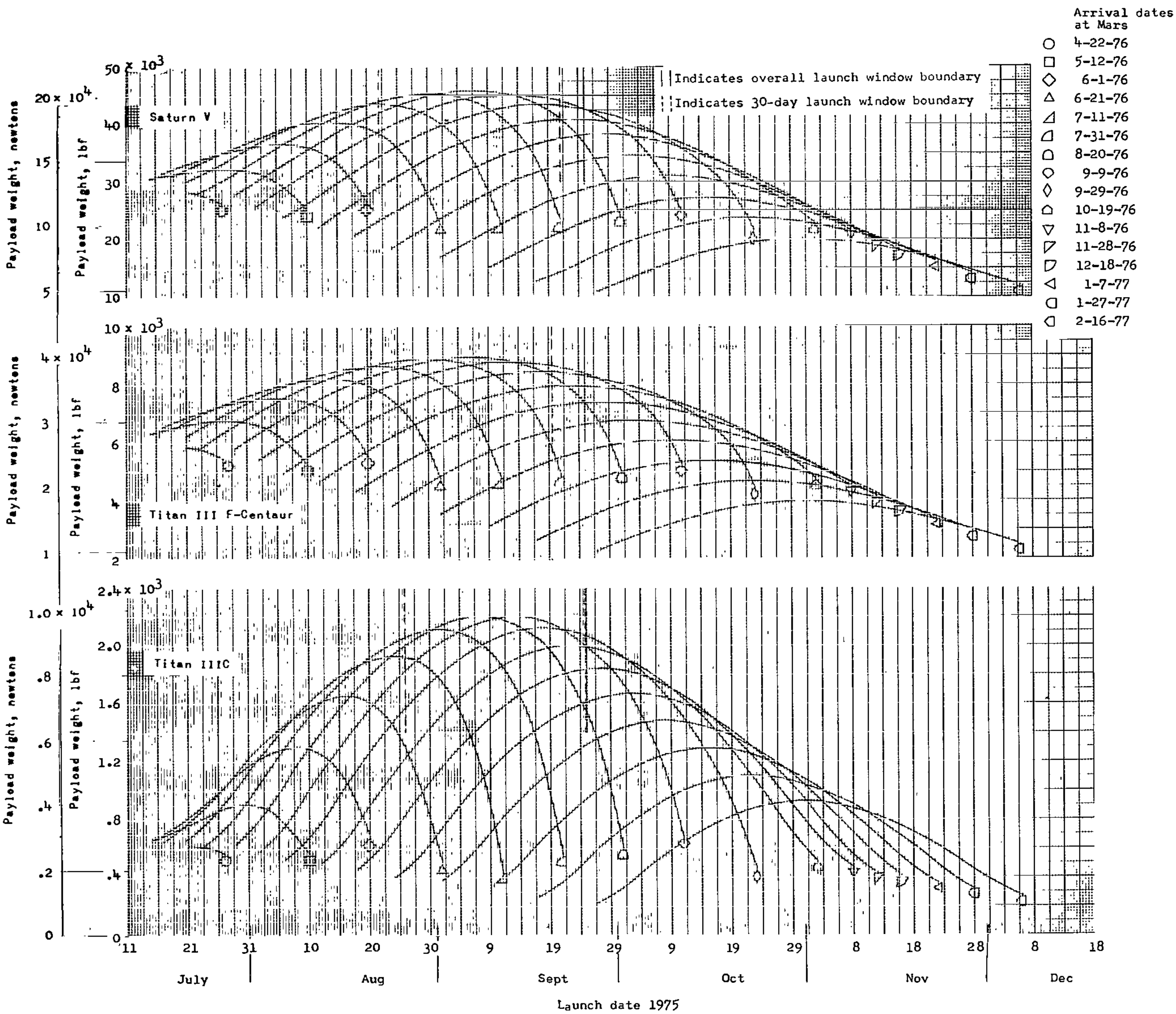

Figure 16.- Payload in Mars orbit as functions of launch date for three launch vehicles for the 1975 type II opportunity.

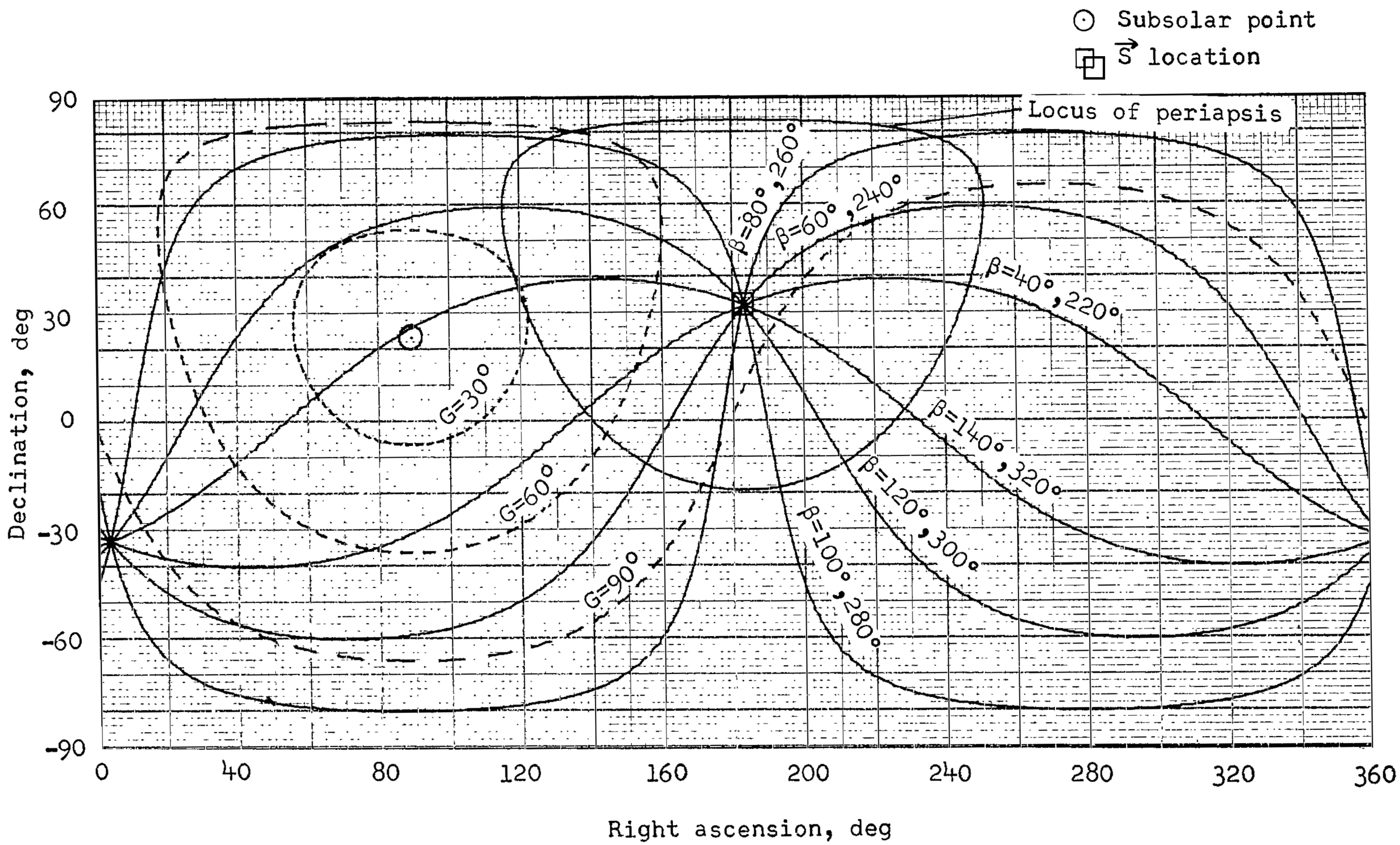

(a) August 20, 1975, launch and July 11, 1976, arrival.

Figure 17.- Relative orbit and sunlighting geometry for typical 1975 type II trajectories.

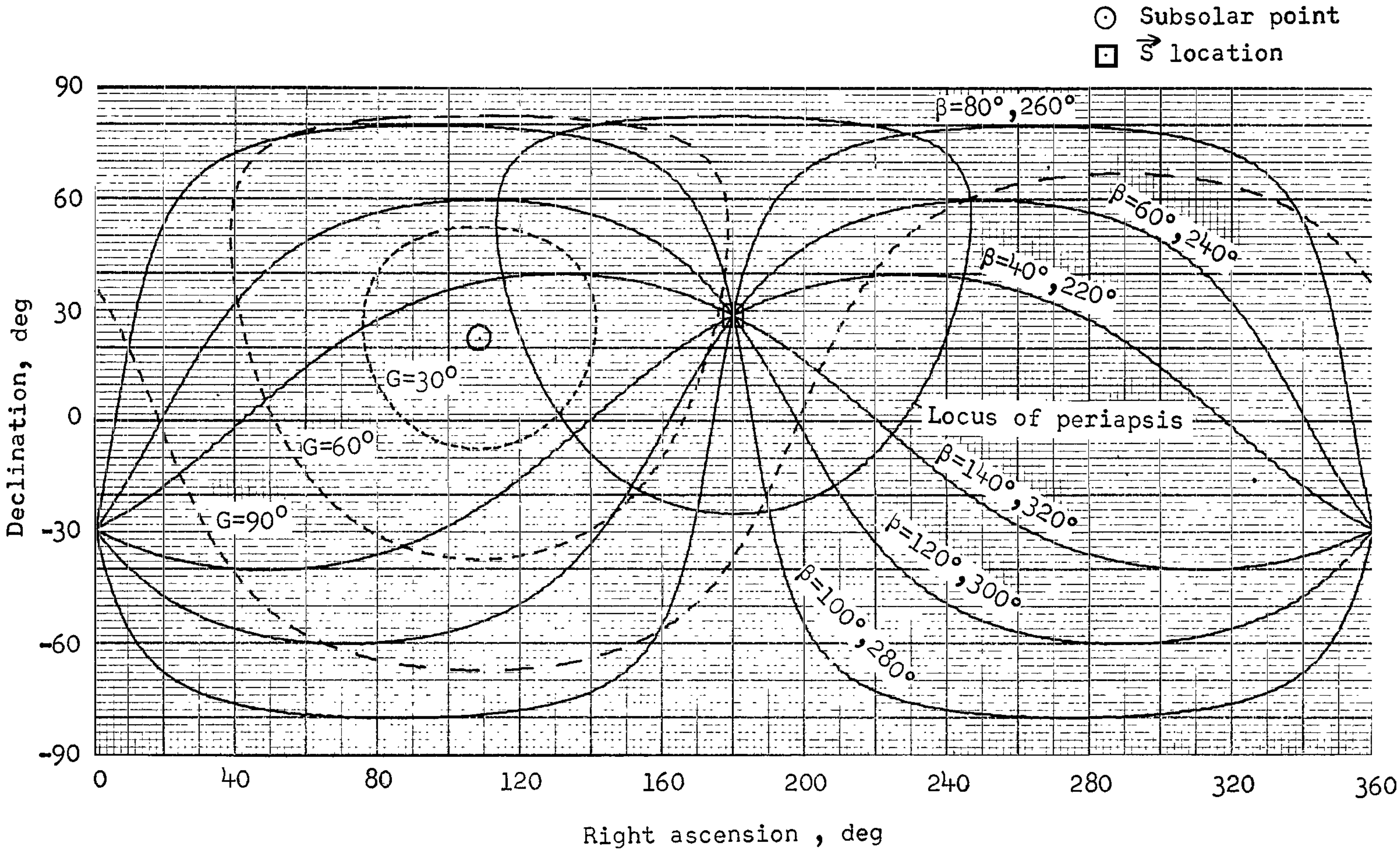

(b) September 7, 1975, launch and August 20, 1976, arrival.

Figure 17.- Continued.

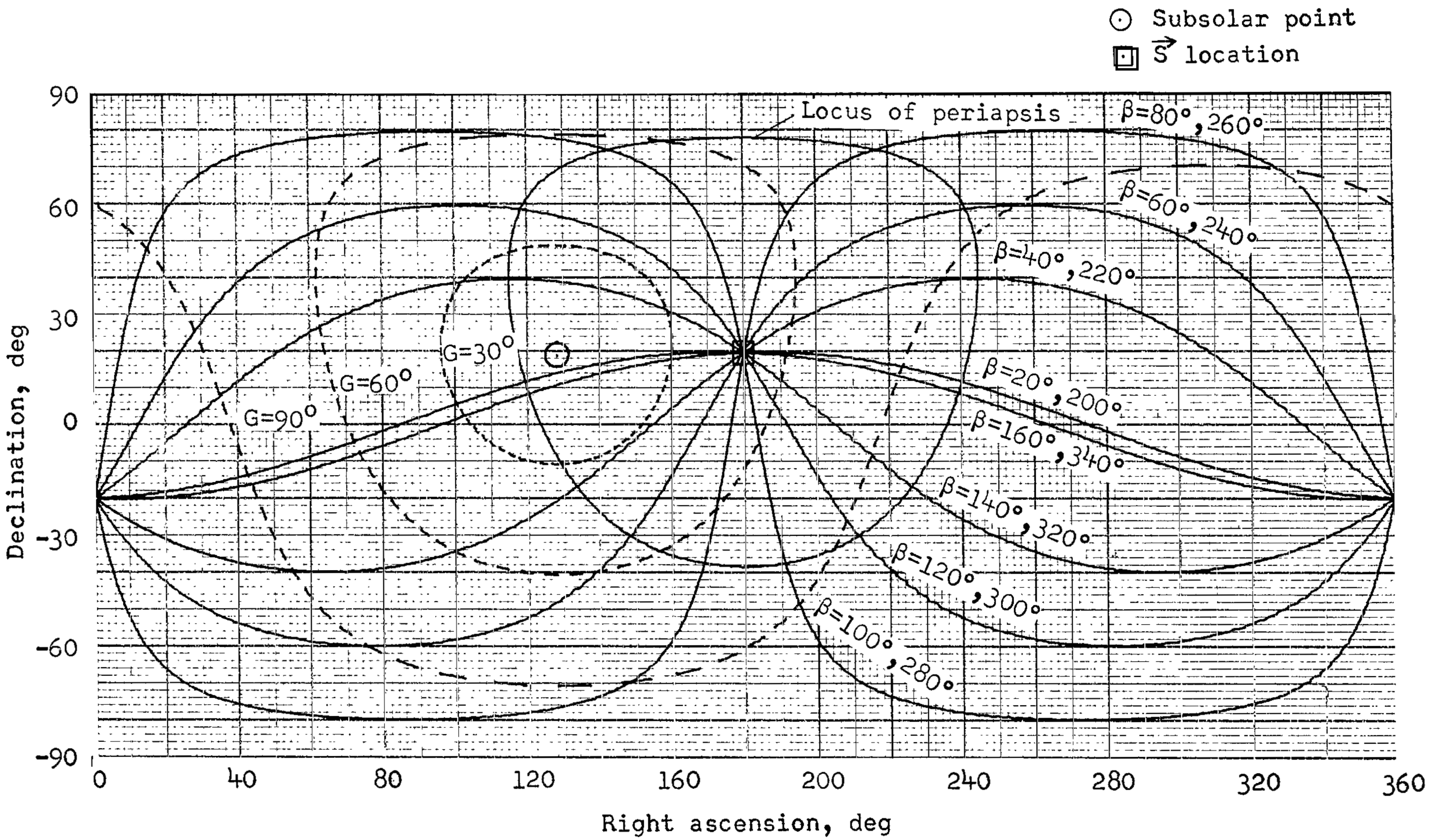

(c) September 25, 1975, launch and September 29, 1976, arrival.

Figure 17.- Concluded.

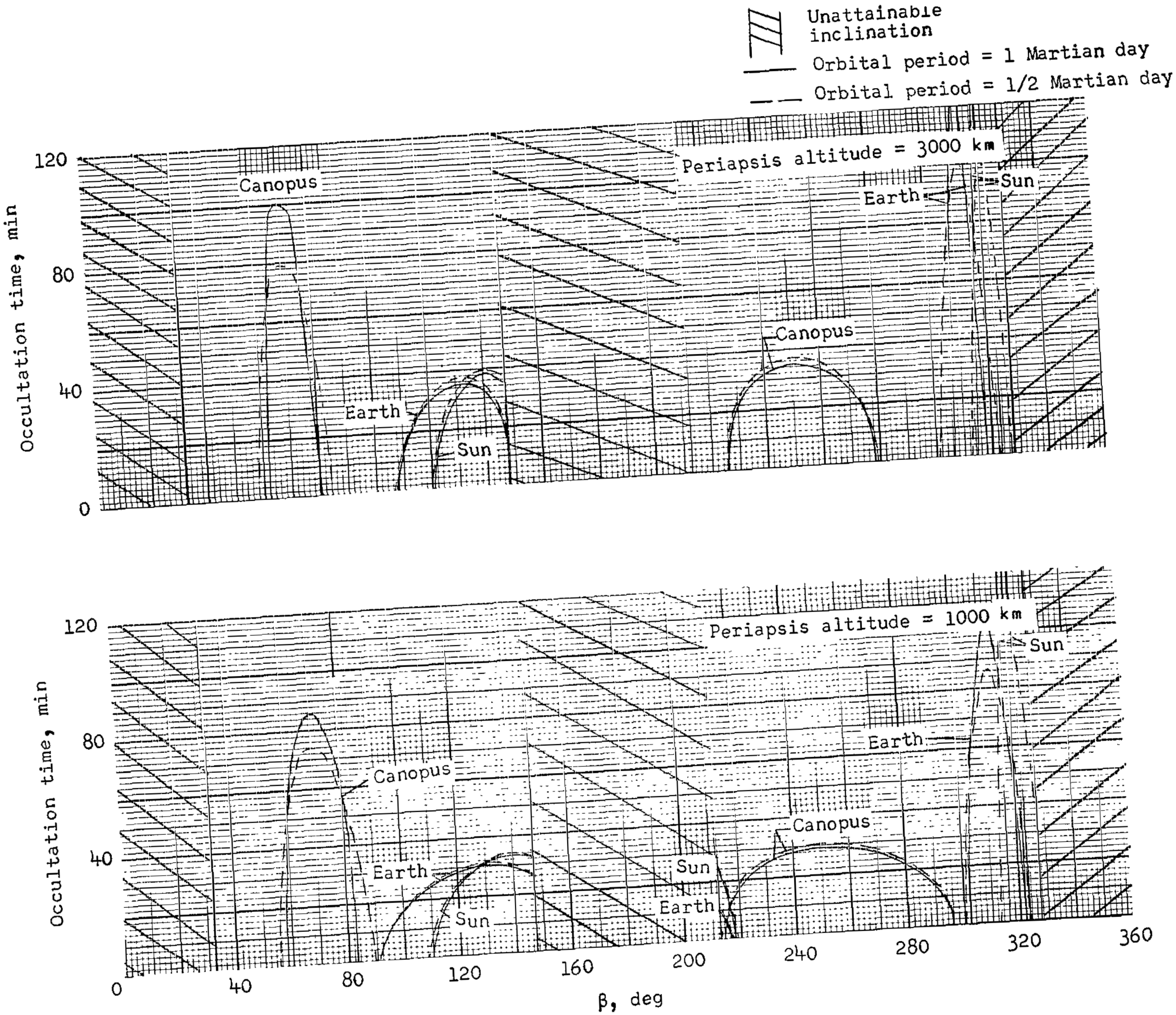

(a) August 20, 1975, launch and July 11, 1976, arrival.

Figure 18.- Occultation characteristics for Mars orbits resulting from typical 1975 type II trajectories.

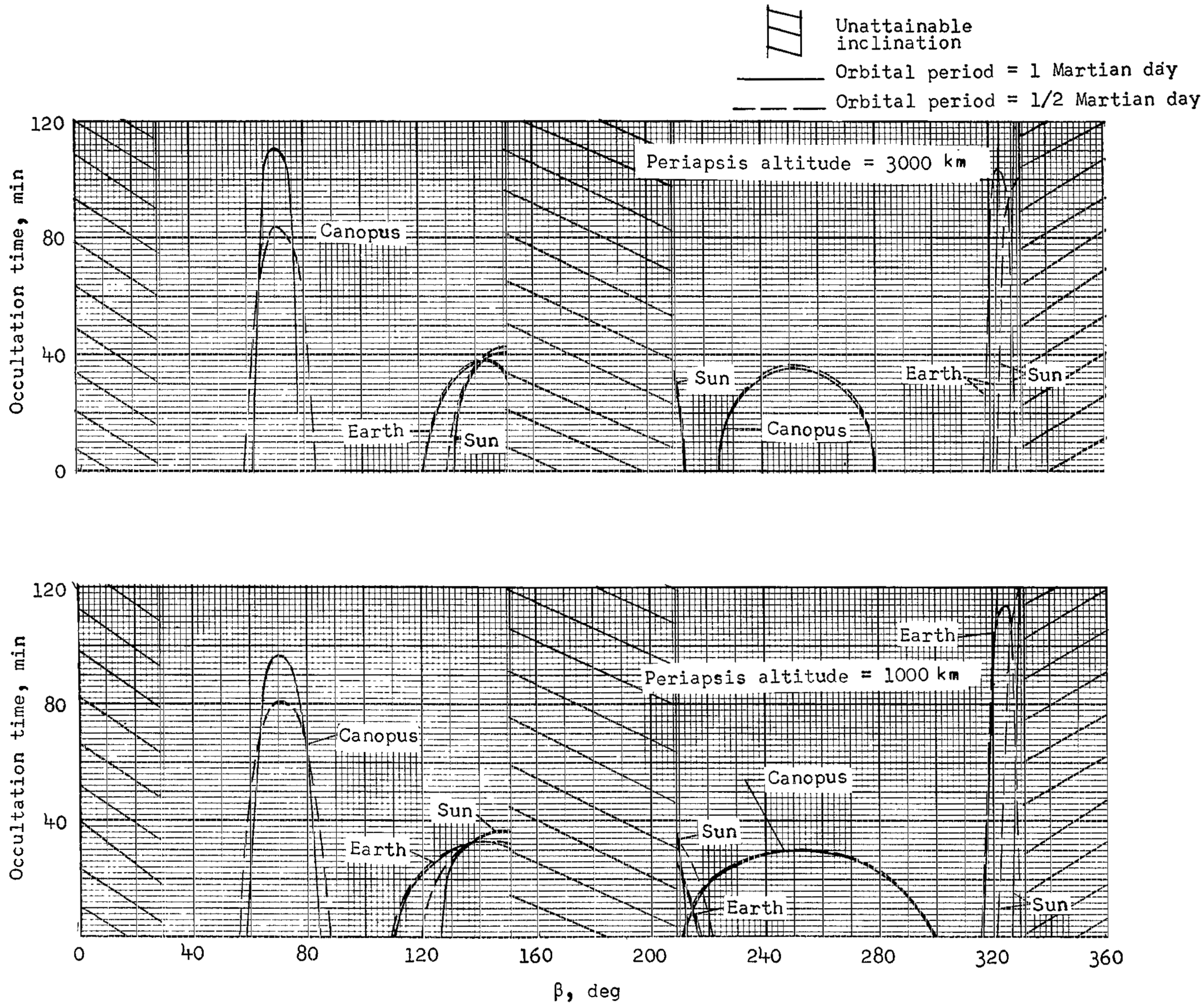

(b) September 7, 1975, launch and August 20, 1976, arrival.

Figure 18.- Continued.

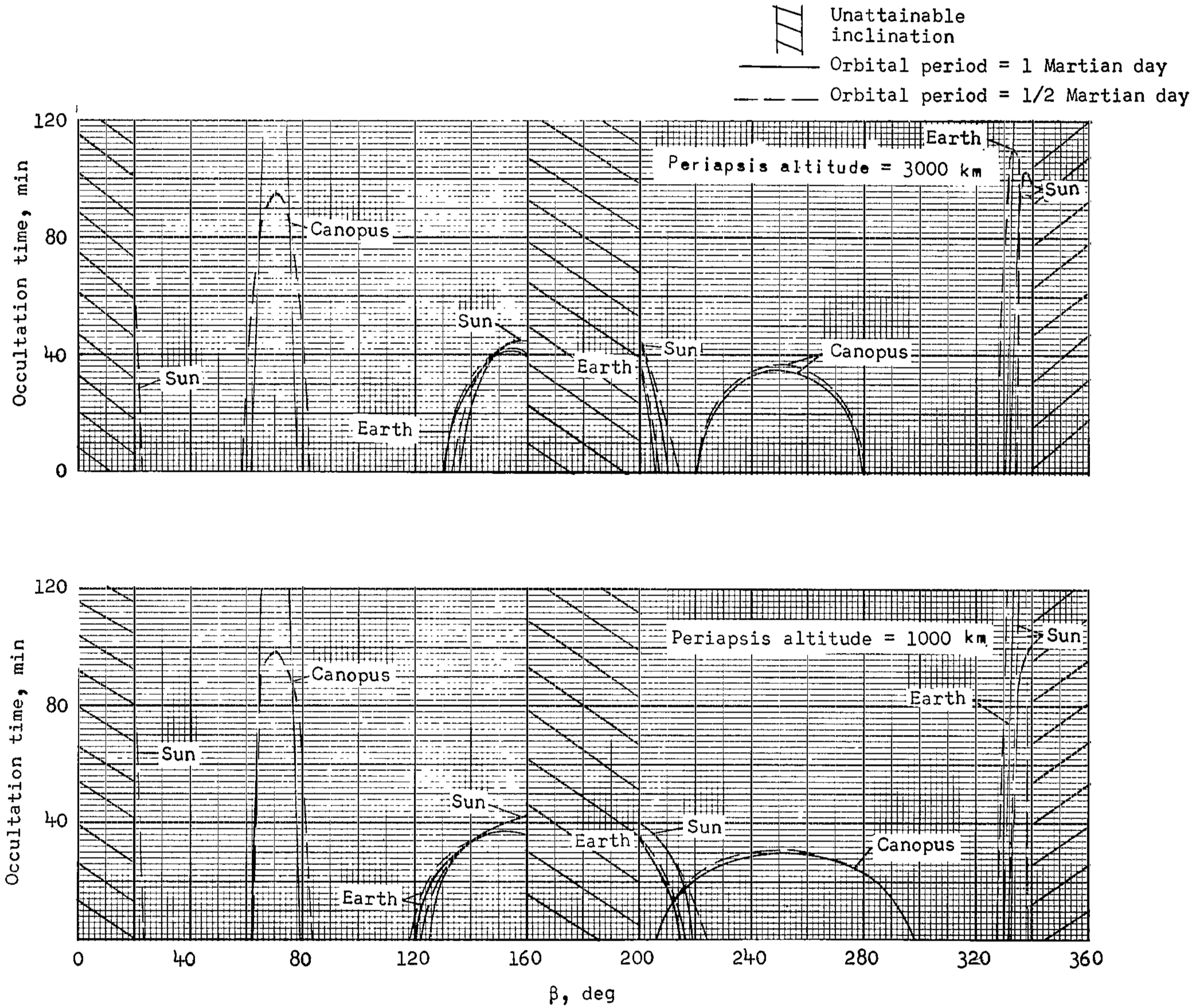

(c) September 25, 1975, launch and September 29, 1976, arrival.

Figure 18.- Concluded.

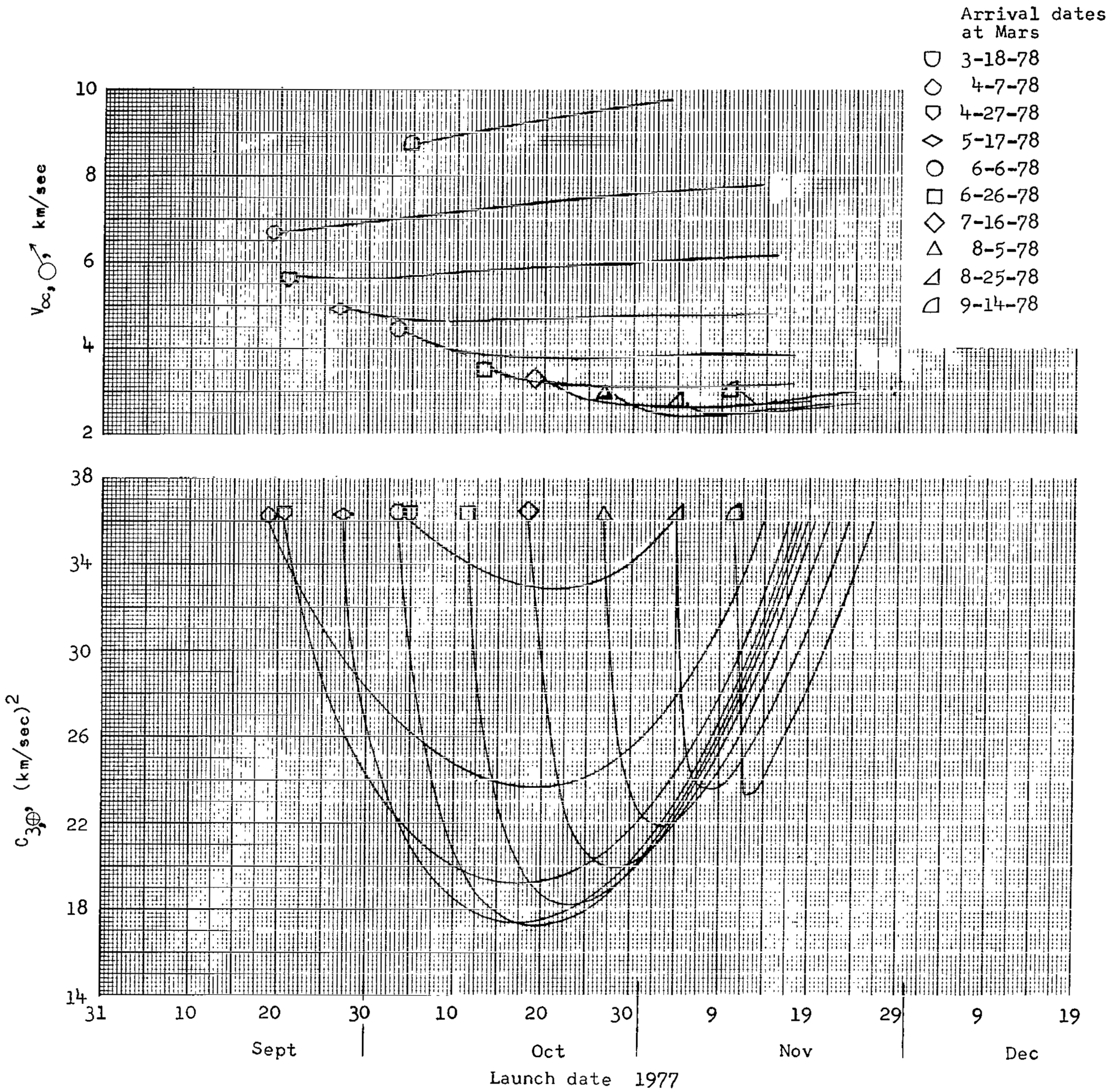

(a) Excess energy at Earth and hyperbolic excess velocity at Mars as functions of launch date for several arrival dates.

Figure 19.- Trajectory characteristics from Earth to Mars for 1977 type I opportunity.

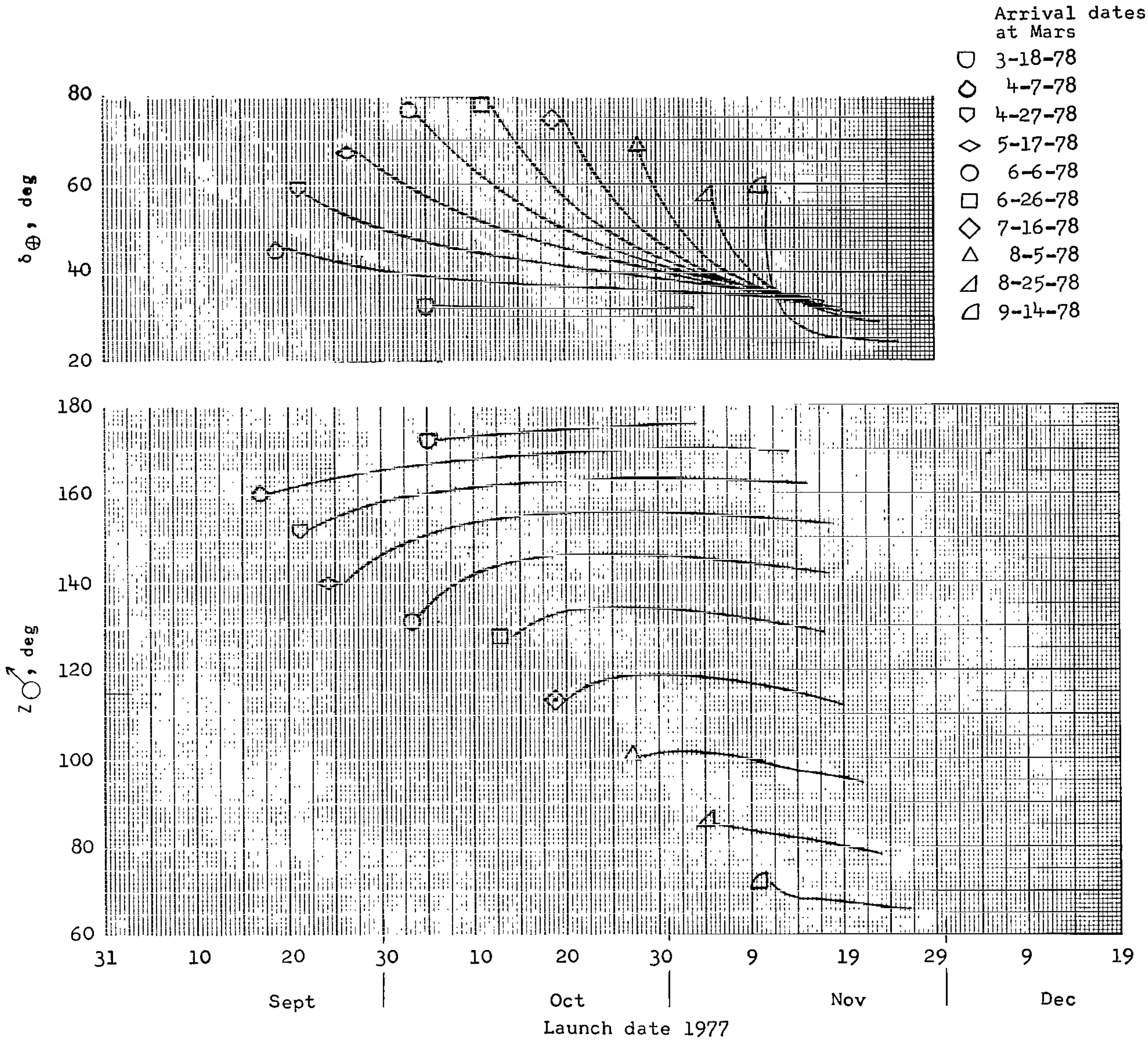

(b) Sun-$\vec{S}$ angle and declination of launch asymptote as functions of launch date for several arrival dates.

Figure 19.- Continued.

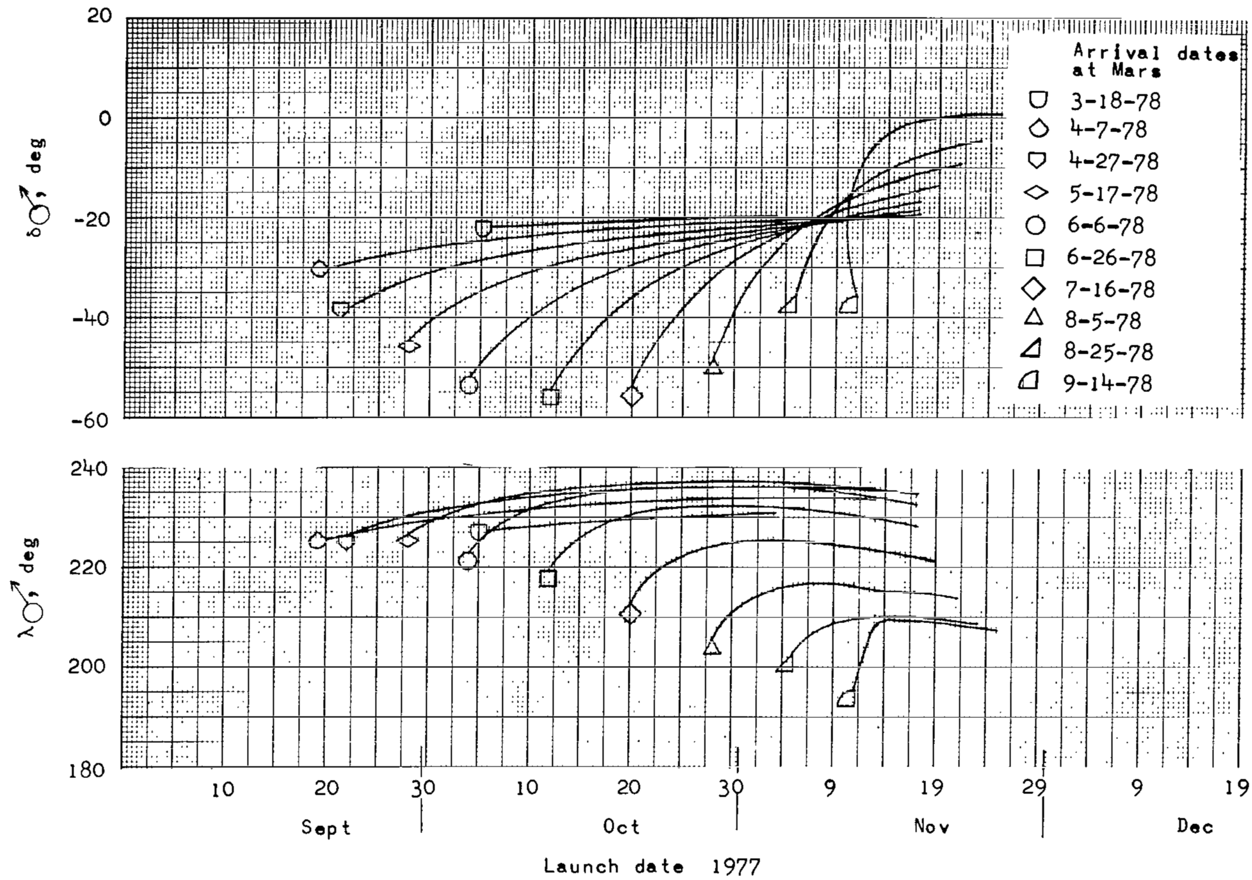

(c) Mars right ascension and declination of $\vec{S}$ as functions of launch date for several arrival dates.

Figure 19.- Concluded.

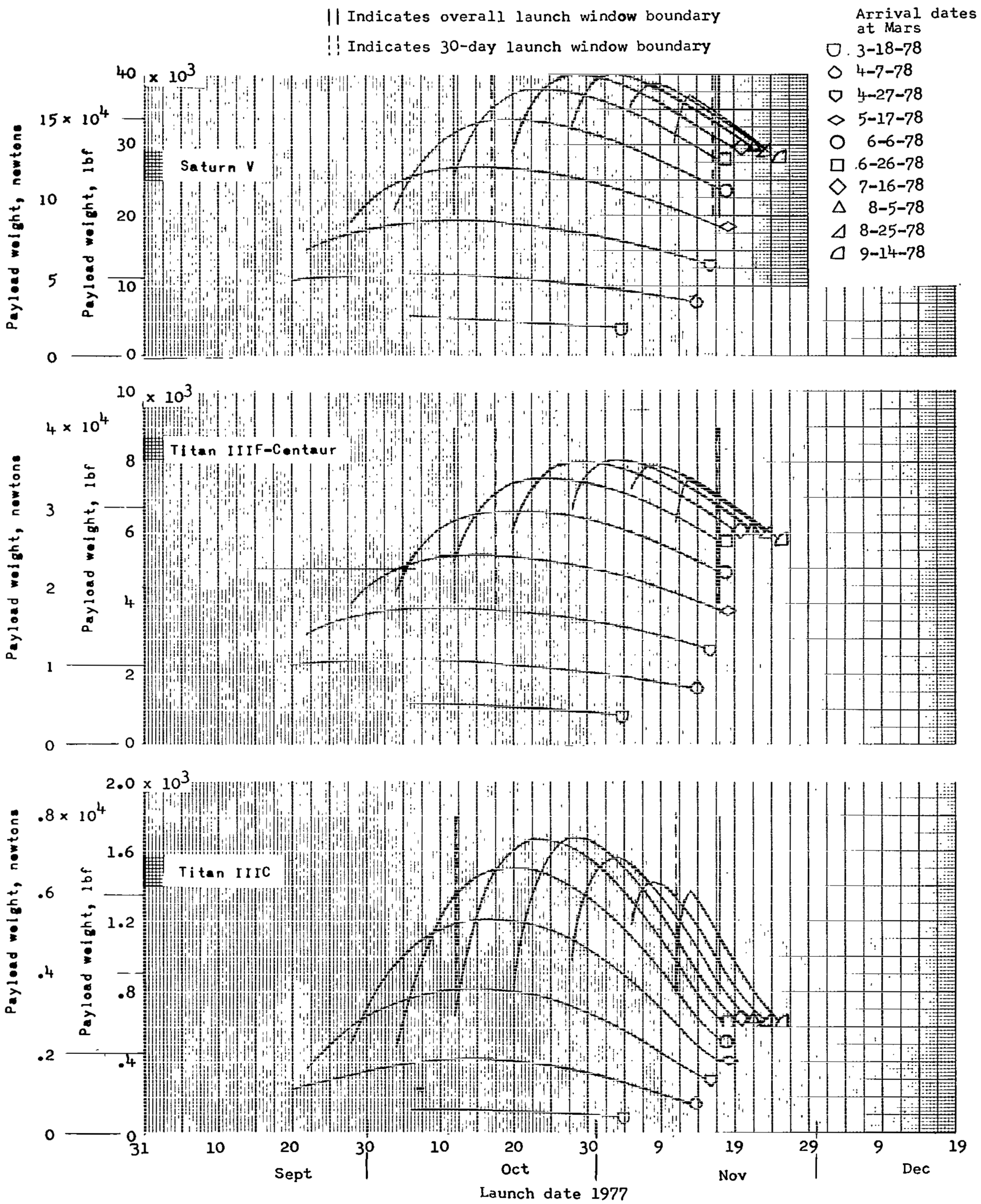

Figure 20.- Payload in Mars orbit as functions of launch date for three launch vehicles for the 1977 type I opportunity.

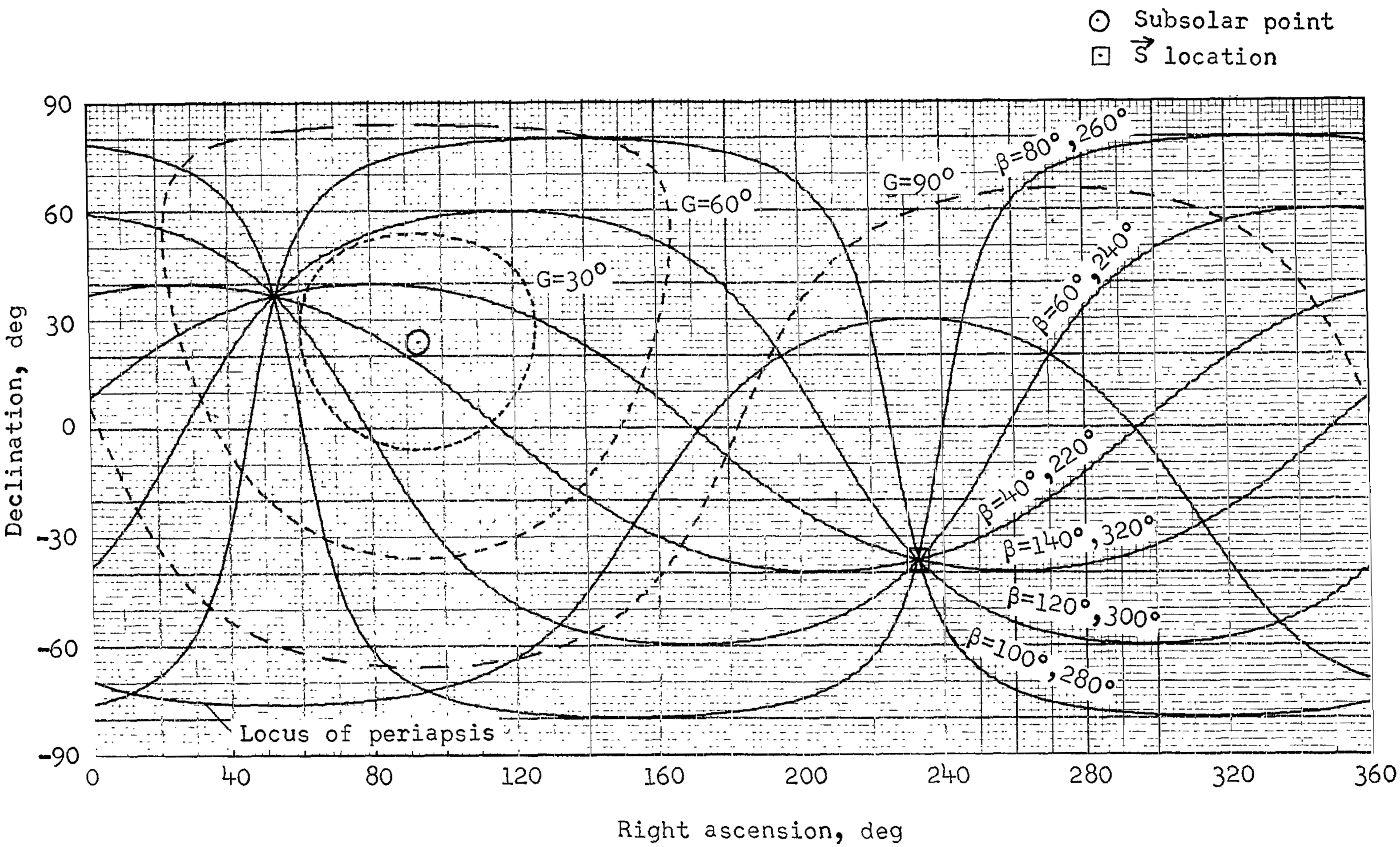

(a) October 12, 1977, launch and June 6, 1978, arrival.

Figure 21.- Relative orbit and sunlighting geometry for typical 1977 type I trajectories.

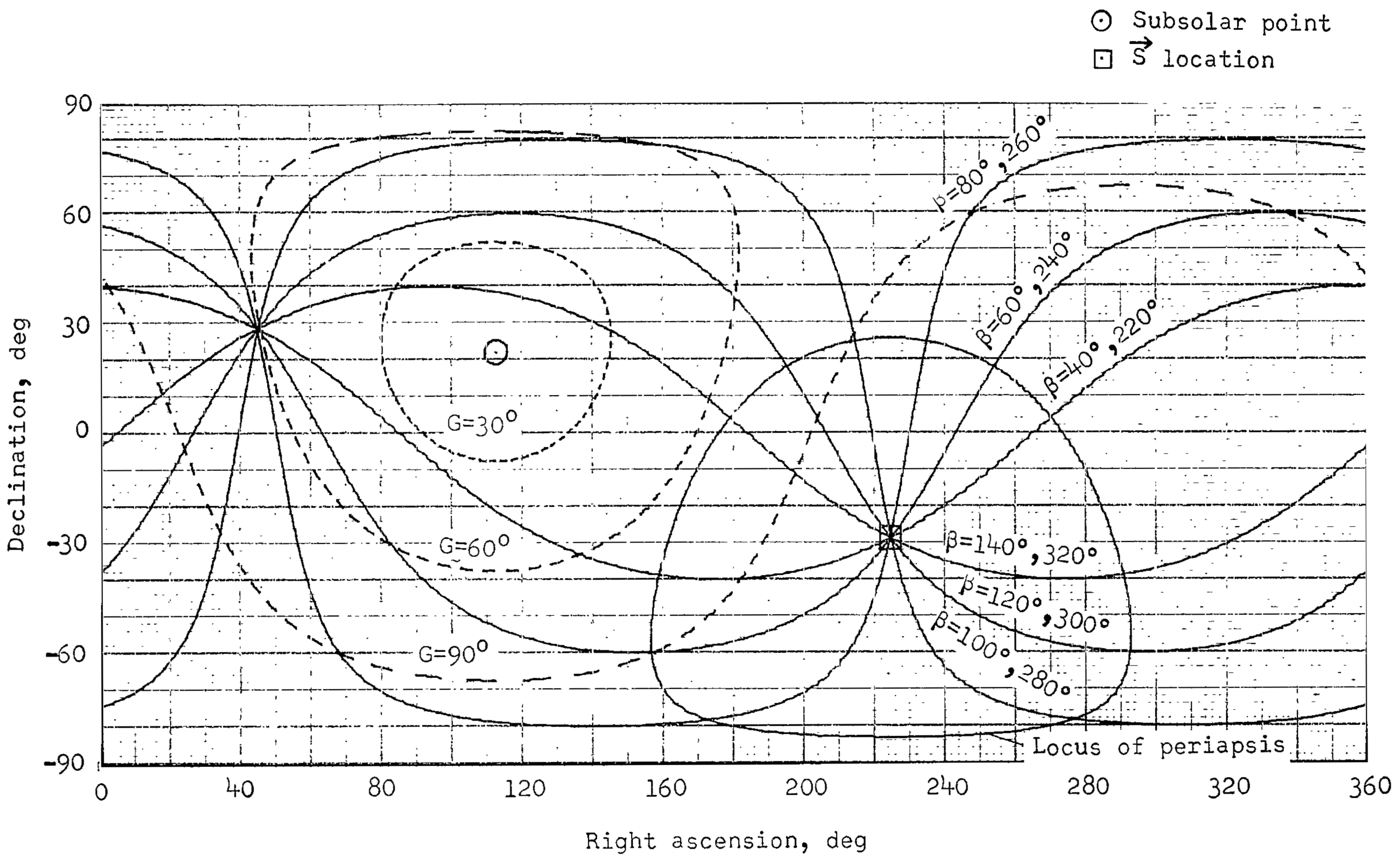

(b) October 30, 1977, launch and July 16, 1978, arrival.

Figure 21.- Continued.

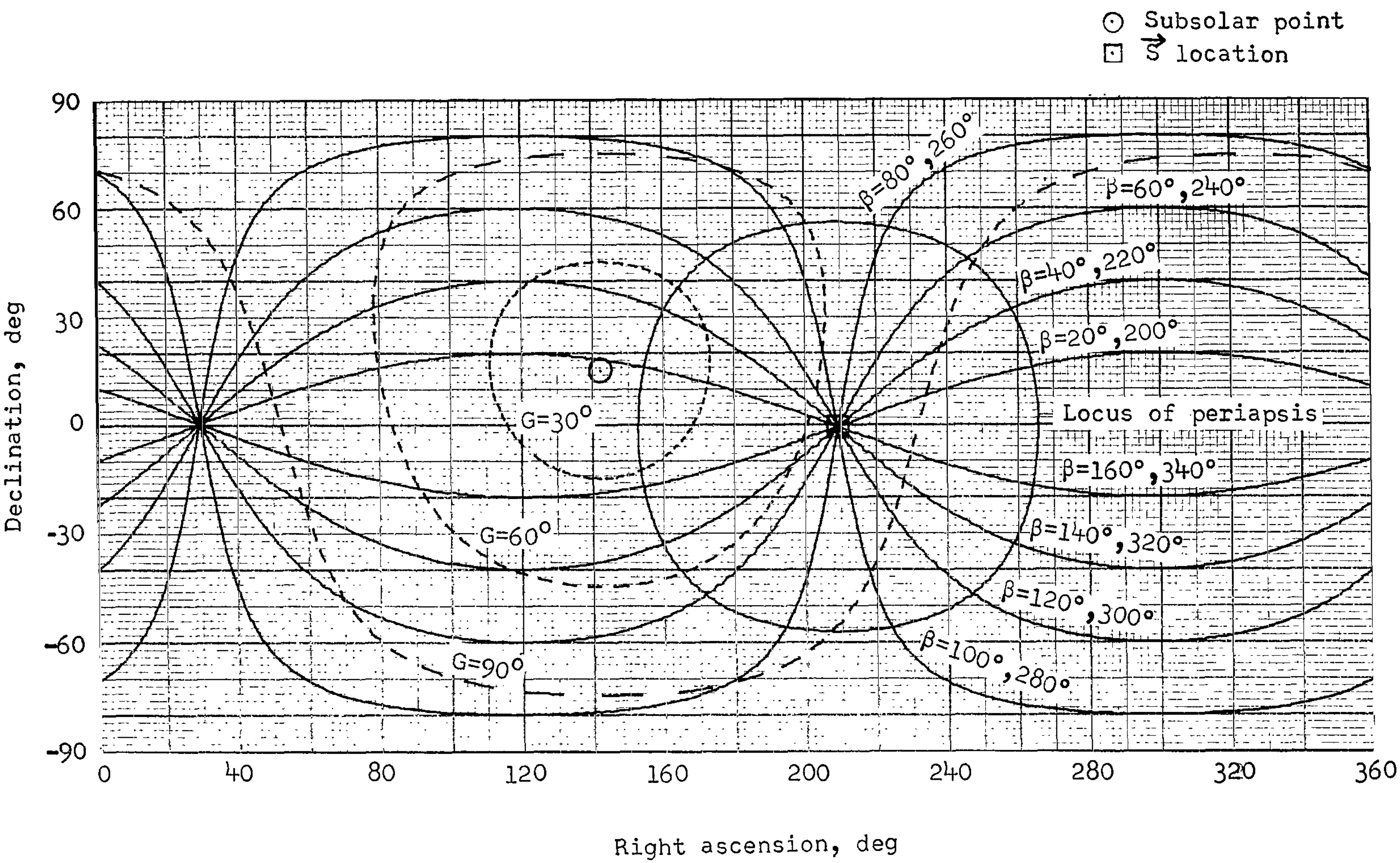

(c) November 17, 1977, launch and September 14, 1978, arrival.

Figure 21.- Concluded.

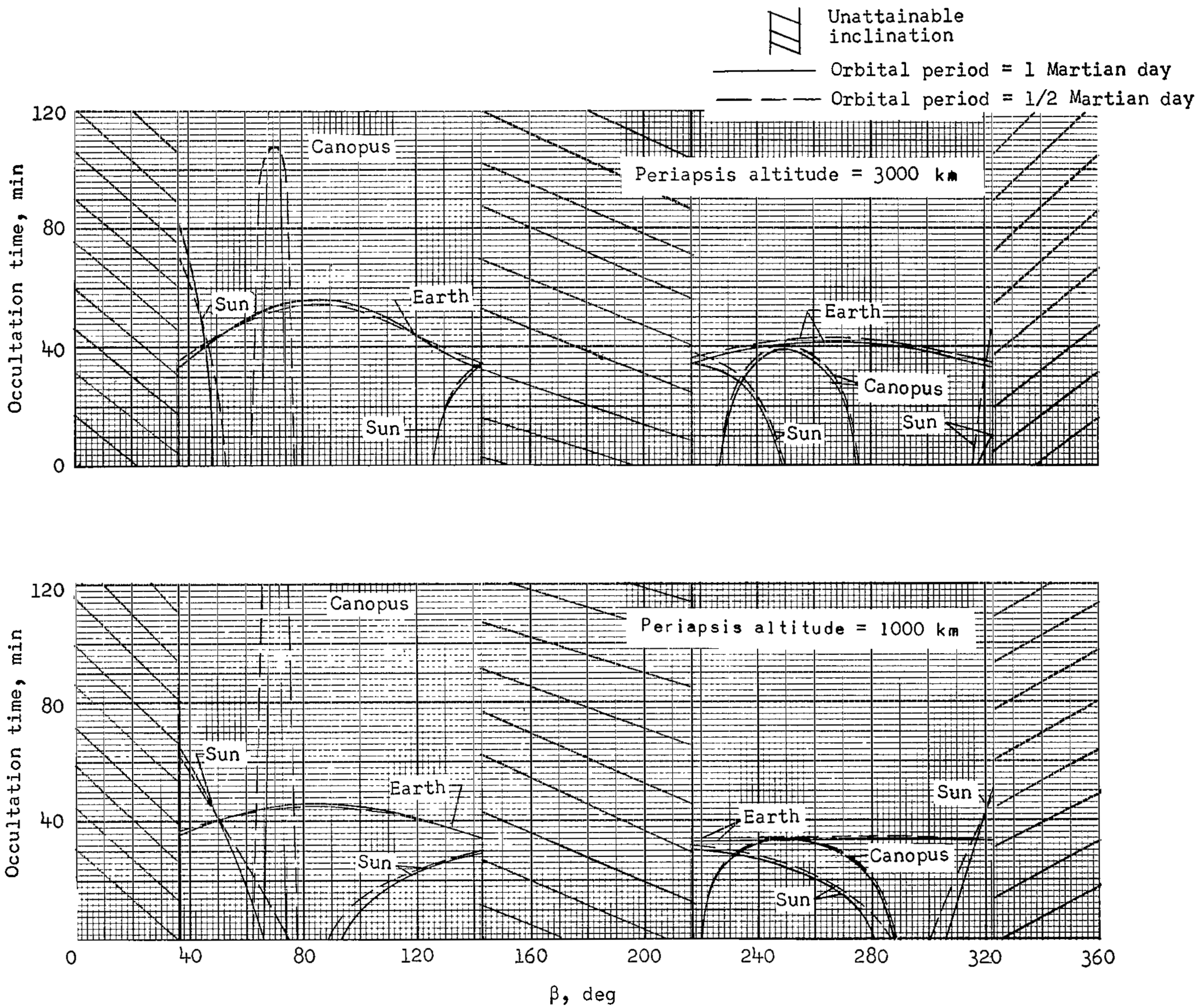

(a) October 12, 1977, launch and June 6, 1978, arrival.

Figure 22.- Occultation characteristics for Mars orbits resulting from typical 1977 type I trajectories.

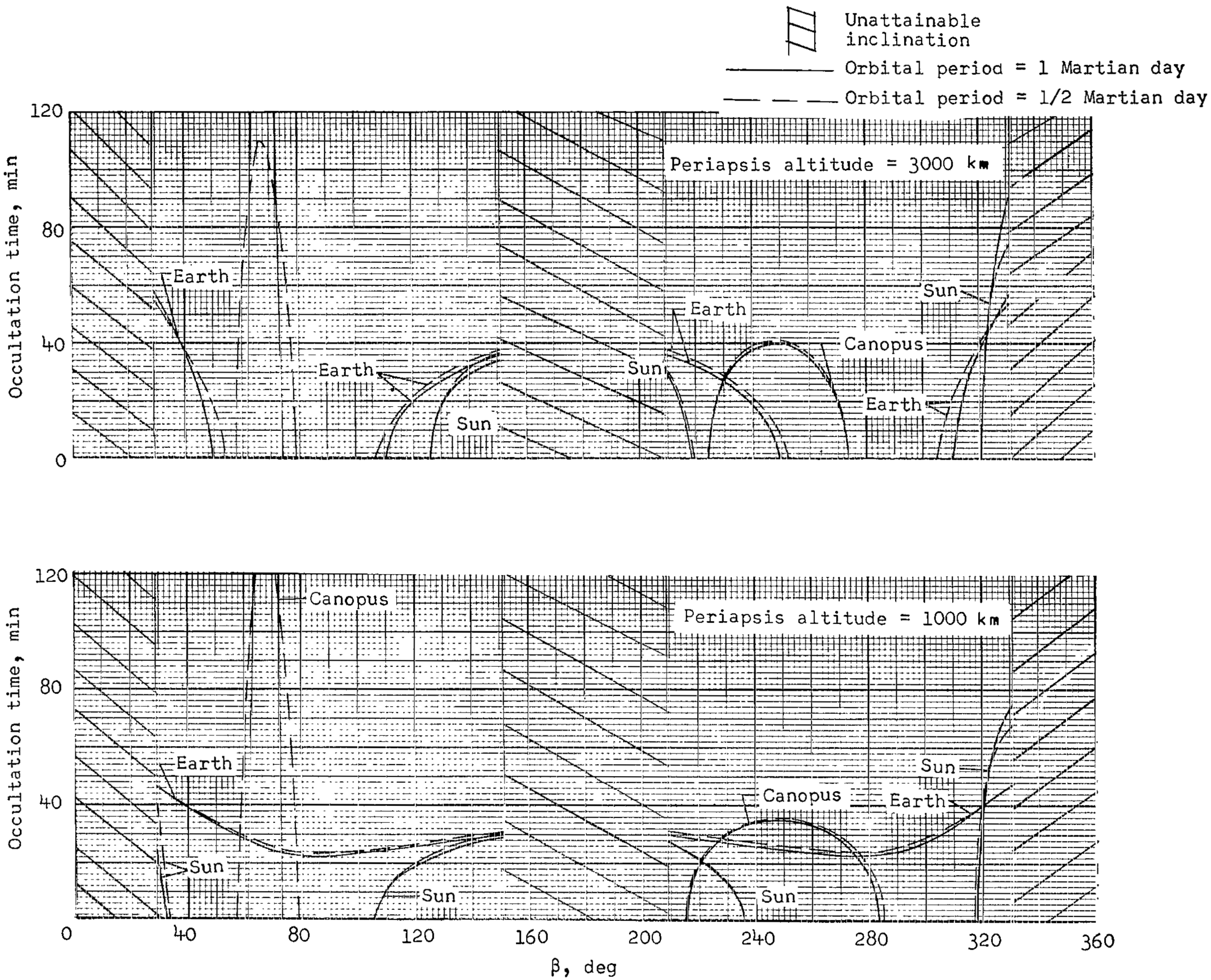

(b) October 30, 1977, launch and July 16, 1978, arrival.

Figure 22.- Continued.

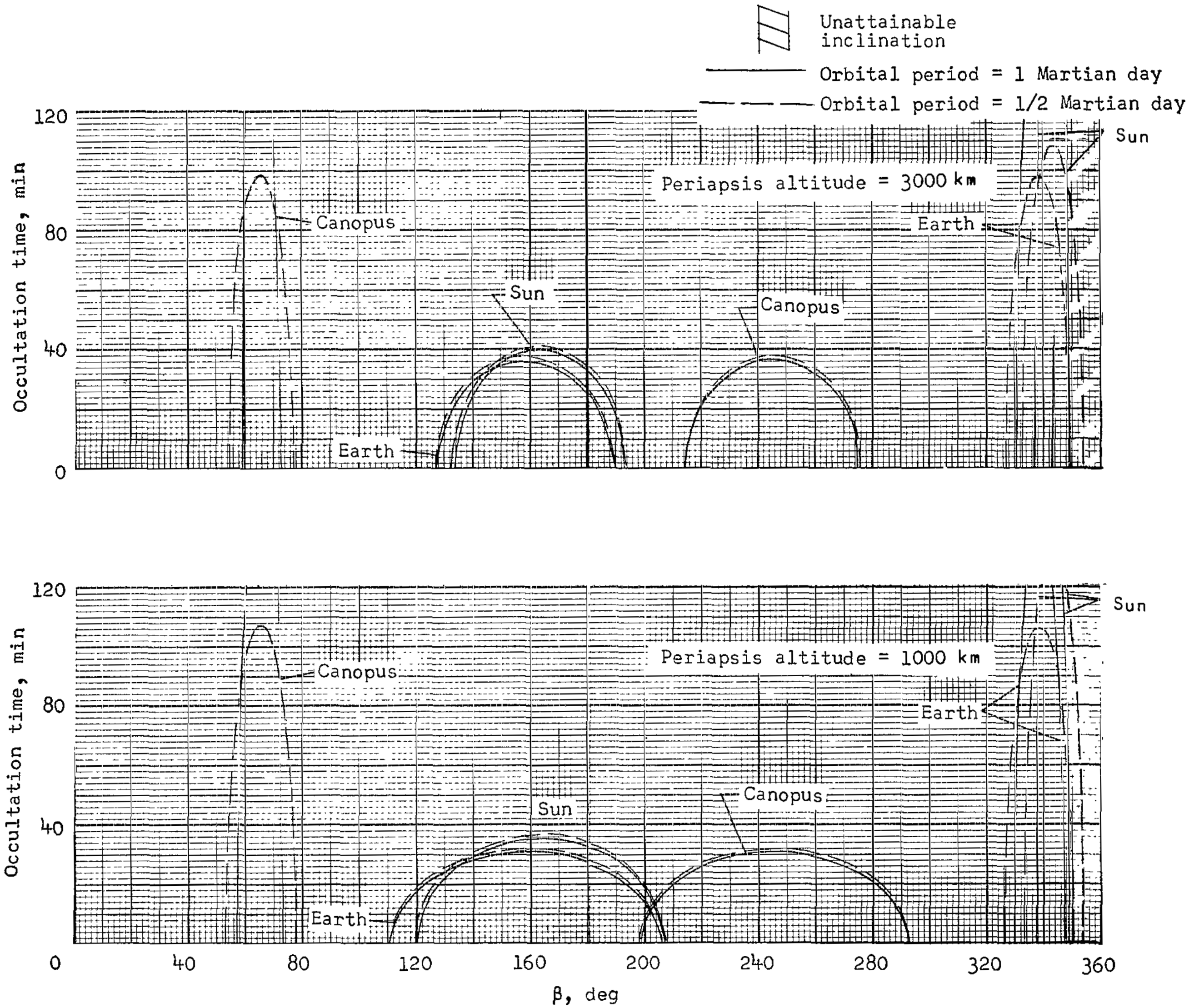

(c) November 17, 1977, launch and September 14, 1978, arrival.

Figure 22.- Concluded.

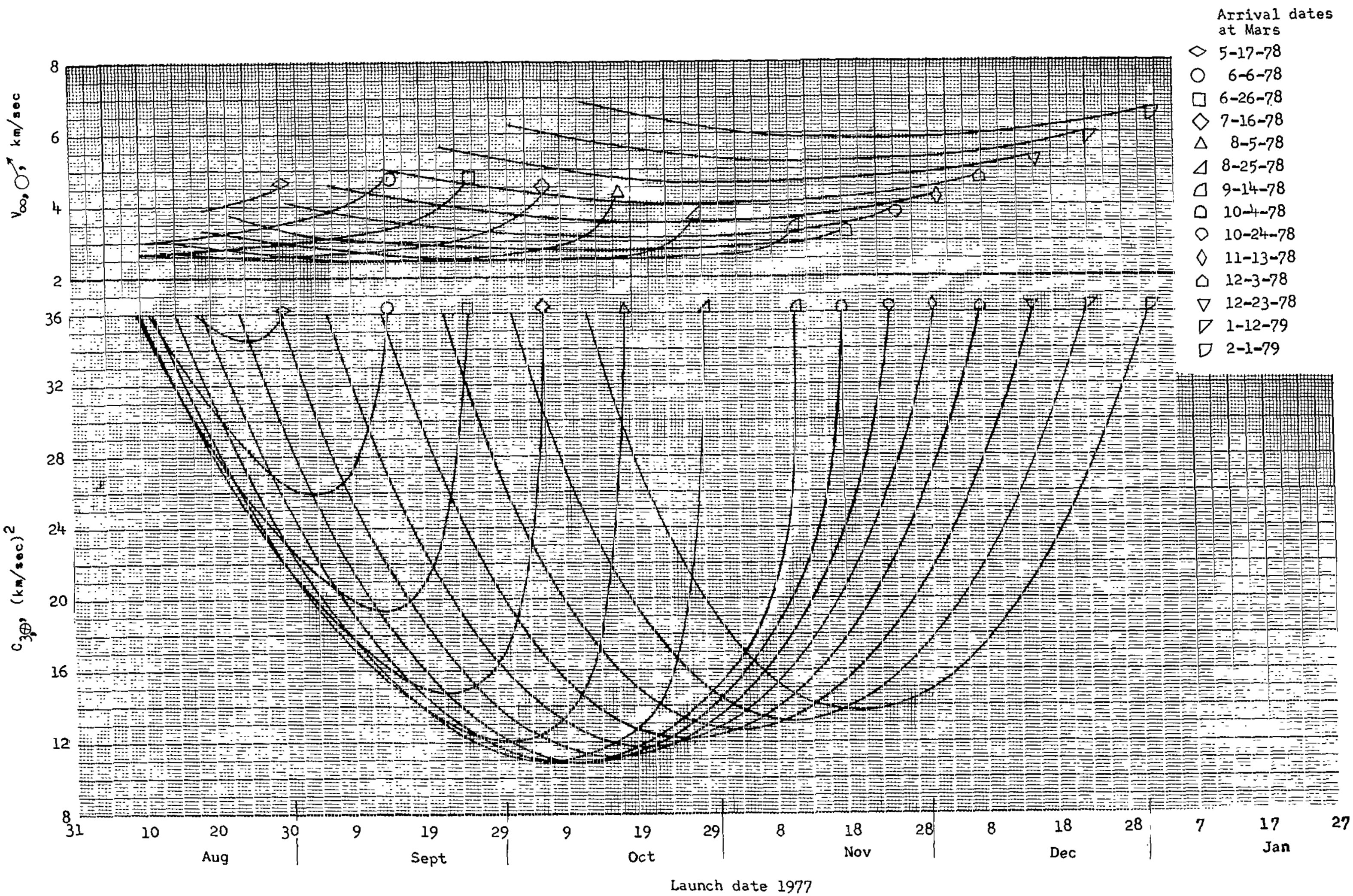

(a) Excess energy at Earth and hyperbolic excess velocity at Mars as functions of launch date for several arrival dates.

Figure 23.- Trajectory characteristics from Earth to Mars for 1977 type II opportunity.

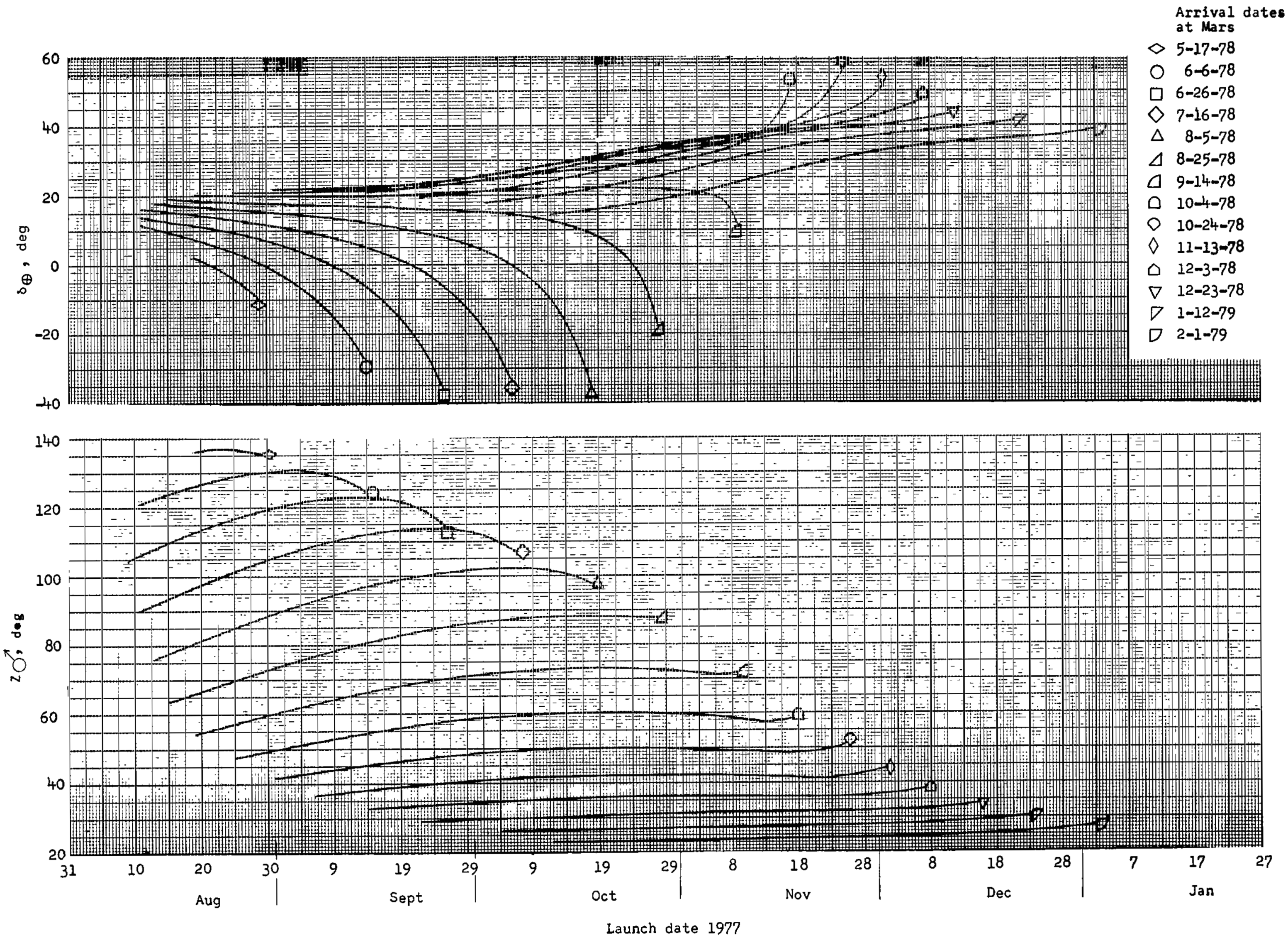

(b) Sun-$\vec{S}$ angle and declination of launch asymptote as functions of launch date for several arrival dates.

Figure 23.- Continued.

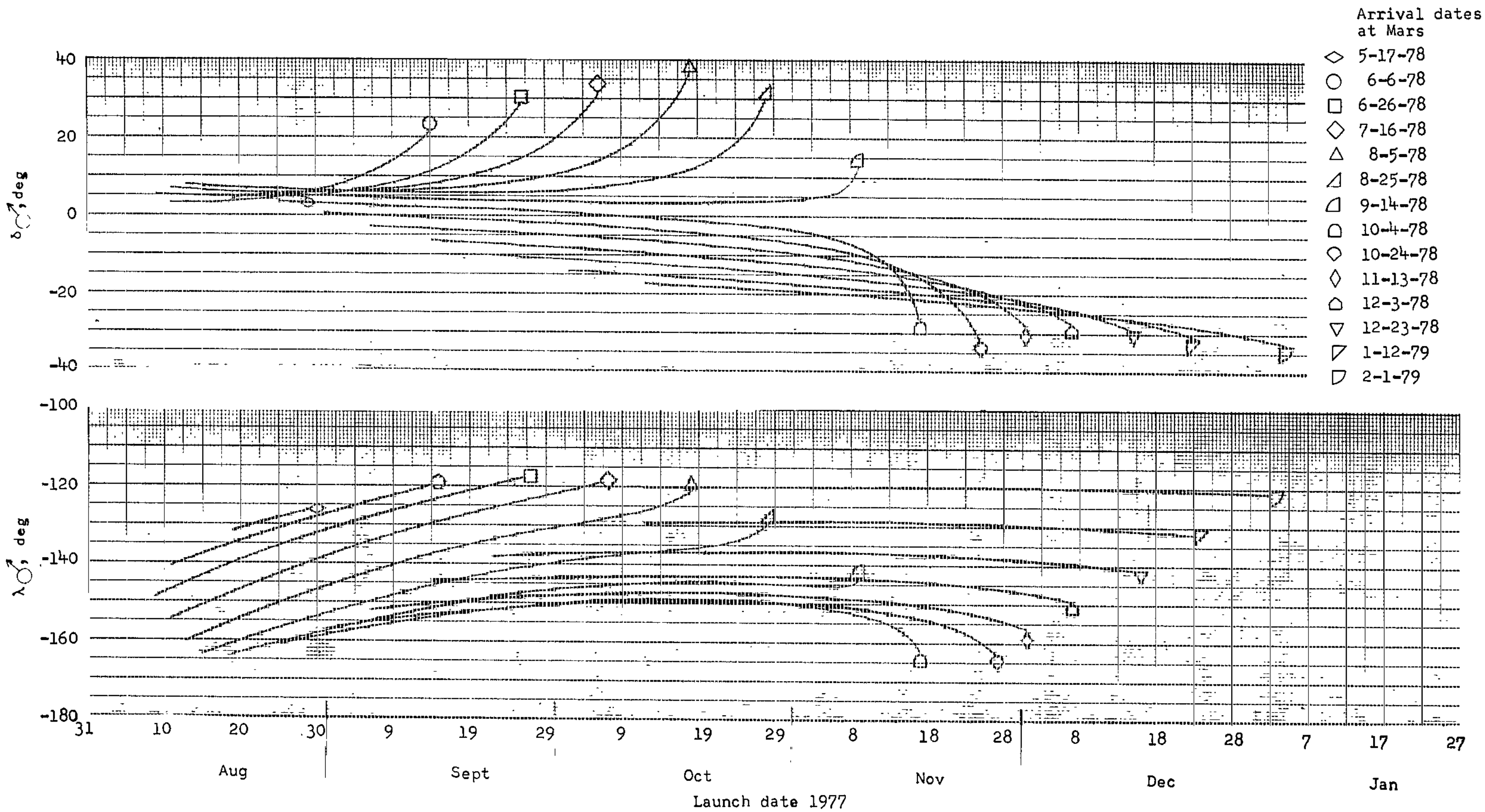

(c) Mars right ascension and declination of $\vec{S}$ as functions of launch date for several arrival dates.

Figure 23.- Concluded.

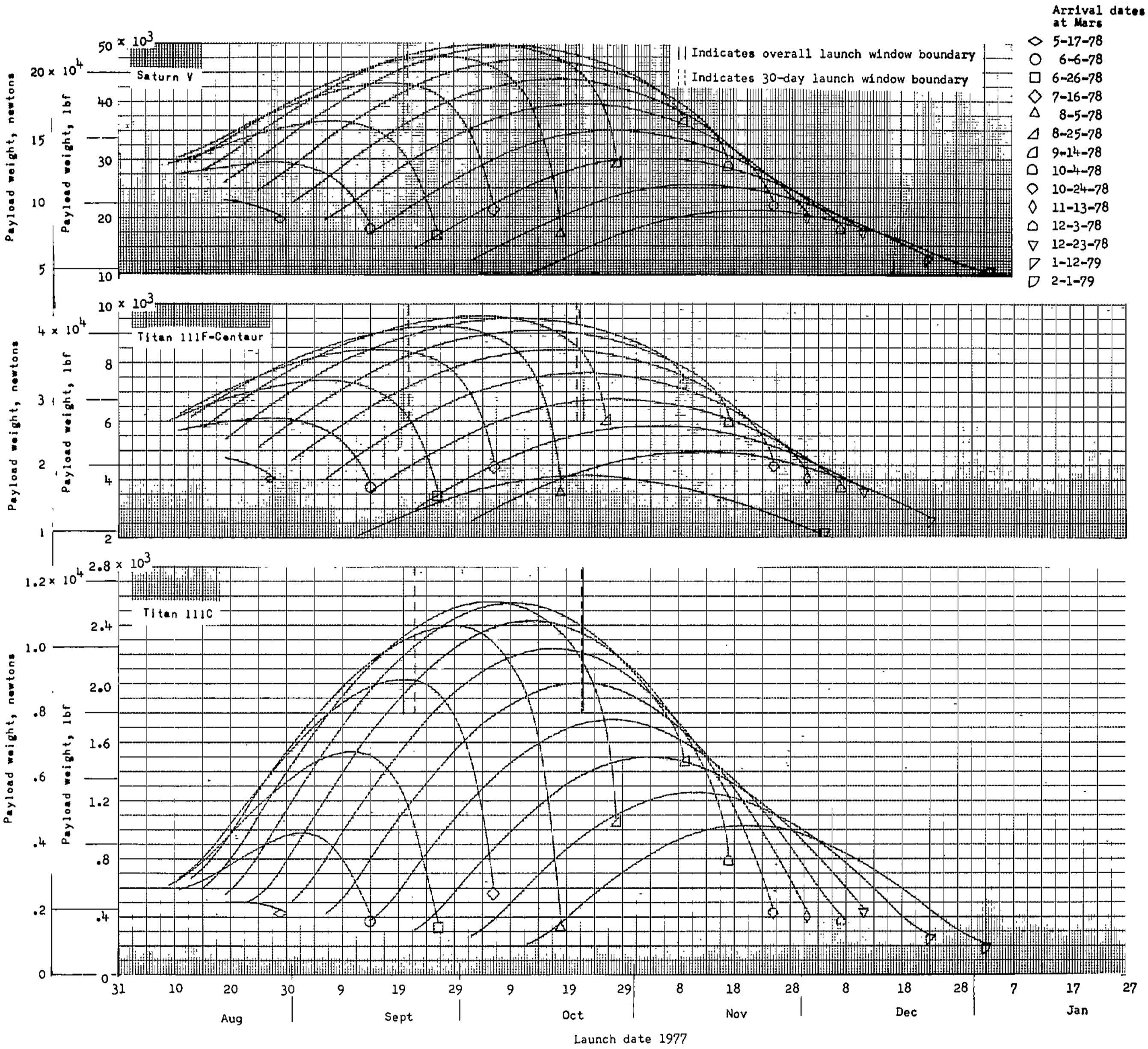

Figure 24.- Payload in Mars orbit as functions of launch date for three launch vehicles for 1977 type II opportunity.

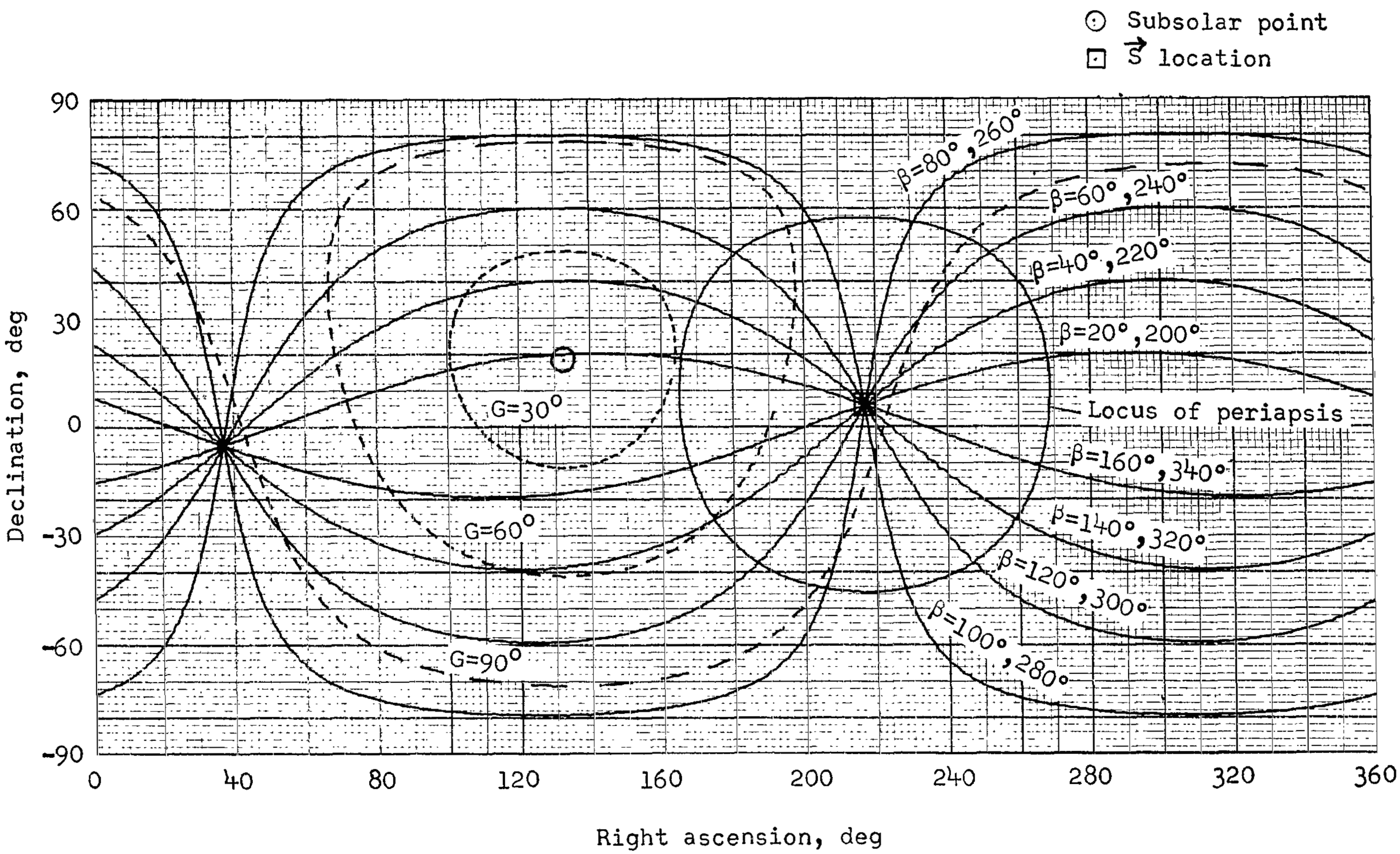

(a) September 20, 1977, launch and August 25, 1978, arrival.

Figure 25.- Relative orbit and sunlighting geometry for typical 1977 type II trajectories.

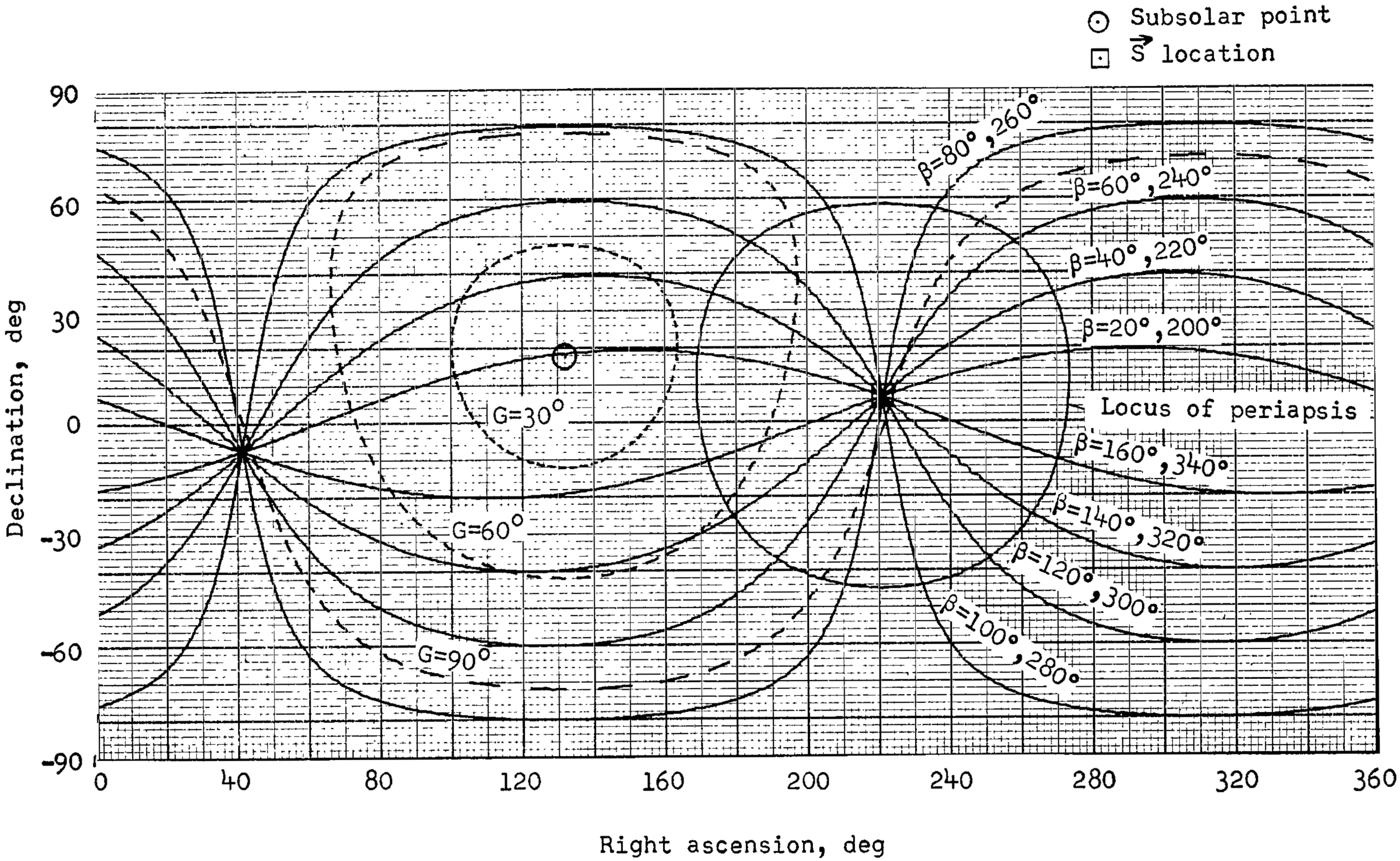

(b) October 6, 1977, launch and August 25, 1978, arrival.

Figure 25.- Continued.

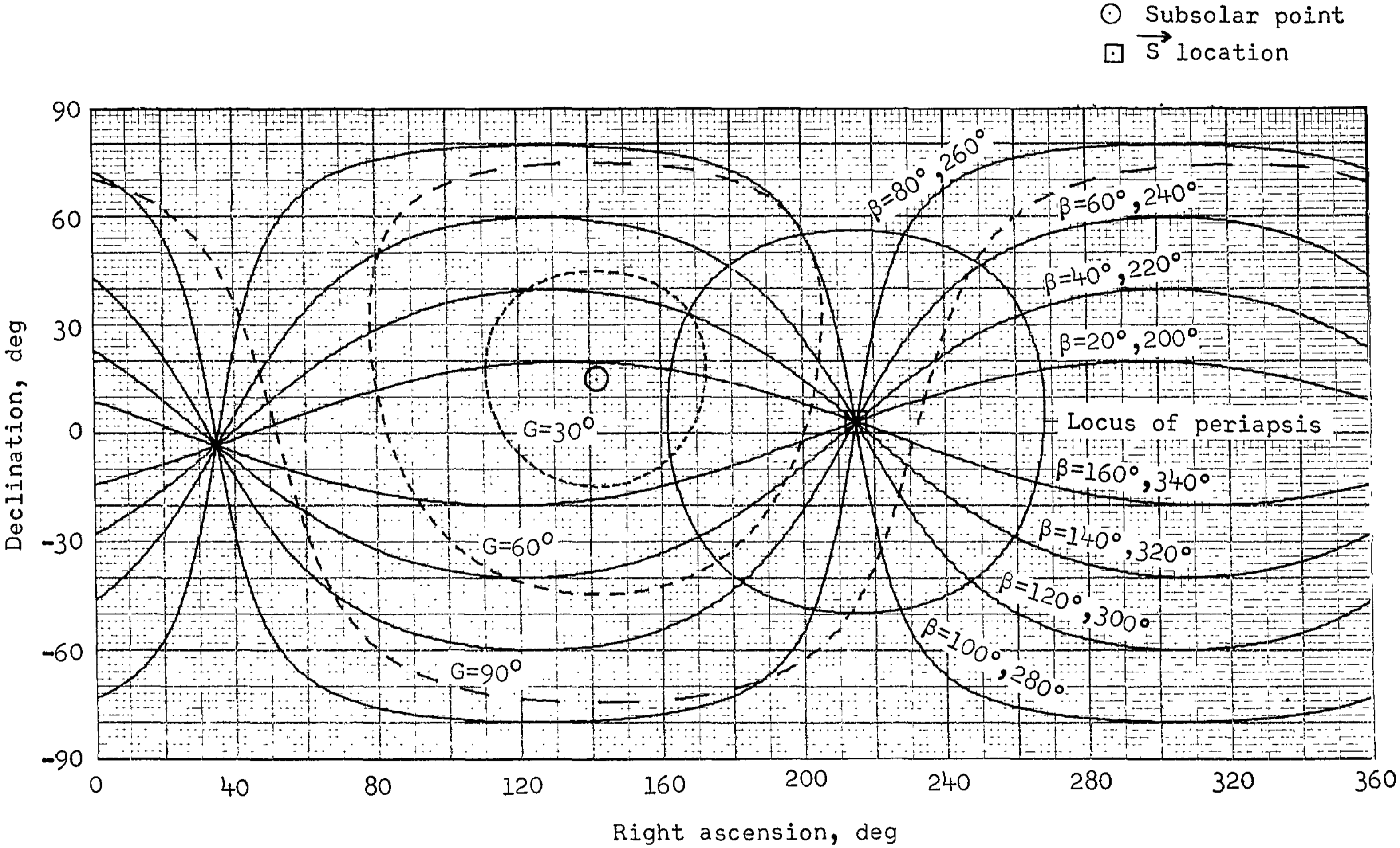

(c) October 22, 1977, launch and September 14, 1978, arrival.

Figure 25.- Concluded.

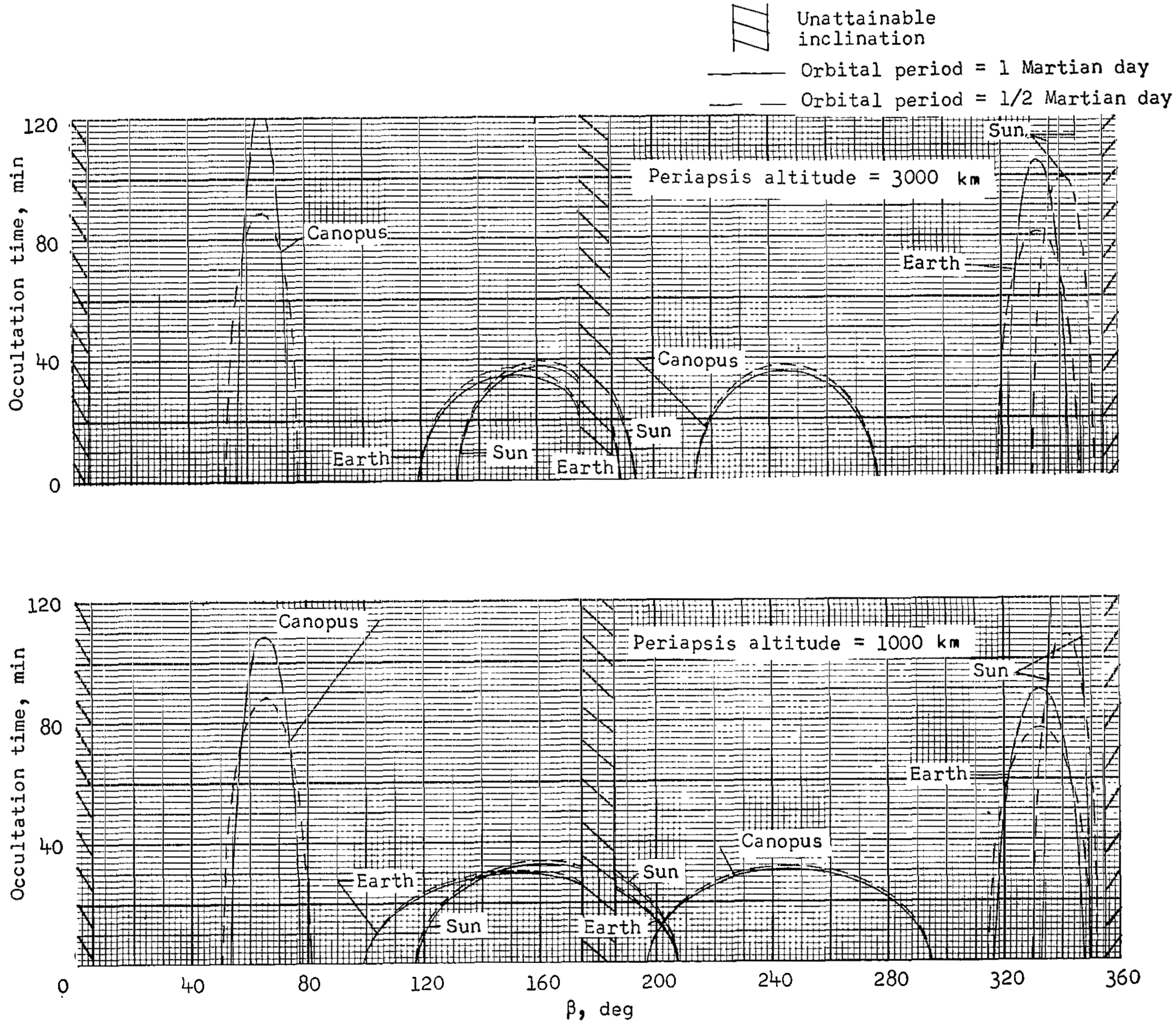

(a) September 20, 1977, launch and August 25, 1978, arrival.

Figure 26.- Occultation characteristics for Mars orbits resulting from typical 1977 type II trajectories.

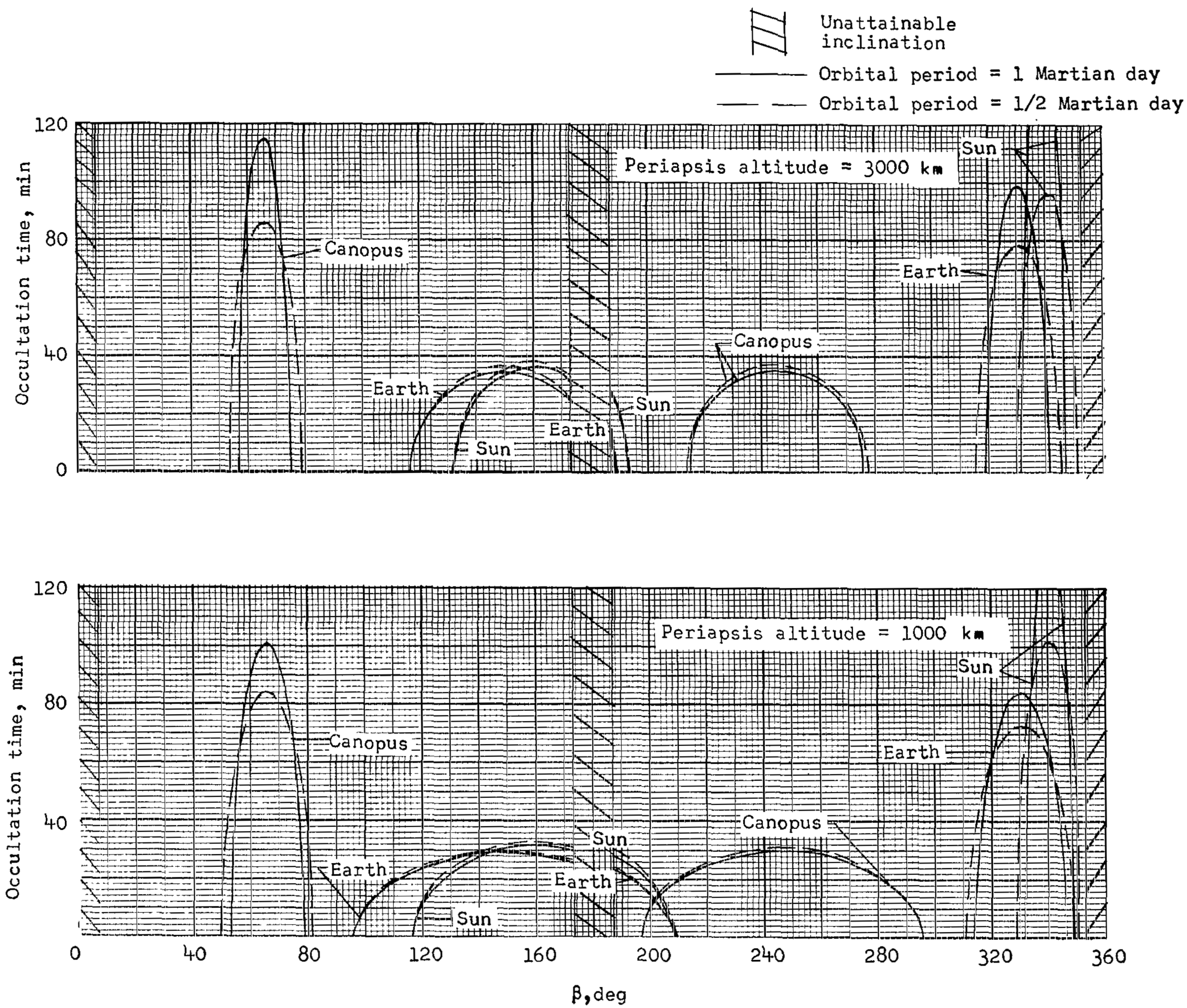

(b) October 6, 1977, launch and August 25, 1978, arrival.

Figure 26.- Continued.

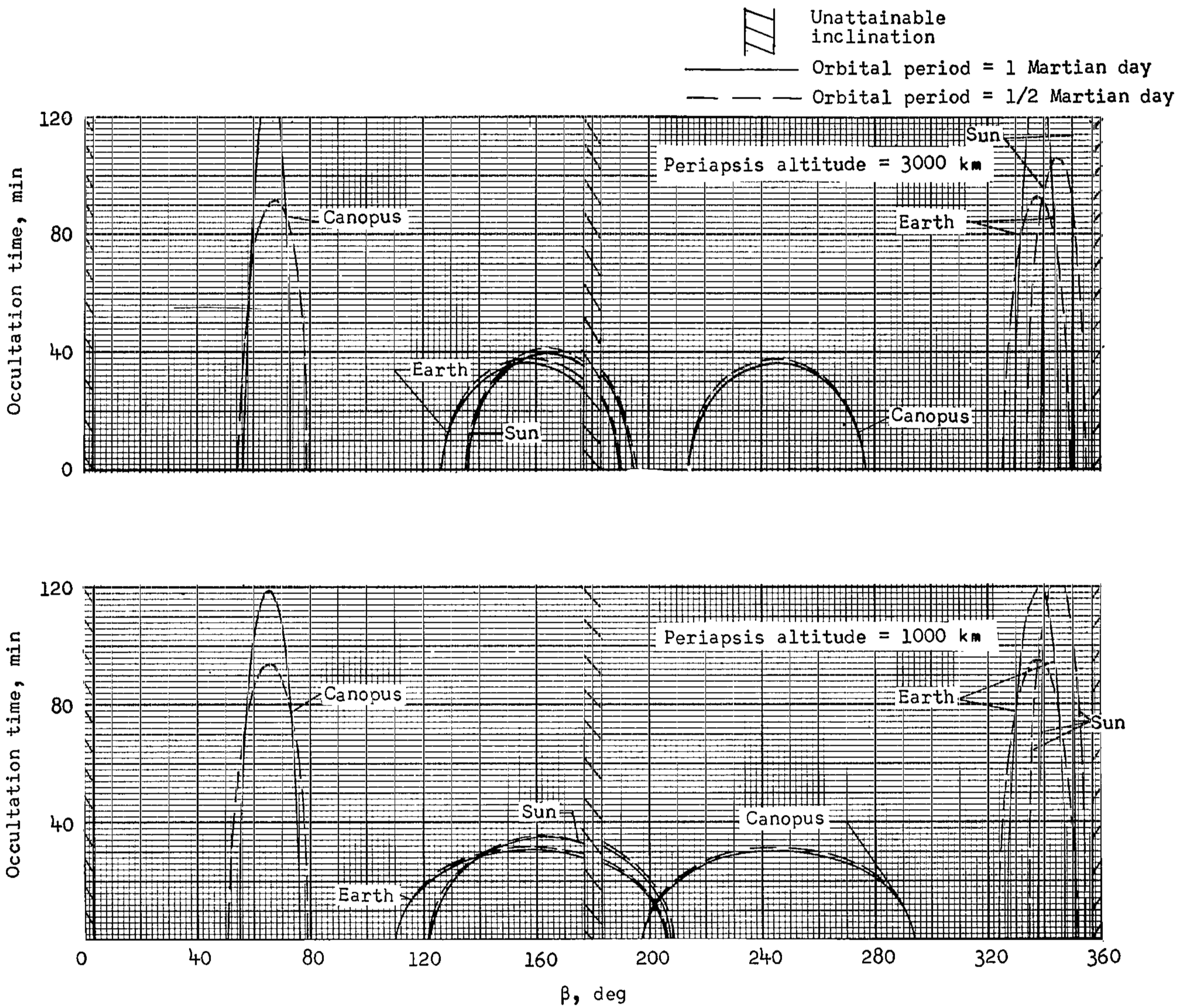

(c) October 22, 1977, launch and September 14, 1978, arrival.

Figure 26.- Concluded.

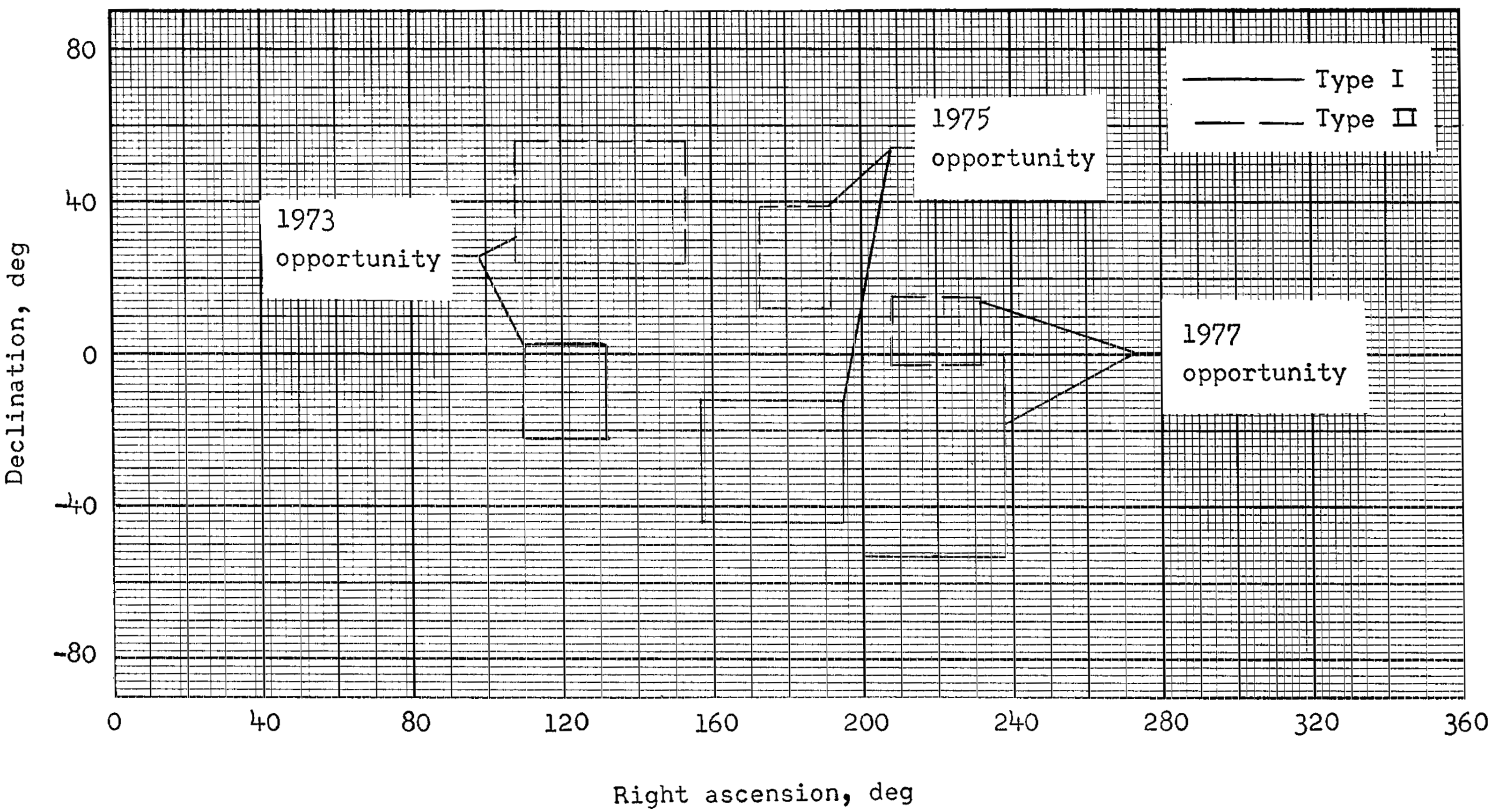

Figure 27.- Loci of approach asymptotes for launch opportunities studied.

NATIONAL AERONAUTICS AND SPACE ADMINISTRATION
WASHINGTON, D. C. 20546

OFFICIAL BUSINESS

FIRST CLASS MAIL

POSTAGE AND FEES PAID
NAL AERONAUTICS AND
CE ADMINISTRATION

01U 001 55 51 3DS 70225 00903
AIR FORCE WEAPONS LABORATORY /WLOL/
KIRTLAND AFB, NEW MEXICO 87117

ATT E. LOU BOWMAN, CHIEF,TECH. LIBRARY

POSTMASTER: If Undeliverable (Section 158 Postal Manual) Do Not Return

"The aeronautical and space activities of the United States shall be conducted so as to contribute . . . to the expansion of human knowledge of phenomena in the atmosphere and space. The Administration shall provide for the widest practicable and appropriate dissemination of information concerning its activities and the results thereof."

— NATIONAL AERONAUTICS AND SPACE ACT OF 1958

NASA SCIENTIFIC AND TECHNICAL PUBLICATIONS

TECHNICAL REPORTS: Scientific and technical information considered important, complete, and a lasting contribution to existing knowledge.

TECHNICAL NOTES: Information less broad in scope but nevertheless of importance as a contribution to existing knowledge.

TECHNICAL MEMORANDUMS: Information receiving limited distribution because of preliminary data, security classification, or other reasons.

CONTRACTOR REPORTS: Scientific and technical information generated under a NASA contract or grant and considered an important contribution to existing knowledge.

TECHNICAL TRANSLATIONS: Information published in a foreign language considered to merit NASA distribution in English.

SPECIAL PUBLICATIONS: Information derived from or of value to NASA activities. Publications include conference proceedings, monographs, data compilations, handbooks, sourcebooks, and special bibliographies.

TECHNOLOGY UTILIZATION PUBLICATIONS: Information on technology used by NASA that may be of particular interest in commercial and other non-aerospace applications. Publications include Tech Briefs, Technology Utilization Reports and Notes, and Technology Surveys.

Details on the availability of these publications may be obtained from:

SCIENTIFIC AND TECHNICAL INFORMATION DIVISION
NATIONAL AERONAUTICS AND SPACE ADMINISTRATION
Washington, D.C. 20546